RESEARCH AND TECHNOLOGY

ANNUAL REPORT 1982

George C. Marshall Space Flight Center

Research and Technology Office

ANNUAL REPORT

Fiscal Year 1982

RESEARCH and TECHNOLOGY

November 1982

Prepared by the

Research and Technology Office
Science and Engineering Directorate
GEORGE C. MARSHALL SPACE FLIGHT CENTER

TABLE OF CONTENTS

TABLE OF CONTENTS

RESEARCH PROGRAMS CONT'D

TABLE OF CONTENTS

TECHNOLOGY DEVELOPMENT CONT'D

ILLUSTRATIONS

ILLUSTRATIONS CONT'D

ILLUSTRATIONS CONT'D

INTRODUCTION

The Marshall Space Flight Center is pleased to present its annual Research and Technology program report for fiscal year 1982. In many ways, this was a banner year for MSFC since new and exciting results occurred, specifically in both the Solar and Magnetospheric Physics elements. New thrusts have been initiated in systems studies, directed toward defining technology developments necessary to enable the evolutionary space station program and its related elements. Significant progress has been made in other areas of our program, and special significance is attached to both materials and processes improvements which will have a positive impact on reducing the costs of operations for MSFC's Shuttle developed elements.

The product of our Research and Technology is knowledge. In keeping with the NASA charter, we have striven to dissemimate this knowledge through the presentation and publication of 83 reports, 42 of which appeared as refereed articles in reference journals. Additionally, our program has resulted in 48 patent disclosures this year and 41 patent awards from both this and the previous year's work.

The readers are invited to contact the researchers whose names appear at the end of each segment. Additional copies of this report can be obtained from the Research and Technology Office, ER01, Marshall Space Flight Center, AL 35812.

ADVANCED STUDIES

SPACE STATION

The next major space program logically should be the development of a space station. This would be a manned facility in low-Earth orbit and capable of performing a variety of scientific and operations missions. Such a facility would significantly extend the Nation's capabilities in space. Besides supporting science and applications missions, the Space Station could service unmanned platforms and free-flying spacecraft. A Teleoperator Maneuvering System (TMS) would be used to return spacecraft to the station or to provide remote servicing, whichever is the most effective. The Space Station would also be used to support Orbit Transfer Vehicles (OTV) for placing payloads in high energy orbits, including geosynchronous placement and retrieval and planetary injection. Although the specific configuration is still yet to be determined, Figure 1 depicts a typical early Space Station composed of a resources module with solar array, a core module for crew support and a berthing adapter for adding on other modules. Mission equipment such as laboratory modules, TMS docking/servicing parts, OTV hangars, and a large space structural assembly are also shown in the illustration.

During the past year, MSFC has conducted a large number of related studies, both in-house and under contract. The "Evolutionary Science and Applications Manned Space Platform Study" (SAMSP) was completed in the Spring of 1982. This major study by McDonnell-Douglas defined and evaluated approaches and concepts for evolving a space platform to a permanent manned facility. Tasks included the analysis of requirements for a manned station, identification of alternate concepts and systems analyses and comparisons.

At the same time, MSFC continued in-house investigations of alternative evolutionary concepts. A major emphasis was given to defining an early availability, low-cost minimal capability station which could be upgraded to satisfy more demanding future requirements. Part of this activity included

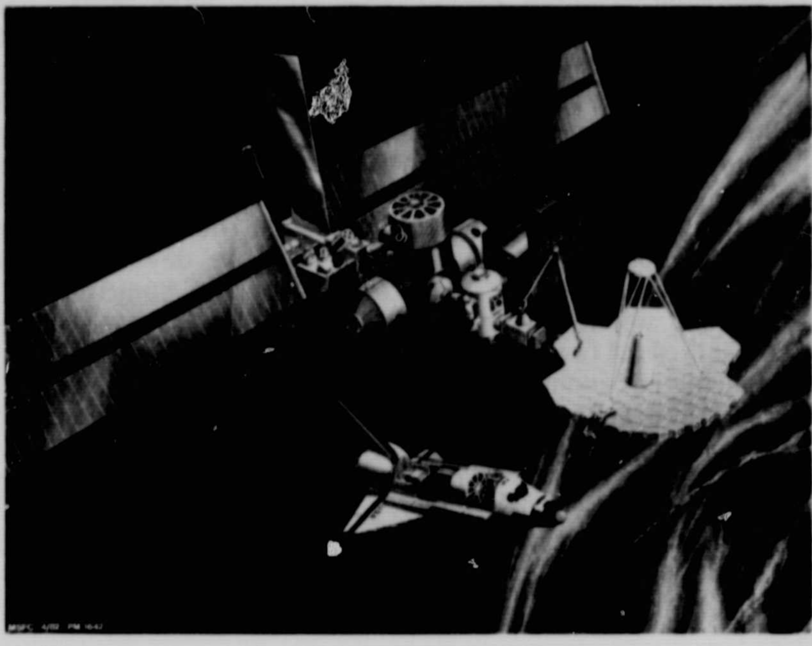

Figure 1. An Early Space Station Configuration.

studying the use of Spacelab designs and hardware as an element of the Space Station. Subsystems analyses were conducted on electrical power, communications, data management, thermal control, structures, life support, attitude control and propulsion subsytems, in addition to overall systems analyses and integration studies. Various flight demonstration tests were also defined for investigating the interactions of large solar arrays with the orbital environment. Operational approaches such as on-orbit servicing and formation flying were investigated. Mission/payload analyses were performed. MSFC also participated in and supported Agencywide working groups and panels on Space Station technology requirements and definitions.

In the fall of 1982, studies were initiated to identify and analyze the potential role an early Space Station could play as a test-bed in developing the longer range, operational capabilities required. Large space structures, satellite servicing, and OTV servicing were selected for emphasis. These studies are expected to provide insight into early Space Station missions.

MSFC also continued advanced development activities in related areas. The Electrical Power System (EPS) testing was continued to determine the performance of high voltage electrical power systems using programmable power processors and the operation and charge control of high voltage NiCd batteries. A 112 cell, 33 ampere-hour (AH) battery completed 5,555 simulated low-Earth orbits since the test was initiated and is being replaced with a second 88 cell, 55 AH battery. During this year, the 33 AH battery was used to investigate charge control techniques in efforts to achieve optimum performance under various operational conditions and to investigate the effects of high rate pulse discharge demands on the battery. An 88 cell, 55 AH battery, which has thus far completed nearly 6,000 orbits, was also used to investigate charge control techniques.

Simulation evaluations were performed on the development model of the TRW Berthing Mechanism. These tests were conducted in the six-degree-of-freedom simulation facility and simulated the mating of the space platform to an adapter attached to the Orbiter. The tests consisted of mating the Berthing Mechanism under various degrees of misalignment, including combinations of axes simultaneously. The probe was supported from a fixed mounting structure on the ceiling, and the cylinder was attached to a load limiting system on the six-degree-of-freedom platform. The platform, driven by six hydraulic struts, simulated the mass, inertia and the motion response of the space platform during mating.

Neutral Buoyancy tests were conducted which demonstrated MDAC space platform orbital maintenance and contingency operations. These tests verified the basic hardware design and maintenance concepts and the thresholds of man's ability to work in space using simple Extravehicular Activity (EVA) support equipment and tools. The tests included: (1) the EVA manual deployment and rigidization of a payload part; (2) the EVA removal and replacement of a Control Moment Gyro (CMG), Solar Array, and boxes mounted on cold plate areas of the platform main body; and (3) the manual deployment of appendages by means of EVA hand cranking.

CMG testing was continued to validate CMG design modifications. The CMG Spin Bearing Life test successfully accumulated over 6,000 hours without any anomalies. The CMG Slip Ring Life test successfully accumulated over 2,800 hours without any anomalies. The outgassing test indicates that the seals which were added to prevent excessive lubricant outgassing are fully effective. (L. Powell/PM01/205-453-5310)

TELEOPERATOR MANEUVERING SYSTEM (TMS)/REMOTE SATELLITE SERVICER

MSFC has performed or directed a number of mission applications and systems definition studies aimed at defining an optimized remotely controlled orbital service vehicle system needed to extend and complement the basic capabilities of the Shuttle Orbiter. This new vehicle for the STS inventory, referred to as a TMS, will deliver or retrieve payloads at altitudes far beyond the effective or economic use range of the basic STS. With the use of redundant TV cameras, TMS can provide good quality video pictures back to a TMS operator/controller located in the Shuttle crew cabin, or on the ground, in support of a remote viewing or satellite inspection mission. The TMS may utilize either a mono-propellant (hydrazine) or bi-propellants for its primary propulsion system; an inert cold gas attitude control system is optional on TMS for maneuvering the TMS in and around payloads where contamination control requirements are severe.

While broadening the STS "sphere of influence" relative to accomplishing major payload altitude and plane changes with a TMS, the Orbiter is then operated at lower altitudes (160 nautical miles), where it is more efficient. As a result, much more payload can be delivered on a single Shuttle flight, thereby reducing the payload cost per flight and offering more opportunities for the manifesting of multiple payloads on each flight. The resulting economic benefits, made available by TMS use, are substantial.

TMS configurations range in weight from 2800 to 4,000 lb. (dry weight), and carry between 5,000 - 7,000 lb. of propellant. Growth options with larger propellant capacities have also been studied. Typically, a representative TMS configuration can deliver a 10,000 lb. spacecraft to a 1,000 nautical mile altitude and then return to the Orbiter for retrieval and reuse. It can retrieve a 1,000 lb. spacecraft from an altitude of 1500 nautical miles. A growth configuration can move a 4,000 lb. spacecraft to an altitude of 1300 nautical miles, make a payload plane change of 8°, which is very demanding, then return back to the Orbiter for retrieval and reuse.

More recently, MSFC studies are investigating a space-based TMS, as shown in Figure 2. In this scenario, the TMS is operated as a major adjunct to the space station, providing both local and remote servicing support to payloads operated in the vicinity of the space station. TMS will also handle the transfer of resupply cargo and payloads from the STS to the space station.

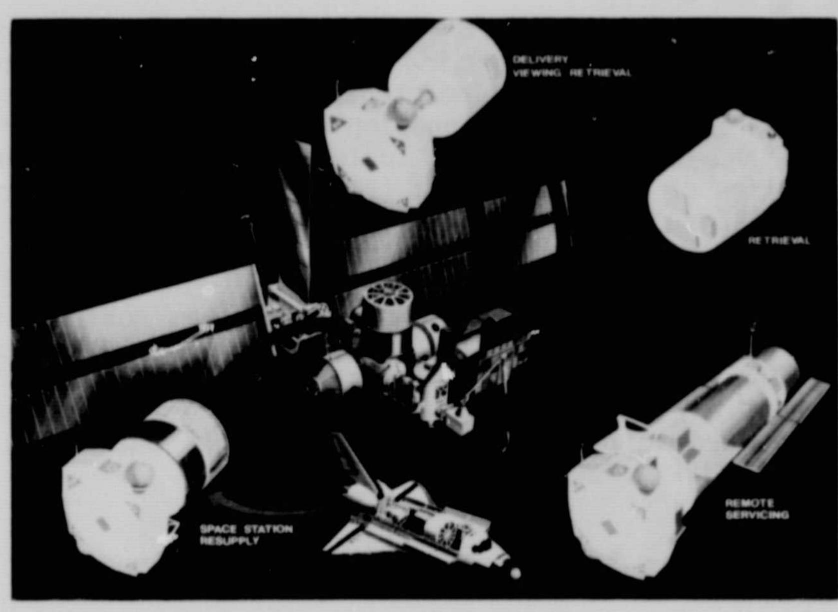

Figure 2. Space-Based Teleoperator Maneuvering System.

TMS is modular in design to permit the addition of growth features as more demanding future missions evolve. Beyond basic payload placement, retrieval, viewing, and subsatellite uses, the TMS is compatible with the addition of advanced mission kits to accommodate remote modular servicing/repair of spacecraft, large structures assembly support, and more autonomous robotic functions, such as space debris retrieval. An early TMS is expected to fly in the 1987-88 time frame. (D. C. Cramblit/J. R. Turner/PS04/205-453-0367)

GROUND LAUNCHED TRANSPORTATION SYSTEMS

Shuttle Derived Vehicles (SDV) (Figure 3) continued to be studied as means to improve performance, reduce cost and increase payload volume. MSFC is investigating the use of flyback liquid rocket boosters on the Shuttle in order to reduce turn-around time and improve operational performance. Methane, propane and RP were investigated as fuel for the Liquid Rocket Booster. Replacement of the Orbiter with a cargo carrier and a recoverable, reusable Propulsion/Avionics module continues to be investigated as a launch vehicle with increased payload performance and increased payload volume capability. This Shuttle Derived Vehicle could supplement the STS Program. Other launch vehicle concepts that are being investigated include the removal of the Orbiter and the placement of a single or dual SSME under the External Tank with the payload container mounted on top of the External Tank ("in-line" configuration) and the combination of Solid Rocket Motors to form an all-solid motor launch vehicle, except for the terminal stage (SRB-X). An Aft Cargo Carrier (ACC) attached to the bottom of the ET is being investigated as a means of increasing the payload volume capability of the STS. Scale model tests are being performed at MSFC to determine launch environment conditions for design purpose.

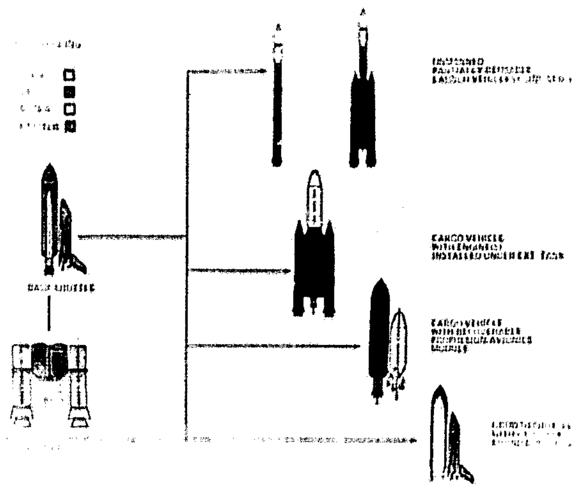

Figure 3. Shuttle-Derived Ground Launch Vehicle Concepts.

In addition to studies to define SDV configuration options, emphasis has been placed on identification of technologies applicable to Shuttle-derived vehicles, and the degree of benefits to be derived from such technology advances. Technology areas identified include: (1) LOX/hydrocarbon propulsion technology, for potential application in reuseable liquid rocket booster stages; (2) Structures, materials, and thermal protection systems (TPS) technology for potential reduction in weight, turn-around time and costs; (3) Avionics and recovery systems technology: (4) Manufacturing and quality assurance technology for reduction in manufacturing time, testing and costs; and (5) Operations technology for the reduction of vehicle turn-around requirements and launch procedures. (M. Page/PS06/205-453-3425)

HIGH ENERGY UPPER STAGE (HEUS)

An aeroassisted version of a High Energy Upper Stage using high performance chemical propulsion systems is shown in Figure 3. HEUS vehicles are needed for transporting payloads of up to 7,000 kilograms between low-Earth orbit and geosynchronous orbit. Interplanetary missions are also anticipated which need similar capability. Studies conducted during 1979/81 define specific mission applications, requirements, and candidate evolutionary vehicle concepts. These studies have identified and initiated definition and technology studies of deployable aeroassisted vehicle concepts which offer significant performance improvement for reusable transportation to geosynchronous orbit. Requirement studies identified the need for a very short stage which can deliver a very long but substantial mass to high Earth orbit. HEUS concepts were identified and defined which utilize a toroidal oxidizer tank around the engine to minimize stage length. An alternative concept has been studied which involves launching the HEUS in an aft cargo canister below the External Tank of the Shuttle, thereby freeing the total Orbiter cargo bay for payloads.

Technology studies aimed at improving the performance of cryogenic stages have been underway for several years and involve advanced engine studies, cryogenic propellant management breadboard testing, and cryogenic propellant tank design and verification. (Robert E. Austin/PS04/205-453-2769)

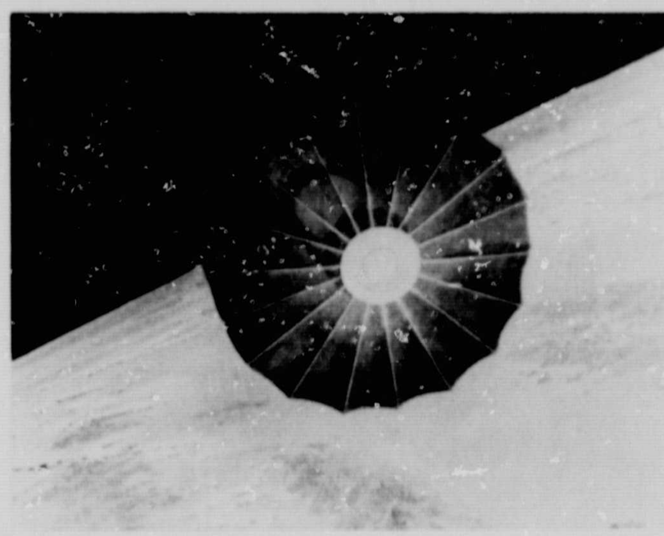

Figure 4. Aeroassisted High Energy Upper Stage.

GEOSTATIONARY PLATFORMS

Earlier studies of Operational Geostationary Platforms of the 1990's have suggested that the lowest cost operational concept might be a complex of docked modules, each carried up by a separate shuttle mission. Such a platform was studied in more detail in FY 1982. Comparison of the new study results with earlier findings showed this version had, in fact, significantly lower life-cycle costs than a comparable constellation of independent modules, all in the same geosynchronous slot. This study was limited to consideration of only one conservative mission set but the conclusion is applicable in general.

Other earlier conclusions concerning Operational Geostationary platforms were also substantiated. These platforms offer clear economic benefits when compared to use of conventional satellites for future communications missions. They offer new economical opportunities for large scale frequency reuse which will be necessary in the 1990's to alleviate the orbital arc and frequency spectrum crowding problem currently being experienced, especially in long distance telephone, data/facsimile transmission and video links.

A single shuttle-launched experimental platform, which would demonstrate as an integrated system the communication and platform technologies, is needed in 1990 to pave the way for the Operational Geostationary Platforms of the 1990's and beyond. Based on updated requirements, technology projections, and payload data, four such Experimental Geostationary Platform concepts were further studied and a baseline version then studied in detail as a point design. This baseline platform included 10 and 15 meter diameter antennas of different construction concepts, deployable truss structures, a good mix of science and applications payloads, both C-band and UHF technology demonstrations, thermally stable structures, docking and servicing capability, high frequency high voltage AC power, high efficiency power system components, experimental active stabilization, experimental North-South stationkeeping, and other advanced technologies. This platform weighs 12,000 lbs and provides 8 kW of power.

A second-generation operational direct broadcast mission was defined and a 4-platform operational system, utilizing 17/12 GHZ for time zone coverage, was analyzed. This system had, on each platform, 40 channels using two 2.9 meter reflectors, 200 watt TWTA's, 5250 kg mass, and a 30 KW power source. Possibilities for a direct broadcast Experimental Geostationary Platform were studied. It was determined that the Baseline Experimental Geostationary Platform could be easily modified to accommodate a direct broadcast mission.

Technologies that would be demonstrated by this Platform include: deployable structures and structural mechanisms; active stabilization of large space structures; high efficiency AC power system; LEO-to-GEO transfer of deployed structures; automated unmanned servicing at GEO; platform intermodule docking; and integrated attitude control system for docked platform modules; multi-beam antennas; scanning-beam antennas; accurate beam pointing; interplatform links; onboard communication switching and processing; a platform communications controller/processor; link performance enhancement techniques; high effective isotropic radiated power and small earth station antenna; dual polarization Ka-band; and use of high-power, long-life spacecraft traveling wave tube amplifiers. New technologies this platform would demonstrate, in addition to those listed previously, would be the use of high power TWTA's in a geostationary application, a larger power system, and a high capacity heat dissipation system in space. (R. Durrett/PS06/205-453-2817)

ADVANCED X-RAY ASTROPHYSICS FACILITY

Pre-phase B activities in FY82 included detailed program planning, a Phase A study incorporating numerous analyses performed over the last several years, continued technology support, and operation of the X-ray Test and Calibration Facility for analyzing the scattering properties of flat samples. One of the technologies advanced involved the Charge Injection Device (CID) for application to the AXAF Aspect System. CID's offer one approach to achieving the precision required for the location of X-ray objects and for reconstruction of X-ray images through data analysis. Another technology was advanced composites, such as Graphite-metal matrix materials, which promise strength, lightweight, and thermal stability needed for high performance space optical systems. In the area of X-ray optics, two significant programs were initiated with industrial optical vendors to grind, polish, and assemble sets of mirror blanks into imaging systems which can be tested with X-rays in the MSFC X-Ray Test and Calibration Facility. These mirror assemblies are expected to exhibit the optical performance required by AXAF to meet program goals. (C. Dailey/PS01/ 205-453-0162)

COHERENT OPTICAL SYSTEM OF MODULAR IMAGING COLLECTORS (COSMIC)

At microwave wavelengths large ground-based interferometers are routinely employed for high resolution astronomical observations. However, the difficulties of dealing with wavelengths 5 orders of magnitude smaller than microwave have made this a less attractive technique for achieving similar advances with ground-based observations at UV/visible wavelengths. In addition, ground-based problems of atmospheric absorption and observation fundamentally limit the possible advances. Space will overcome these barriers as well as provide the necessary undistrubed environment.

ORIGINAL PAGE
BLACK AND WHITE PHOTOGRAPH

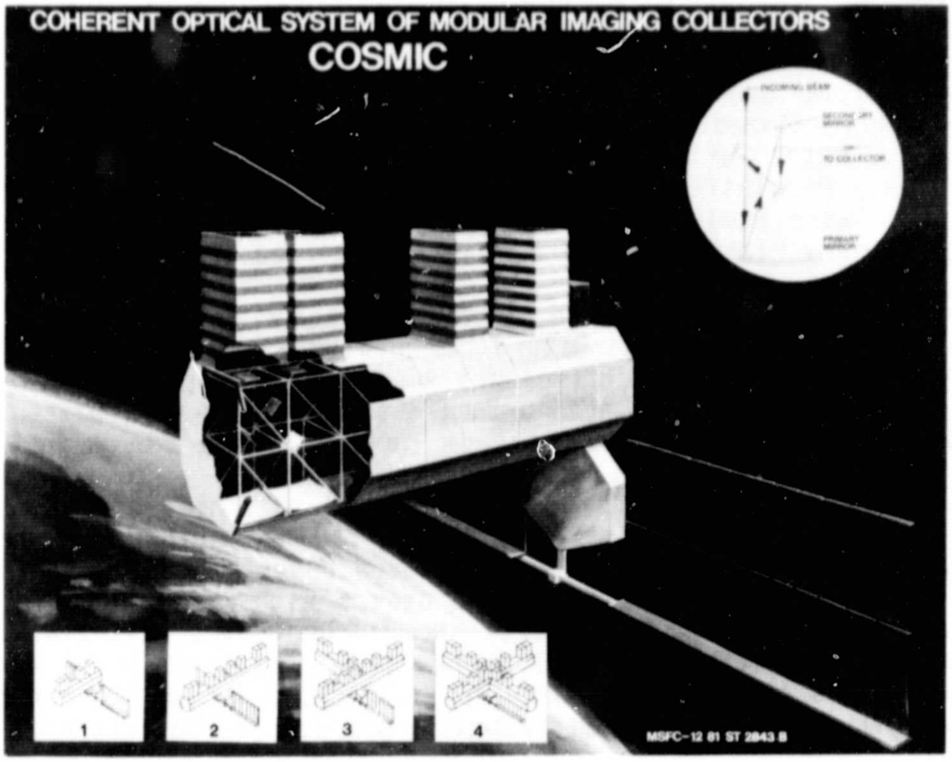

Figure 5. Space-Based Coherent Optical System of Modular Imaging Collectors.

The capability to construct large systems in space and the development of advanced optical control technology to maintain accurate baselines and alignments will allow the development of an array of coherent optical telescopes--this array, the optical analog of a radio VLBI, was studied to determine the advantages of phase-coherent arrays combined into a large equivalent aperture imaging system. It was determined that images with angular resolution in the milliarcsecond range can be achieved.

Figure 5 shows an artist's concept of COSMIC and the evolutionary construction of a large cruciform array. The initial linear array contains four Afocal Interferometric Telescopes (AIT) with a Beam Combining Telescope (BCT) at one end. The COSMIC spacecraft module pivots from its launch position at the end of the BCT to its deployed position below the BCT. The solar arrays deploy from stowed positions alongside the telescope module. The focal plane of the BCT and sunshades are extended above the telescope apertures.

The concept of a minimum redundancy array of telescopes is borrowed from radio astronomy and applied to optical systems. The AIT's are identical and all feed through fold flats, which compensate for the variations in the optical path lengths to the BCT. A collecting area of about 3m^2 per AIT gives the initial COSMIC configuration three times the collecting area of the Space Telescope. This, coupled with a factor of six increase in angular cresolution, means that COSMIC will have a faint-object-detectivity advantage over Space Telescope comparable to the advantage Space Telescope has over ground-based observatories.

The Smithsonian Astrophysical Observatory is assisting NASA in the scientific definition and analyses of the image reconstruction methods. Scientific objectives have been established, and mission and system requirements have been established. (M. Nein/PS02/205-453-3430)

Traub, W. A. and Gursky, H.: "Coherent Arrays for Optical Astronomy in Space," in Optical and Infrared Telescopes for the 1990's, Vol. 1, ed. A. Hewitt, Kitt Peak National Observatory, pp. 250-262, 1980.

Nein, M. E. and Davis, B. G.: "Conceptual Design of Coherent Optical System of Modular Imaging Collectors (COSMIC)," in Advanced Technology Optical Telescopes, SPIE Vol. to appear in 1982.

GRAVITY PROBE-B (GP-B)

Gravity Probe-B, containing the Relativity Gyroscope Experiment, is one of the few known laboratory tests of general relativity. The experiment seeks to measure two components of the precession of a gyroscope as predicted by the general relativity theory. The precession is small. In the low Earth orbit proposed for Gravity Probe-B, the largest component, the geodetic effect, is 6.9 arc sec/year while the smaller, the motional or gravimagnetic effect, is only 0.050 arc sec/year. The gravimagnetic effect is the gravitational analog of magnetism. Neither its magnitude nor its existence has ever been demonstrated in any other test of relativity. Only in a satellite where the support forces on the gyroscope can be minimized is it possible for the relativistic precession to dominate that from classical sources. The measurement of the geodetic effect to the proposed accuracy of 0.001 arc sec/year is a factor of 30 more accurate than any previous test. Such accuracy will permit the testing of relativity theories with unprecedented precision. Observation of the gravimagnetic effect should provide clues to the nature of quasars, the most powerful sources of energy in the Universe. The 1981 report of the National Academy's Committee on Gravitational Physics identified the detection and accurate measurement of the gravimagnetic effect as the number one priority for space relativity in the 1980's.

In the fall of 1980, MSFC initiated an in-house systems definition of the GP-B spacecraft. This activity was supported by Stanford University which is the parent organization of the Principal Investigators for this experiment. The results of this design activity were presented to several review groups earlier this year. Presentations on both the technical and programmatic aspects of the project were made to the MSFC Project Review Board (May 1982) and to the Center Review Board (June 1982). These groups thought the project was challenging, but accomplishable. An abbreviated review was held with the National Academy of Science Committee on Gravitational Physics in May 1982, and it reaffirmed its endorsement of GP-B as the centerpiece of its strategy in gravitational physics for the 1980's. In June 1982, OSSA convened a non-advocate group composed of scientists and engineers from various universities and from other NASA organizations to review GP-B and assess its technical and programmatic readiness for flight. This group stated that GP-B was a difficult but exciting experiment that should be supported for flight by NASA. Based on the results of these reviews, OSSA has requested an FY84 new start on the GP-B instrument with a mission new start in late FY86.

A parallel advanced development effort at both Stanford and MSFC has been in effect this past year and is continuing. During the past year, a repeatable procedure has been developed to polish very homogeneous quartz balls (rotors for the experiment gyroscopes) to a sphericity of less than one microinch. Development work is continuing on the techniques and equipment to put uniform thin films of niobium on the quartz balls. (A. Neighbors/PF16/205-453-1790)

PINHOLE OCCULTER FACILITY

The Pinhole Occulter Facility (POF) is a Shuttle-based facility which will study the solar corona in several wavelengths, and it will also form hard X-ray images of the sun and celestial objects. It uses a long deployable boom to position an occulting mask between imaging instruments and the sun (see Figure 6). This mask contains a system of multiple pinholes which

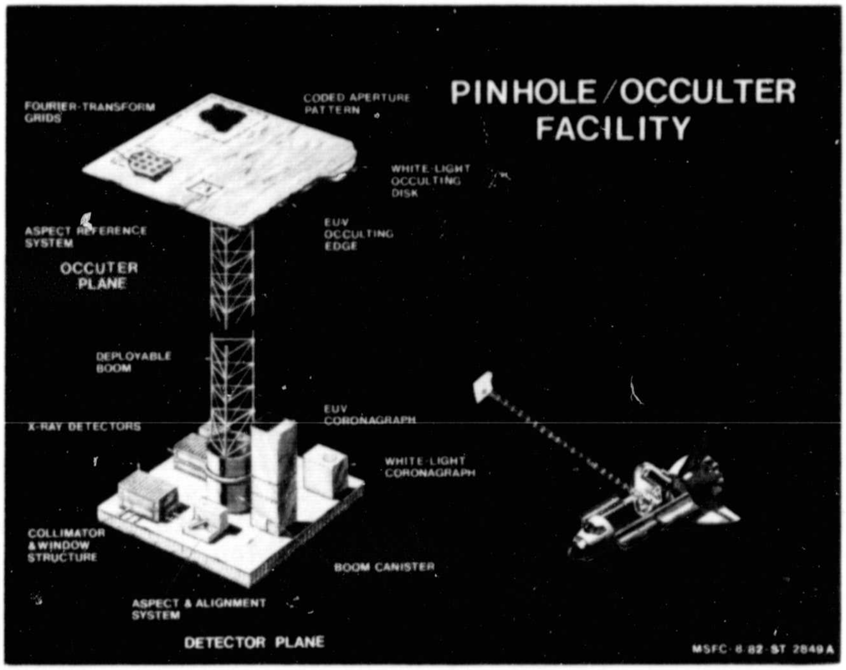

Figure 6. Pinhole Occulter Facility.

form X-ray images of the sun on a series of X-ray detectors. The mask also serves as an external occulter for white light and ultraviolet coronagraphs. The deployable boom, the occulting mask, and the instruments are all pointed and stabilized by a gimbal pointing system. The system can also be used to form high resolution images of celestial objects in much higher energies than possible by other X-ray imaging techniques.

The POF science working group has finished its final report which will be published this year. A conceptual design of a pointing and an alignment system has been defined and preliminary analysis indicated that the scientific requirements can be satisfied using modified control laws for a standard Spacelab pointing system such as the AGS or IPS. (J. Dabbs/PS02/205-453-3430)

ORIGINAL PAGE
BLACK AND WHITE PHOTOGRAPH

ORIGINAL PAGE
BLACK AND WHITE PHOTOGRAPH

LARGE INTERFEROMETERS IN SPACE

During the 1980's Space Astronomy will, without doubt, make discoveries and raise questions that require the use of more powerful astronomical instruments in order for us to understand the diverse astrophysical phenomena that will be unveiled. To meet these needs, large astronomical facilities with greatly improved angular resolution and large collecting areas will be placed in space above the absorbing and distorting interference of the Earth's atmosphere.

Figure 7. Very Long Baseline Interferometer - Retrievable Space Antenna.

The capability to assemble large structures in space and the existence of advanced technology for maintaining precise baselines and accurate pointing of large systems will make possible interferometers in space. Two such concepts currently under study by MSFC are the orbiting Very Long Baseline Interferometer (VLBI) and a phase-coherent UV/visible telescope array.

Radio interferometry observations of celestial sources are routinely made on Earth using atomic frequency standards to synchronize radio telescopes separated by as much as intercontinental distances. Angular resolution of magnitude superior to that of Earth-based optical telescopes has been achieved. By placing one or more observing elements in Earth orbit and making observations in concert with those on the ground, significant advantages over purely ground-based systems may be obtained.

An initial step would be to utilize the capability of the Space Shuttle to demonstrate orbiting VLBI by deploying a large retrievable antenna attached to the Shuttle. This mission, which could be a part of the Large Deployable Antenna Flight Experiment under study by MSFC and aerospace contractors during the past several years, would provide an on-orbit test of a large (> 50 meter) antenna system (which also has potential applications in defense, communications and Earth observations among others). An artist's concept of one possible antenna is shown in Figure 7. During the mission, about three days would be devoted to VLBI observations. An alternative system now under study at MSFC is a 15 meter antenna aboard the Shuttle that could later be used on the Space Platform or perhaps on an Explorer class mission. Although a large aperture antenna is desirable, an important set of bright sources could be observed with a space antenna as small as 5 to 10 meters in diameter.

During 1981, a technical working group was established to assist in the science and mission design of a VLBI experiment. Scientific objectives and mission and system/subsystem requirements for performing a VLBI demonstration have been established. (S. Morgan/PS02/205-453-3430)

Morgan, S. H. and Roberts, D. H., (editors): Shuttle VBLI Experiment: Technical Working Group Summary Report, NASA TM-8249, NASA-George C. Marshall Space Flight Center, July 1982.

Preston, R. A., Burke, B. F., Doxsey, F., Jordan, J. F., Morgan, S. H., Roberts, D. H., and Shapiro, I. I.: "The Future of VBLI Observatories in Space," International Conference on VLBI Techniques, Centre National D'Etudes Spatiales, Toulouse, France, September 1982.

RESEARCH PROGRAMS

ATMOSPHERIC SCIENCES

Global Weather Research

Research efforts under the Global Weather Program are directed toward understanding global-scale dynamics via diagnostic and modeling studies wherein satellite data play a major role. Emphasis is on: (1) the synoptic-scale cyclone and the role of latent heat release in its evolution, and (2) the evolution and structure of planetary-scale flows.

Significant progress in diagnosing the impact of condensational heating in synoptic flows was made this year. Large-scale condensation was investigated via quasi-geostrophic and semi-geostrophic vertical motion calculations (Pennsylvania State University), while heating rates by deep, moist convection were obtained by a diagnostic cumulus parameterization (Purdue University). In addition, a diagnostic evaluation of heat and mass transport by cumulus clouds utilizing IR imagery from GOES geostationary satellites was developed in-house. Theoretical aspects of the heating of synoptic-scale flows were investigated via a second-order, nonquasigeostrophic, two-layer analytical model. All of these studies addressed the enhanced growth rates of storms that occur when latent heat release offsets adiabatic cooling resulting from upward motion ahead of synoptic-scale storms.

Investigations in planetary-scale flows were focused this year on the index cycle which is a measure of the variability of the zonally averaged flow around the Earth. A quasi-geostrophic spectral model was developed which demonstrated that the index cycle depends on forcing both by topographic effects as well as thermal forcing related to baroclinicity. In addition, data from the Earth Radiation Budget (ERB) satellite experiment have been utilized to construct zonally averaged diagnostic heat budgets for the winter of 1974-1975. An interesting finding has been the tendency of poleward transports of heat and westerly momentum to oscillate at periods in the 5- to 10-day range in late fall and early winter, but to suddenly begin executing large amplitude, 20-day oscillation in mid-winter.

A preliminary investigation into the viability of a Space Shuttle/ Spacelab atmospheric science experiment was also conducted. A Shuttle-launched complement of meterorological research sensors could be targeted to a variety of scientific questions. Composites of multispectral measurements from sensors currently under development would allow a more comprehensive analysis of atmospheric structure than now available. Suggested science issues would include: (2) spatial structure of atmospheric moisture and quantitiative precipitation mapping; (2) lightning mapping; (3) the role of convection in producing poleward and interhemispheric mass, momentum, and thermodynamic energy transports; and (4) cyclone intensification over oceanic regions. (F. Robertson/ES82/205-453-2463 and G. Fichtl/ES82/205-453-0875)

Dutton, J. A., Fundamental Theorems of Climate Theory - Some Proved, Some Conjectured, SIAM Review, 24, 1-33, 1982.

Shirer, H. N., Improving Spectral Models by Unfolding Their Singularities, J. Atmos. Sci., 39, 610-621, 1982.

Tang, C. M. and Fichtl, G. H., The Role of Latent Heat Release in Baroclinic Waves - Without B-Effect, J. Atmos. Sci. (in press).

Design of the Atmospheric General Circulation Experiment (AGCE)

Previous laboratory experimental modeling of large-scale atmospheric flows has been limited to cylindrical geometries. However, in the low-gravity environment of Spacelab, a true spherical model can be realized. A radial dielectric body force can be used to simulate planetary gravity, and the complicating effects of terrestrial gravity disappear.

For a successful experiment, it must be possible to produce strong baroclinic (wave cyclone) instability. Because of mathematical difficulties, the design calculations, to insure that this instability criterion will be satisfied, cannot be performed using analytical methods. Sophisticated computer codes are needed. During the past year, the two codes required were completed. The first code calculates axisymmetric basic state flows for specified dimensions, fluid boundary temperature configurations, and rotation. The second code examines the stability of these basic states. Using these codes, systematic design studies are now being performed. Figure 8 shows an example of a basic state flow. These codes make use of new numerical time-stepping techniques for faster convergence. This work is being performed in conjunction with Dr. G. Roberts (SAI), Dr. K. Kopecky (Drake University), and Dr. T. Miller (MSFC).

To link the AGCE studies more closely to atmospheric research, a computer general circulation model (GCM) was stripped down to approximate a simplified Earth. A large number of runs with this GCM were recently completed. This work was performed by Dr. J. Geisler (University of Utah), Dr. E. Pitcher (University of Miami), and Dr. R. Malone (Los Alamos Scientific Laboratory).

Backup scientific work to assist in formulating well-posed scientific studies for the AGCE and to help in interpreting the results are being performed in conjunction with Dr. B. Antar (University of Tennessee Space Institute), Dr. R. Gall (University of Arizona), Dr. F. Leslie (MSFC), and Dr. T. Singler (MSFC).

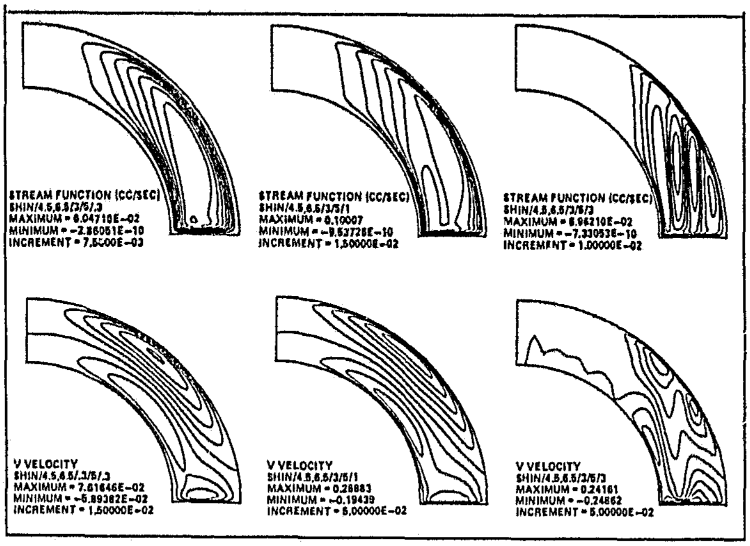

Figure 8. Design Considerations for the Atmospheric General Circulation Experiment.

This research has been sponsored by the Global Weather Program of the Office of Space and Terrestrial Applications under RTOP 146-30-06 (Theoretical Studies of Atmospheric Processes). (W. W. Fowlis/F. W. Leslie/ES82/205-453-2047)

Fowlis, W. W. and Davis, M. H., (editors): The Numerical Studies Program for the Atmospheric General Circulation Experiment (AGCE) for Spacelab Flights, NASA CP-2200, 1981.

Homsey, R. J. (editor): Feasibility Study - Atmospheric General Circulation Experiment, NASA CR-161889 (2 volumes), September 1, 1981.

Antar, B. N., and Fowlis, W. W., (editors): Baroclinic Instability of a Rotating Hadley Cell, J. of the Atmos. Sci., 38, 2130-2141, 1981.

Keramidas, G. A., Brebba, C. A., Miller, T., and Gall, R.: Numerical Calculation Experiment. In Proceedings of the International Conference on Computational Methods and Experimental Measurements, (Springer-Verlag, New York), 1982.

Fowlis, W. W. and Roberts, G. O.: The Numerical Design of a Spherical Baroclinic Experiment for Spacelab Flights. In Proceedings of the International Conference on Computational Methods and Experimental Measurements, July 1982.

Leslie, F. W., Hyun, J. M., and Fowlis, W. W.: Numerical Solutions for the Spin-up from Rest of a Homogeneous Fluid in a Cylinder, J. of Fluid Mechanics (accepted for publication).

Miller, T. L. and Gall, R. L.: Thermally Driven Flow in a Rotating Spherical Shell: Axisymmetric States, J. of the Atmos. Sci., (submitted).

Geisler, J. E., Pitcher, J. E., and Malone, R. C.: Rotating-Fluid Experiments with an Atmospheric General Circulation Model, J. of the Atmos. Sci., (submitted).

Mesoscale Sampling

The AVE/VAS (Atmospheric Variability Experiment/Visible and Infrared Spin-Scan Radiometer Atmospheric Sounder) Ground Truth Field Experiment was conducted in cooperation with the Operational Satellite Improvement Program and NASA's Severe Storm and Local Weather Research Program. The AVE/VAS experiment was important to the VAD demonstration because it provided, via a special mesoscale rawinsonde network, a fundamental data set upon which the VAS sounding assessment and evaluation will be made. The experiment was managed by the Marshall Space Flight Center.

The AVE/VAS rawinsonde network consisted of a regional area, centered over the U.S. plains, where 24 NWS (National Weather Service) rawinsonde stations were employed to collect upper level data. Nested within the central region is a meso-B scale network of rawinsonde sites (12) with a separation of around 120 km. During the experiment days, radiosonde releases were made at all sites from 1200 through 0600 GMT at 3-hour intervals. The timing of the radiosonde observations was closely related to the sounding times from the GOES VAS system.

During the period from March through May 1982, four primary AVE/VAS periods were carried out. These were: March 6-7, March 27-28, April 24-25, and May 1-2. The 3-hour rawinsonde observations began at 1200 GMT on the first day and went to 0600 GMT on the following day. The VAS data acquisition continued through 1200 GMT on the second day at 3-hour intervals. Seven rawinsonde observations were made on each experiment day at each of the 24 regional and 12 special network sites. In addition to the four formal experiment days, the special network rawinsonde sites were run at 6-hour intervals between 1200 and 0000 GMT on February 6-7, 1982, to checkout the rawinsonde equipment. VAS data were also taken at 3-hour intervals. In addition to the VAS and rawinsonde data, digital radar data were collected at the NWS radar site at Stephenville, Texas, and at Texas A&M University at College Station. Both radar sites are within the meso-B network.

These data are currently being processed to allow for an objective comparison between ground-based rawinsonde profiles of temperature and moisture and those derived from the VAS instrument. A complete description of these research results is expected in 1983 as part of a continuing program to better utilize space technology in understanding atmospheric processes. (J. Arnold/ES84/205-453-2570)

Lightning Research

Research on atmospheric electricity is directed toward the development of an optical lightning mapper sensor to operate from geostationary orbit. During 1982, work included the initiation of sensor studies which focus on techniques to remove large background "noise" due to illuminated clouds from large-scale mosaic detector arrays and basic research aimed at obtaining measurements of lightning characteristics from above thunderstorms.

The data acquisition effort included the use of a NASA U-2 aircraft flying a package of eight instruments over severe thunderstorms in the vicinity of Oklahoma and the southwestern United States, and the Shuttle based Nighttime-Daytime Optical Survey of Lightning (NOSL) instrument. Of particular value are data of large-scale lightning development and propagation obtained during STS-4.

Unique data sets which should answer most of the questions needed for the development of the lightning mapper were recorded during the U-2 flights. Data on the spatial, temporal, and spectral characteristics of optical lightning emissions were obtained, much of which can be correlated with ground-based data recorded at the National Severe Storms Laboratory. This should greatly improve our ability to interpret the lightning data. It is anticipated that the spectral data will be particularly valuable both to the development of the lightning mapper and in understanding the characteristics of lightning channels occurring in the upper regions of clouds. (H. Christian/ES83/205-453-2463)

Nighttime-Daytime Optical Survey of Lightning (NOSL) Experiment

The primary objective of this program was to conduct exploratory research on lightning and severe storms with a simple, low-cost detector from orbital altitude using the Space Shuttle. Additional objectives were to provide preliminary information from space-based observations with NOSL that might be of value to a proposed lightning mapper satellite development program.

The NOSL experiment was first flown on the STS-2 as a part of the OSTA-1 science payload. The experiment was crew-operated, and a very limited amount of experiment time was available due to the shortened mission duration. Even this limited time established that the system operated very successfully. Photography was obtained for five ocean storms and the electro-optical pulses were positively identified.

The experiment was reflown on STS-4, and both photographic and electro-optical data were collected. Photographic data of a large lightning bolt (> 50 km in length) showed a propagation velocity of 10^5 m/s. This bolt branches into a wye, and preliminary brightness data and the branching indicate that it is probably a cloud-to-ground-type bolt. Thirty intracloud flashes were recorded during the night pass over the South American storm, which was photographed on two orbital passes. Eight day storm systems were photographed over land and water, and electrooptical data were obtained. Analysis of the data is continuing, and the experiment will be reflown on STS-6 in January 1983. (O. Vaughan/ES83/205-453-Ø941)

Behavior of Multiphase Media at Very Low Intergranular Stresses - Interactions with Atmospheric Processes in the Boundary Layer

A peer group review, initiated by the chairman of the OAST Physics and Chemistry Experiments in Space (PACE) Working Group, endorsed a proposed Spacelab experiment to study the constitutive behavior and solid-fluid interactions of multiphase (solid, liquid, gaseous) media under very low intergranular stress fields. Among many other applications, the value of these investigations would be to considerably enhance our fundamental understanding of erosional, depositional, and mass-wasting mechanisms, as well as other transport phenomena that occur in large regions of the Earth's surface as a result of interactions between atmospheric geologic processes in the boundary layer. Such processes, although not understood as yet, are the dominant factors for the transformation of habitable regions into deserts which currently constitute one third of the world's land area.

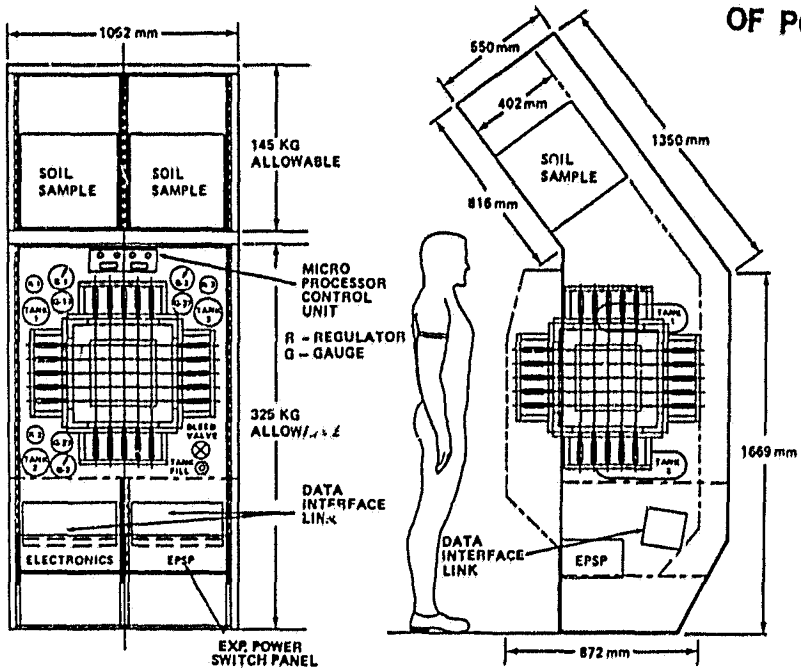

Figure 9. Experiment Definition of the Multiaxial Cubical Test Cell.

A most likely candidate apparatus for such an experiment has been studied extensively at MSFC and is shown in Figure 9. (N. C. Costes/ES81/ 205-453-0946)

Costes, N. C. and Sture, S.: The Potential of In-Space Research on Liquefaction Phenomena and Related Soil Behavior; Special Contribution in Proceedings, International Conference on Recent Advances in Geotechnical Earthquake Engineering and Soil Dynamics, St. Louis, Missouri 3, 929-959, April 26-May 3, 1981.

Bonaparte, R. and Mitchell, J. K.: Development of Experimental Concepts for Investigating the Strength Behavior of Fine-Grained Cohesive Soil in the Spacelab/Space Shuttle Zero-G Environment, NASA CR-3365, April 1981.

Sture, Y. H. Ko, Mitchell, J. K., and Costes, N. C.: Development of an Experimental Concept for Investigating the Constitutive Behavior of Particulate Materials in the Spacelab/Space Shuttle Zero-G Environment, Phase I-II Proposal to PACE, advocated by MSFC, September 1979.

Atmospheric Turbulence

Doppler Lidar Field Experiments

Scientists at NASA and a number of outside institutions are studying data obtained with the MSFC Doppler Lidar System. Data obtained during the summer 1981 flight experiments have been provided during 1982 to research at the University of California, Battelle Northwest Laboratories, University of Nevada, Lassen Research, University of Oklahoma, and University of Chicago. These unique data consist of wind fields measured by the airborne lidar in the clear air surrounding severe storms and in a variety of other atmospheric phenomena. Preliminary results indicate that a number of very significant findings will be made as a result of the analysis of these data which are on a scale that has not been heretofore available.

The Doppler Lidar System participated in the Joint Airport Weather Studies (JAWS) field experiment during 1982. Ground-based Doppler measurements of wind were made during this very successful cooperative field experiment sponsored by the National Center for Atmospheric Research and the University of Chicago. The lidar data will be used together with other data to study the physics of cumulus dynamics and to develop aircraft terminal wind shear systems. Together with a group from NOAA/Environmental Research Laboratories, dual Doppler lidar wind measurements were made in the clear air surrounding cumulus storms. These data will complement the radar measurements made at the same time in the precipitous regions and should help in the understanding of thunderstorm gust fronts and turbulent downbursts. Support for the MSFC Lidar System is provided by the NASA Office of Space Science and Applications Severe Storms and Local Weather Research Program. (D. Fitzjarrald/ES82/205-453-3104)

Vortex Dynamics

An effort to study tornado-like flows under the OSSA Severe Storms and Local Weather Program includes numerical simulation of laboratory vortices. Modeling a laboratory simulator (rather than the actual natural phenomenon) has the advantages of laboratory measurements to compare with, in order to validate the code and easily evaluate boundary conditions. In addition, the present interest lies in a mechanically-driven vortex whose morphology depends on certain nondimensional parameters which have been matched to atmospheric conditions. The most relevant parameter is the swirl ratio S which may be thought of as a measure of the imposed circulation relative to the volume flow rate through the convective system. It is proportional to the fluid inflow angle with respect to a radial. As this parameter is varied from zero to unity, the vortex structure changes from a thin laminar votex, to a fully turbulent one with a central downdraft, to a multiple vortex system.

The evolution of the flow which produces a vortex is of much interest. Shortly after start, the meridional circulation develops and the streamlines change very little qualitatively thereafter. The flow enters the domain from the far field, turns up as it approaches the axis, and then flows out of the system. This circulation carries angular momentum into the domain from the far field. Although angular momentum is not completely conserved due to viscous dissipation, the tangential velocity begins to increase rapidly as the fluid flows to smaller radii. During this time, the surface pressure begins to fall. After several seconds of experiment time a concentrated columnar vortex forms on the axis, and a steady flow is achieved.

The tangential velocity near the surface away from the core resembles a potential vortex while the core itself rotates nearly as a solid body (i.e., a Rankine-combined vortex). Far from the axis of the vortex, the tangential velocity is independent of height. When the swirl ratio S increases, the radial position of the velocity maximum (and by definition the core radius) increases. The vertical position is relatively low to the ground where the fluid approaches close to the axis. The height of the velocity maximum also diminishes with increasing swirl so that as the ambient circulation is increased, the location of the velocity maximum gets closer to the ground and increases in magnitude. When the swirl ratio is large, an axial downdraft develops aloft and inside the core of the vortex. This may be interpreted as vortex breakdown where a stagnation point appears on the axis and separates the updraft from the downdraft. As swirl is increased further, the stagnation point descends to the surface and the meridional flow exhibits a two-cell structure-downdraft along the axis to the surface turning upward at the core radius. At higher values of the swirl ratio, the radial extent of the downdraft increases along with the core radius. (F. W. Leslie/ES82/205-453-2047)

B-57B Gust Gradient Program

The objective of the Gust Gradient Program is to obtain detailed data on turbulence in severe environments (e.g., in the vicinity of thunderstorms, which can be used to aid in the design of aircraft and in pilot training). The heart of the program is the B-57B aircraft which has three component velocity probes on each wing tip and on the nose so that variations of turbulent gusts can be measured across the wing (see Figure 10). Four NASA Centers (MSFC, Dryden Flight Research Facility, Langley Research Center, and Ames Research Center) are involved in this program. MSFC's function in the program is data analysis.

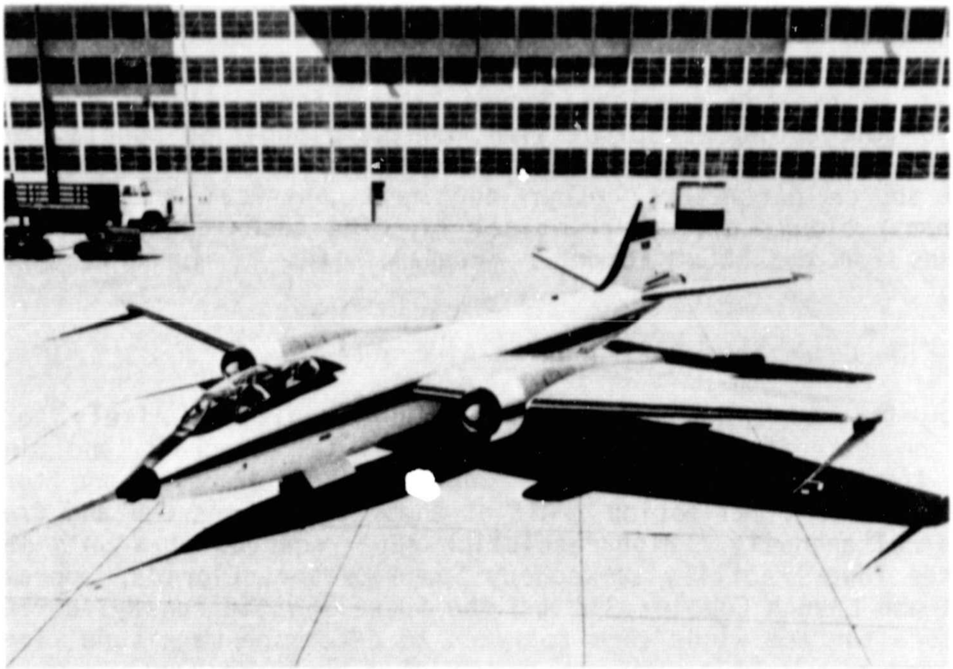

Figure 10. Instrumented B-57B Aircraft.

During July of 1982, the B-57B collected data in the Denver, Colorado area in conjunction with the JAWS (Joint Airport Weather Studies) project. Its flights were supported with three Doppler radars, a network of surface meterorological stations, an aircraft-positioning system, and other data sources. The B-57B's position was indicated on the radar screen so that MSFC personnel could direct the aircraft to areas of severe turbulence. On three days, the B-57B encountered severe turbulence. Weather phenomena observed during the series of tests included tornadoes and funnel clouds,

ORIGINAL PAGE
BLACK AND WHITE PHOTOGRAPH

numerous thunderstorm outflows which pose a serious hazard to aircraft, and hail. Data analysis is in the very early stages, but preliminary results are extremely promising. If early expectations are realized, these data sets could become classical. (W. Campbell/ES82/205-453-1886 and D. Camp/ES82/205-453-2047)

User's Manual for the Rocket Exhaust Effluent Diffusion Model (REEDM)

Marshall Space Flight Center (MSFC) has pursued the development of computerized atmospheric dispersion models for predicting the behavior of rocket exhaust clouds in the troposphere since the mid-1960's. These models are routinely used to assess the environmental impact of exhaust products from rocket engines with respect to air quality standards, toxicity thresholds, and potential bio-ecological effects and to evaluate requirements, if any, for launch constraints. This program revealed the need for the development of a realtime dispersion prediction capability. The results of the program provide measurements for use in verifying the accuracy of the model predictions as well as providing a data base which could be used in making model improvements. These results, including a computer code for using the data, were published and disseminated to various users. This computer code has been used to assess the environmental impact of Space Shuttle operations and to support the first launches of the Space Shuttle. The purpose of this document is to provide complete documentation for: (1) mathematical descruotuib of the atmosphere dispersion models, cloud-rise models, and other mathematical formulas used in the current version of the REEDM code; (2) Vehicle and source parameters, other pertinent physical properties of the rocket exhaust cloud, and meterological layering techniques; and (3) user's instructions for the REEDM computer program. (R. E. Turner/ES84/205-453-4175)

Low-Level Flow Conditions Hazardous to Aircraft

An investigation has been completed on conditions likely to be encountered on takeoff or landing by conventional aircraft and the Space Shuttle. Low-level flow conditions known to be hazardous are turbulence wind shear, and vertical motion. All of these conditions can and frequently do occur simultaneously. High-resolution data recorded at NASA's 150-Meter Ground Winds Tower Facility at Kennedy Space Center, Florida, approximately midway between Launch Complex 39B and the Space Shuttle runway, during high-to-gale-force surface winds were analyzed to determine magnitude, frequency, duration, and simultaneity of occurrence of turbulence (gustiness and gust factor), wind shear (speed and direction), and vertical motion (updrafts and downdrafts), along with temperature inversions. Graphic and tabular presentations of mean and extreme values and simultaneous occurrences are included as a function of tower height, layer, and/or distance for six, 5-second intervals (one interval every 100 seconds) of parameters sampled simultaneously at the rate of 10 speeds, directions, and temperatures per second for approximately a 10-minute period. Two similar analyses during high vertical motions and strong low-level temperature inversions with associated parameters are being made for information, comparison, and flight-simulation purposes. (M. Alexander/D. Camp/ES82/205-453-2087)

Alexander, Margaret B. and Camp, Dennis W.: Significant Events in Low-Level Flow Conditions Hazardous to Aircraft, NASA TM (proposed).

Shuttle Gust Model

The Atmospheric Sciences Division of MSFC is responsible for developing atmospheric models to be used to evaluate the Space Shuttle ascent loads and performance. To fulfill this purpose, a 5-parameter bivariate gamma probability distribution was developed to provide the joint statistical relationship between gust length and gust magnitude in a discrete vector wind gust model. This 5-parameter distribution, having two-shape parameters, two-scale parameters, and a correlation parameter, reduces to the well-known 4-parameter distribution where the shape parameters are equal. Properties of this distribution are given in Smith et al. (1982). This distribution has other applications in reliability theory, signal-to-noise ratio (radar tracking error analysis), and vibration mechanics. (O. E. Smith/ES81/205-453-3101)

Smith, O. E. and Austin, L. D.: NASA Technical paper 1988, entitled Sensitivity Analysis of the Space Shuttle to Ascent Wind Profiles, 1982.

Smith, O. E., Adelfang, S. I. and Tubbs, J. O.: NASA TM-82483, entitled A Bivariate Gamma Probability Distribution with Application to Gust Modeling, 1982.

MAGNETOSPHERIC PHYSICS

Magnetospheric Plasma Characteristics

Magnetospheric low-energy plasma study is a dominant part of the MSFC space plasma physics activities. During this period, data were collected and analyzed from two different spacecraft, the International Sun-Earth Explorer (ISEE) satellite, and the Dynamics Explorer-1 (DE-1) satellite. In addition, data are currently being analyzed from the Spacecraft Charging at High Altitudes (SCATHA) satellite. A great number of fundamental discoveries concerning the origin and energization of this low energy component have been made during the past year. In addition, the success of the DE spacecraft has provided a wealth of new information on the interchange of ionization between the magnetosphere and ionosphere.

Retarding Ion Mass Spectrometer

Instrument development activities supported by SRT funds over the past several years were important precursers to the successful design and development of the Retarding Ion Mass Spectrometer (RIMS) instrument which was flown on the DE-1 spacecraft. Launched in August 1981, the instrument was put into a fully operational status in early October. The instrument has functioned well throughout the mission and has returned exciting new information on the composition and dynamics of low energy (0 - 50 eV) ions in the Earth's ionosphere and magnetosphere. The unique orbit of the DE-1 spacecraft permits the sampling of the ion distribution along the magnetic field lines for the first time.

The DE-1 RIMS data have revealed two significant discoveries so far in the mission. In one of the early orbits, the RIMS instrument made the first measurements of the polar wind, a flow of ionization from the ionosphere out into the magnetosphere which was theoretically predicted more than 14 years ago (Figure 11). The unique capabilities of the mass spectrometer on the spinning spacecraft, combined with a method of biasing the instrument aperture to offset the effects of a positive spacecraft potential, made this measurement possible. A second major discovery involved the first measurements of nitrogen ions at high altitudes in the magnetosphere (Figure 12). The N^+ ions were found to be streaming out of the Earth's polar regions

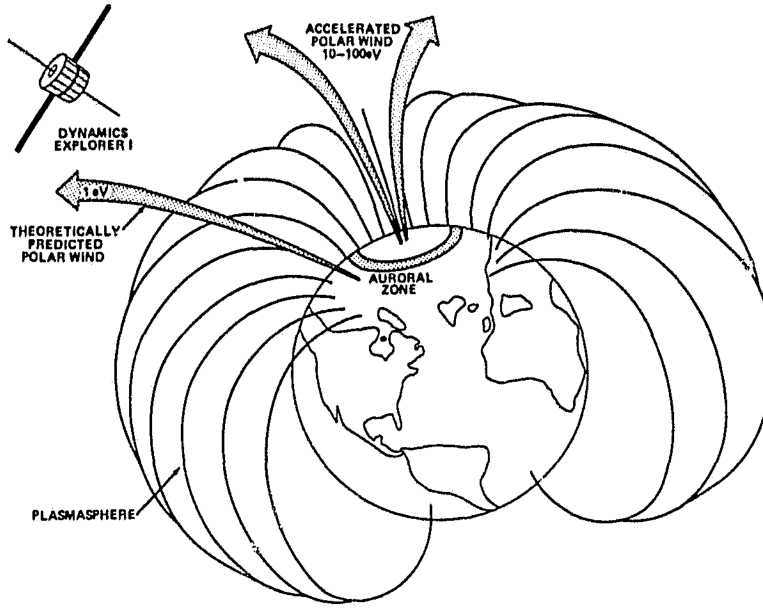

Figure 11. Illustration of the Theoretically Predicted Polar Wind Streaming up the Earth's Magnetic Field Lines.

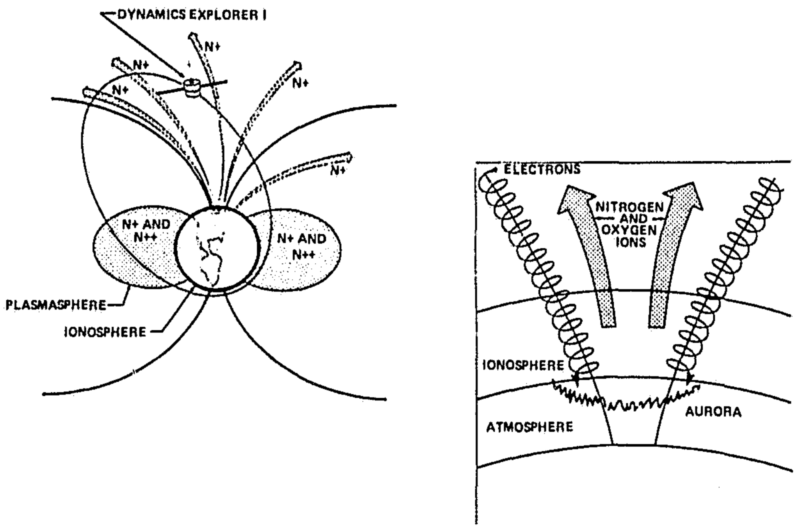

Figure 12. Location of N^+ and N^{++} Ions Along the DE-1 Orbit.

while N^{++} ions were found to be accumulating in the torroidal-shaped plasmasphere which surrounds the middle-latitudes of the Earth out to altitudes of 5 Earth radii. This latter discovery was made possible by the unique capability of the RIMS instrument to separate the N^+ ions from the more prevelent O^+ ions found throughout the magnetosphere.

The RIMS instrument was developed by MSFC in concert with scientists at the University of Texas at Dallas (UTD), and the results are being analyzed cooperatively by scientists from MSFC and five universities, UTD, Stanford, University of Michigan, Utah State University, and the University of Alabama in Huntsville. (Charles R. Chappell/ES51/205-453-3036)

Chappell, C. R., Fields, S. A., Baugher, C. R., Hoffman, J. H., Hanson, W. B., Wright, W. W., Hammack, H. D., Carignan, G. R., and Nagy, A. F.: The Retarding Ion Mass Spectrometer on Dynamics Explorer-A. NASA TM-82418, April 1981.

Chappell, C. R., Fields, S. A., Baugher, C. R., Hoffman, J. H., Hanson, W. B., Wright, W. W., and Hammack, H. D.: The Retarding Ion Mass Spectrometer on Dynamics Explorer-A. Space Science Instrum., 5 (4), 477 1981.

Chappell, C. R.: Cold Plasma Distribution Above a Few Thousand Kilometers in the Auroral Zone. To appear in High Latitude Space Plasma Physics, Proceedings of Nobel Symposium 54, Kiruna, Sweden, March 23-25, 1982.

Fields, S. A., Baugher, C. R., Chappell, C. R., Reasoner, D. L., Hammack, H. D., Wright, W. W., and Hoffman, J. H.: Instrument Manual for the Retarding Ion Mass Spectrometer on Dynamics Explorer-1. NASA TM-82484, May 1982.

Chappell, C. R.: Initial Observations of Thermal Plasma Composition and Energetics from Dynamics Explorer-1. Geophys. Res. Lett., September 1982.

Chappell, C. R., Green, J. L., Johnson, J. F. E., and Waite, J. H., Jr.: Pitch Angle Variations in Magnetospheric Thermal Plasma--Initial Observations from Dynamic Explorer-1. Geophys. Res. Lett., September 1982.

Chappell, C. R., Olsen, R. C., Green, J. L., Johnson, J. F. E., and Waite, J. H., Jr.: The Discovery of Nitrogen Ions in the Earth's Magnetosphere. Geophys. Res. Lett., September 1982.

Light Ion Mass Spectrometer

Analysis of data from the Light Ion Mass Spectrometer (LIMS) on the SCATHA satellite has continued. A characterization of the plasma characteristics in the plasmasphere and plasmatrough regions in terms of density, temperature, mass composition, and flow velocity has been made. With these analyses, it was possible to distinguish among the cold, plasmaspheric plasma and other plasma populations. Figure 13 shows the spatial distribution of the different populations on each day. The most significant result of the analyses was that the plasma through region outside of the plasmasphere was populated by warm plasma distributions with temperatures ranging from 5 to 15 electron volts and a He+/H+ ratio significantly less than that seen in the plasmasphere. These data explain a contradiction in earlier measurements of the average plasmasphere boundary, and as well indicate the presence of mechanisms acting to produce energization of ionospheric ions to populate the outer magnetosphere. The analysis of these data contributes not only to our knowledge of low-energy plasma dynamics in near Earthspace but also to our understanding of the interactions of spacecraft with their surrounding plasma environment. (D. Reasoner/ES53/205-453-3037)

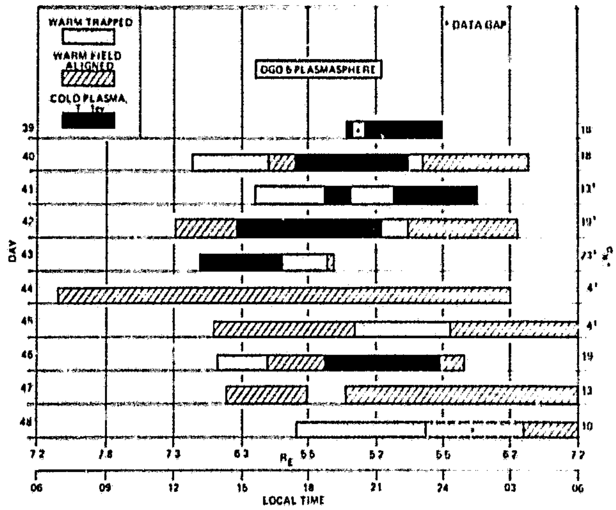

Figure 13. Distribution in Local Time of the Different Types of Plasma Populations Seen with the LIMS on Scatha.

Reasoner, D. L., Chappell, C. R., Fields, S. A., and Lewter, W. J.: Light Ion Mass Spectrometer for Space-Plasma Investigations. Rev. Sci. Instrum., 53 (4), 1982.

Reasoner, D. L., Craven, P. D., and Chappell, C. R.: Characteristics of Low Energy Plasma in the Plasmasphere and Plasma Trough. (to be published)

MSFC/NASA NEEDS Network

The MSFC/NEEDS network is designed around the construction of the DBMS (data-based management system) here at MSFC. The DBMS is a part of the NEEDS (NASA end-to-end data system) program. This program is developing concepts and demonstrating technology over the next 5 years that will significantly reduce the time it takes for acquired spacecraft data to reach the experimenter. The part that DBMS plays is to store multiple data bases at a central site in a large archival memory. The MSFC/NEEDS network links several remote users to the DBMS computers here at MSFC. Presently the network is configured so that there are five 'remote' (not at the central site) nodes in the network, the University of Texas at Dallas, Utah State University, Stanford University, the University of Iowa, and Space Science Laboratory at MSFC. Each of the remote nodes has a direct line into the DBMS.

There are several capabilities and features that the MSFC/NEEDS network is developing, making it unique within the space science community. The NEEDS network provides remote nodes with access to growing space science data bases and brings scientists throughout the country more closely together in a common working computer environment. Unlike the Dynamics Explorer network, where the remote sites have only terminals (supporting one person at the remote site at a time), the MSFC/NEEDS network will support many users simultaneously at each remote node. These users can participate at their institutions in a number of network functions involving the central NEEDS computer facilities and other remote computer facilities. Data files and graphics files can be transferred to and from the NEEDS DBMS and other remote facilities. Program execution can be accomplished at any of the network nodes, even though it has been initiated from a different node. The DBMS facility has a growing library of analysis software that can be transferred to remote nodes or executed at a central site. For example, the user at a remote site can initiate a library program at the central site which reads and analyzes data out of the archival mass memory (AMM) and then have the results transferred to his node. At this stage of development, an interim AMM is being used which employs simple disk storage. All of the nodes have the capability for message routing, enabling remote users to communicate with each other as if a direct phone line existed between them, even though they may not be "adjacent" nodes. Since the network has become operational, several papers have been written which without the NEEDS network facility would have been extremely difficult or impossible. The most important feature of this network is remote user data access which is clearly demonstrated during workshop periods. A workshop period enables physicists to solve a science problem by interactive analysis utilizing computing capabilities already resident at the scientist's institution as well as the DBMS facilities. All users have access to the entire data set before, during, and after the workshops. This enables everyone to become familiar with the data sets and to learn how to use the network before the workshop. The workshop activities can also continue long after the initial meeting, thus permitting the maturing of scientific ideas. The first workshop was held at MSFC on August 19-20, 1982, with others planned for FY83. A NASA technical manual on this first workshop is currently in preparation. The MSFC/NEEDS network is in its infancy but is having a major effect on NASA's data systems of the future. The network and the Data Systems Users Working Group brings to NASA and the user community needed technology increasing the capabilities of today's scientists. (J. L. Green/ES53/205-453-0028)

Greenstadt, E. W. and Green, J. L.: Data Systems Users Working Group. EOS, 62, No. 6, 50, 1981.

Chappell, C. R.: Initial Observations of Thermal Plasma Composition and Energetics from Dynamics Explorer-1. Geophys. Res. Lett., September 1982.

Chappell, C. R., Green, J. L., Johnson, J. F. E., and Waite, J. H., Jr.: Pitch Angle Variations in Magnetospheric Thermal Plasma--Initial Observations from Dynamics Explorer-1. Geophys. Res. Lett., September 1982.

Chappell, C. R.: Cold Plasma Distribution above a Few Thousand Kilometers in the Auroral Zone. To appear in Hight Latitude Space Plasma Physics, Proceedings of Nobel Symposiun 54, Kiruna, Sweden, March 23-25, 1982.

Chappell, C. R., Olsen, R. C., Green, J. L., Johnson, J. F. E., and Waite, J. H., Jr.: The Discovery of Nitrogen Ions in the Earth's Magnetosphere. Geophys. Res. Lett., September 1982.

Sojka J. J. and Schunk, R. W.: Analysis and Interpretation Techniques For the RIMS Experiment on DE-A. Internal report Utah State University, May 1982.

The low-energy thermal plasma environment in the Earth's magnetosphere was, at first, believed to be completely Maxwellian in distribution having ionospheric temperatures. The low-energy composition measurements from the DE, ISEE, and SCATHA spacecraft have revealed field-aligned, trapped, and conic pitch-angle anisotropies seen with temperatures two orders of magnitude and more above that of ionospheric plasma. Due to the multiplicity of angular anisotropies, new methods must be developed to obtain reliable temperature and density information.

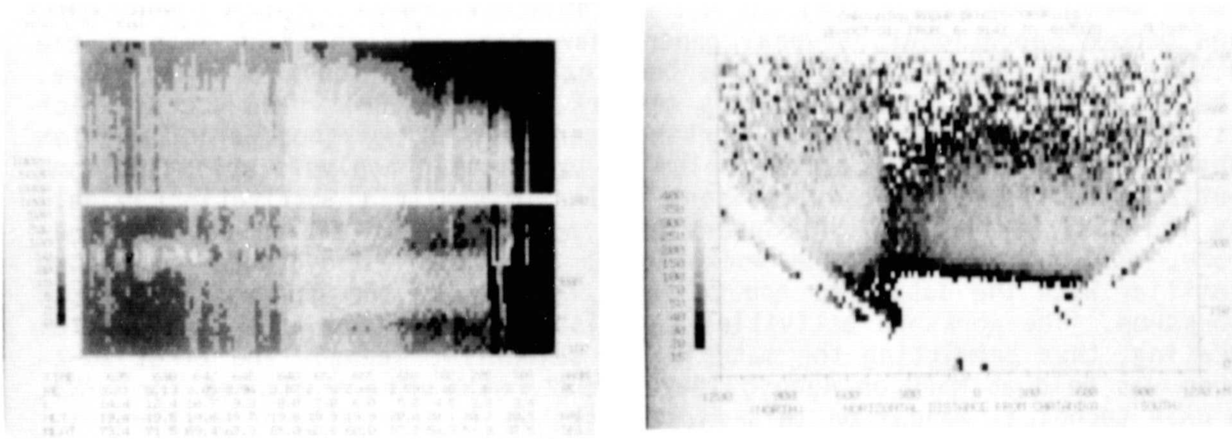

Figure 14. Near Simultaneous Observations of Low-Energy Hydrogen from the DE-1 RIMS and the ground-based Chatanika Radar.

Original multidimensional graphic techniques have been developed to aid the study of low-energy plasma. Several types of spectrograms and three-dimensional contour routines have been developed which are now being applied to data from SCATHA. These routines are of general applicability and are also being used for analysis of DE and ground-based Chatanika radar data. Figure 14 illustrates an extremely quick (in terms of computer and plotting time) spectrogram method used to examine the details of low-energy plasma in the ionosphere and magnetosphere as measured by the Chatanika radar and DE-1. The left panel shows near-simultaneous measurements of the low-energy ionospheric plasma being transported out into the magnetosphere as measured by the DE-1 RIMS experiment as it passed over the Chatanika radar site. The ionospheric signatures of density are seen in the right panel. Basically, the spectrogram technique usually done in color is being used to accentuate the extreme differences that are often found in the distribution of ionospheric and magnetospheric low-energy plasmas. The activities will facilitate the unveiling of the low-energy plasma characteristics interactively. In addition these displays are available for comparison with other experimental and theoretical data sets which reside at other institutions through the NEEDS network. They will enable remote users in the MSFC/NEEDS network to transfer the device-independent plot files to their remote site and convert these files into files displayed on their own graphics devices. These device independent graphics techniques are a key element in conducting future data analysis workshops in which many of the participants are at a remote location. Knowledge gained from these developments can be applied to programs such as DE and Origins of Plasmas in the Earth's Neighborhood in which data sharing between investigators is required. (J. L. Green/ES53/205-453-0028)

Spacecraft-Plasma Interactions

The interactions between a spacecraft and its environment, particularly the plasma population, affect spacecraft systems and plasma measurements, and can cause spacecraft failures. This interaction is best studied with plasma data. The twofold problem, therefore, is to determine the effects of such interactions on the plasma measurements and then use these measurements to study the spacecraft surface potentials, space-charge, sheath, and plasma currents. Important physical processes vary with altitude. Deep in the plasmasphere, high ambient electron fluxes control the spacecraft potential, and thin sheath approximations are valid. As a spacecraft moves outwards from Earth, the photoelectric current due to sunlight gradually becomes the most important term in the balance of ambient particle fluxes, secondary electron fluxes, and photoelectron fluxes. As the spacecraft approaches the plasma sheet (R > 4 RE), it becomes positive, and thicksheath approximations become appropriate. Electrostatic fields become important, particularly as they vary over spacecraft surfaces. Control of such potentials becomes especially important for spacecraft with insulating surfaces, since shadowed insulators can charge hundreds to thousands of volts negative with respect to the spacecraft mainframe. This control is best achieved by plasma emission. Data from five satellites have been studied, and the NASA Charging Analyzer Program (NASCAP) charging model has been installed at MSFC. Data from Applied Technology Satellites -5 and -6 (ATS-5 and -6) on active charge control experiments were analyzed in previous years, and published during this year (Olsen, 1981a & b). These data showed that Plasma emission was an effective method of controlling mainframe and differential charging. This method is currently being advocated for the OPEN mission to enhance particle and field measurements in the magnetosphere. Plasma emission for charge control remains important for spacecraft survival, as recently demonstrated by the problems of a European geosynchronous satellite (Knott, private communication).

Two other projects based on the ATS data set are nearly completed. A paper on a "threshold effect" for spacecraft charging is under review. This work deals with a critical plasma energy required for the charging of spacecraft in eclipse, and is important for the development of instruments designed to monitor the magnetosphere with the objective of spacecraft safety. A second area of work is in the dynamics of the charging process. The difference in charging time scales observed on ATS-5 and ATS-6 in sunlight and eclipse provide an important cornerstone in the development of an understanding of the physical processes involved in spacecraft charging. Comparison of the ATS data with the results from the NASCAP code show that in sunlight the major criterion for spacecraft charging is the existence of shadowed insulating surfaces. Data from the Plasma Composition Experiment (PCE) on ISEE are taken in a retarding potential analyzer mode near and inside the plasmasphere. Analysis of such data for basic plasma paramaters such as density, temperature, and flow direction requires some method for dealing with sheath effects on ion trajectories. An approximate solution to the thin-sheath problem has been developed for use in the analysis of ISEE PCE data (Comfort, et al., 1982). This method is being extended for use in other magnetospheric regions; i.e., the plasma sheet, and for data taken from a detector that is not looking into the ram direction. This will be useful not only for interpreting ISEE data, but also for RPA data from the RIMS, on the DE satellite.

The electrostatic analyzers (ESA) on the SCATHA satellite are well suited for the study of thermal plasma and the variations in the plasma measurements with spacecraft potential. A study of "Hidden Ions" was published based on SCATHA and ATS-6 data in sunlight and eclipse (Olsen, 1982a). This work showed that there is a low-energy ion population near the outer boundary of the plasmasphere that is normally hidden from the ESA by a substantial positive potential; i.e., 5 to 10 V. When the spacecraft is eclipsed, however, the low energy ion population becomes visible to the ESA. This effect was utilized in a study of field-aligned ions using the ATS-6 data set (Olsen, 1982b). Measurements of the "Hidden Ion" population in the magnetosphere as noted above are important, and suggest the need for more active methods of controlling instrument potentials. One method developed for this is to put the instrument package on a boom, and bias the package with respect to the spacecraft mainframe. The S-302 experiment on Geodetic Earth-Orbiting Satellite utilized this method. A study is underway to compare data from the SCATHA and GEOS satellites to determine the usefulness of this method. Data taken by SCATHA when that spacecraft is eclipsed can be compared to GEOS data during a few (fortuitous) conjunctions. Preliminary results show that the method is useful near the outer edge of the plasmasphere.

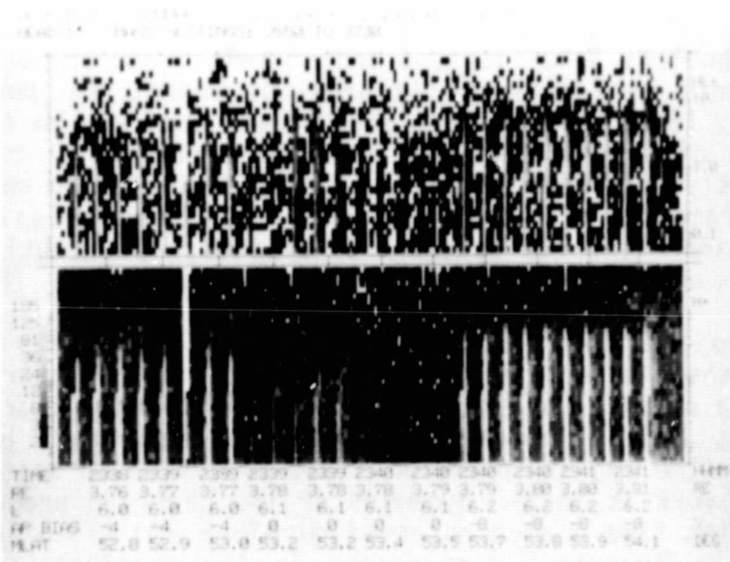

Figure 15. This Energy-Time Spectrograph from the RIMS Shows the H and He Flux of the Polar Wind.

The RIMS on the DE satellite has been in operation for only a year, but has already provided a number of impressive discoveries. The instrument includes the capability of biasing an external aperture plane negatively with respect to the spacecraft. The first operation of the instrument in that mode provided the first measurements of the polar wind at high altitudes. The spacecraft potential normally prevented the measurement of this low-energy population, but the biasing technique brought these field-aligned flows into view (Olsen, et al., 1982; Chappell, et al., 1982). These data are shown in Figure 15, an energy time spectrogram for 3 minutes of data. Preliminary analysis of aperture bias data in equatorial regions, near the plasmapause, show that the "Hidden Ion" population of the ATS and SCATHA satellites is normally visible on DE, at least in the ram detector, because the instrument goes down to zero energy, and is not co-rotating with the plasma as the geosynchronous satellites were. There are still interesting variations in the plasma measurements when the spacecraft is eclipsed, however, even when the shift in potential is small.

The NASCAP was installed on the MSFC UNIVAC 1108 during the last fiscal year. This program is useful for prediction of charging effects, but our current use is to study the effects of variations in spacecraft potentials on the sheath around various spacecraft and the resulting effects on particle detectors. Preliminary results from models of the DE aperture bias experiments and comparison with the polar wind data show that there is an electrostatic barrier in front of the aperture, and that the aperture bias voltage must be large compared to the mainframe potential (Olsen, et al., 1982). (C. Olsen/ES53/205-453-0505)

Chappell, C. R., Green, J. L., Johnson, J.F.E., and Waite, J. H., Jr.: Pitch Angle Variations in Magnetospheric Thermal Plasma -- Initial Observations from Dynamics Explorer-1. Geophys. Res. Lett., September 1982.

Comfort, R. H., Baugher, C. R., and Chappell, C. R.: Use of the thin sheath Approximation for Obtaining Ion Temperatures from the ISEE 1 Limited Aperture RPA. J. Geophys. Res., 87, 5109-5123, 1982.

Olsen, R. C.: Modification of Spacecraft Potentials by Thermal Electron Emission on ATS-5. J. Spacecraft and Rockets, 18, 1981.

Olsen, R. C.: Modification of Spacecraft Potentials by Plasma Emission. J. Spacecraft and Rockets, 18, 462-469, 1981.

Olsen, R. C.: The Hidden Ion Population of the Magnetosphere. J. Geophys. Res., 87, 3481-3488, 1982.

Olsen, R. C.: Field-Aligned Ion Streams in the Earth's Midnight Region. J. Geophys. Res., 87, 2301-2310, 1982.

Olsen, R. C., Comfort, R. H., Chappell, C. R., Waite, J. H., Jr., Johnson, J.F.E., and Shawhan, S. D.: Dynamics Explorer Low-Energy Plasma Observations Using a Variable Aperture Bias. Presented at the 1982 Spring Meeting of the American Geophysical Union.

Body-Plasma Electrodynamic Interaction Studies

The investigation of the electrodynamic interaction of a flowing, rarefied plasma with test bodies in the laboratory is an ongoing effort which continues to contribute to our understanding of this basic physical problem and its applications to spacecraft-space plasma electrodynamic interactions. This has application to the resulting environment of diagnostic instruments, as well as natural body-plasma electrodynamic interactions occurring in the solar system. The laboratory results have proven to be useful in analyzing in situ data, particularly in a recent new look at data from the Ariel 1 and Explorer 31 satellites (Stone and Samir, 1981). In addition, this ground-based effort points the way toward orbital experiments which make use of the same experimental techniques and instrumentation developed for the laboratory to simulate solar system body-plasma interactions such as the interaction caused by the moon Io moving within the Jovian magnetosphere. The dimensionless scaling parameters indicate that the ionosphere provides a similarity to the Jovian environment which makes possible a relatively inexpensive and timely method of investigating such solar system plasma phenomena. This should permit a greater scientific return from subsequent planetary missions (Stone and Samir, 1981; Stone, Samir, and Wright, 1982).

The direction of the laboratory effort in the past year has been to extend the study to include two species plasma flows in order to more accurately simulate the multiconstituent ionospheric plasma. This will permit investigation of the interaction between combinations of heavy and light ions in the presence of strong density and potential gradients. It is thought that this interaction may generate instabilities and oscillations in the wakes of ionospheric satellites. This capability will also provide a more characteristic environment for flight instrument testing and calibration.

A dual ion plasma accelerator has been developed for this purpose that allows the generation of two completely independent streams of ions which are then superimposed and neutralized to form a single binary plasma stream. This permits the selection of different masses, drift energies, and densities for each species of the stream.

The Differential Ion Flux Probe (DIFP), which was previously developed to provide differential vector measurements of ion flow direction, density, and energy, has been successfully flown on the Shuttle STS-3 mission as part of the Plasma Diagnostic Package experiment, and on two Project Centaur Multiple Auroral Probe sounding rocket missions. Initial results have shown how the ionospheric environment is perturbed by the motion of the Shuttle and have given new insights into plasma flow phenomena around large target bodies.

Stone, N. H. and Samir, U.: Adv. Space Res., 1, 361, 1981.

Stone, N. H., Samir, U., and Wright, K. H., Jr.: 1982 Proc. Int. Conf. on Plasma Phys., Gothenburg, Sweden, June 9-15, 1982, p. 13.

Particle Acceleration Mechanisms in the auroral Zone

In December of 1981, two DIFP instruments were provided for the Multiple Auroral Probe (MAP-1 and MAP-2) sounding rocket payloads. The two instruments mounted on the Centaur I payload are shown in Figure 16. This campaign was designed to investigate charged particle acceleration mechanisms in the polar cleft region of the Earth's magnetosphere, with the motion of the thermal ions being provided by the DIFP. Data analysis is still in progress, however, the preliminary results show a strong azimuthal assymetry (around the field lines) of the thermal ion motion with an upward drift within the cleft. As the rocket emerged from the cleft and passed into the polar cap region, the vertical component of the ion motion changed directions and became directed Earthward.

In addition to geophysical effects, it appears that the data set will provide a significant insight into spacecraft charging effects in the polar region of the magnetosphere. (N. Stone/ES53-205-453-0029)

Retarding Potential Analyzer/Differential Ion Flux Probe

The Retarding Potential Analyzer/Differential Ion Flux Probe (RPA/DIFP) was successfully flown on the University of Iowa Plasma Diagnostics Package on the STS-3 mission. The primary scientific objective of the instrument was to study the plasma environment around the Shuttle Orbiter with particular emphasis upon perturbations to the plasma environment produced by the

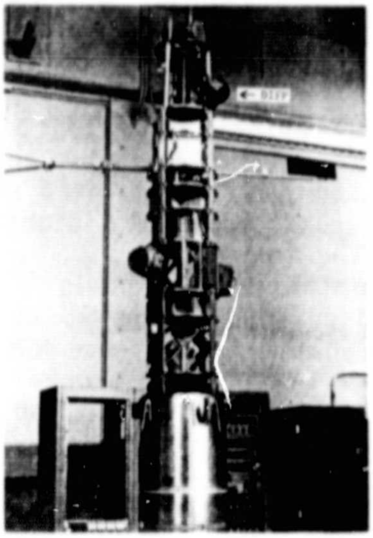

Figure 16. One of two DIFP Instruments on the Centaur Multiple Auroral Probe Sounding Rocket Payload.

Orbiter wake and sheath effects and by electron beam emissions from an onboard electron gun. The instrument performed perfectly in all respects, and approximately 64 hours of flight data were received. Although the data analysis is preliminary at this writing, the data show that the Orbiter produces significant perturbations to the local plasma, with local plasma densities significantly above ambient levels. These are apparently produced by photoionization of outgassing products from the Orbiter. Analysis of directional ion flow data has revealed the presence of multiple ion streams due to the interaction between the Orbiter and the relative plasma flow. (N. Stone and D. Reasoner/ES53/205-453-0029)

Optical Observations of Magnetosphere/Atmosphere Coupling

An instrument development effort has been oriented toward the design of spacecraft instrumention for the imaging of faint source emissions that originate in our magnetospheric environment from natural and artificial stimuli. The imager will have a large dynamic range for high contrast scenes such as those produced by auroral beams. Near UV, visible, and near IR wavelength regimes all have emission features of scientific interest. Solid-state detector arrays (CCD's, CID's, and diodes) have matured over the past few years and are available from several manufacturers. Several devices with spatial resolution > 256 square are available. The main disadvantages of these devices include high dark counts, small formats (typically 7 to 10 mm/array), low gain, and "thermal" accommodation. Their advantages include low power, ruggedness, linear response, low mass, and linear fields.

In the auroral imager development, a CID array with 256x256 pixels has been optically coupled through a fiber optic plug to a 25-mm, two-stage intensifier with 106 gain. This system has been assembled in a test configuration and has demonstrated good optical resolution being maintained from the intensifier through the array itself. This breadboard system is now to the point where it can be packaged and controlled for use as a field useable system. The field system must be rugged, cooled, pointed, and integration controlled to expose varying luminosities of aurora and airglow phenomena.

It was learned from Shuttle-spacecraft applications that it is relatively simple to articulate a small mass. Experience has also shown that it is difficult to cool a pointing system. Optical pipes which carry an image several feet are available which allow one to separate the detection part of the instru- ment from the optical gathering part. A fibre pipe of 4 ft. with a 25-mm rectangular format has been tested for this system and will be used to isolate the detector from the pointed optics. The pipe is flexible and may be articulated freely. The fibre pipes have good transmission from 3800 Angstroms well into the infrared.

Control of the image taking process is simplified in the CID in that the image can be observed or read out as it is being exposed. The control system then can be made dynamic to preserve intensity measurement for varying source brightness (such as found in aurora) by dynamically varying integration time by simply monitoring the buildup with a microprocessor. We have found many attributes in solid-state imaging which can be readily incorporated in the reflight of the Atmospheric Emissions Photometric Imager experiment being flown on Spacelab 1. These concepts permit the design of a low-cost imager with a large articulation freedom in the confined environment found on spacecraft. The devices will be rugged, energy efficient, and environmentally suitable for space physics applications. (G. Swenson/ES53/ 205-453-3040)

SOLAR PHYSICS

Energy and matter stream continuously outward from the Sun. The Study of the generation, the propagation, and the effects (upon the Earth and other planets) of these flows is properly the subject of solar-terrestrial physics. Studies in solar physics, attempting to learn about the Sun itself, blend into solar-terrestrial investigations and increase our understanding of how processes on and in the Sun generate and modulate its outflows. Solar research at Marshall Space Flight Center has continued to explore basic problems related to solar atmospheric structure and activity, as outlined in the following pages.

Solar Maximum Mission (SMM)

The SMM, prematurely interrupted in late 1980 by the loss of the satellite's accurate pointing control, is being considered for repair, refurbishment of instruments, and redeployment. Meantime, analyses of the data obtained during its first active phase continue at Marshall and elsewhere. The international Solar Maximum Year (SMY) program of coordinated observation and analysis has become a Solar Maximum Analysis (SMA) program, with gatherings and workshops planned in conjunction with international meetings of other organizations; in the United States, a series of three SMM workshops is planned for 1983 to foster collaborative investigations of events observed by the SMM experimenters and by ground-based observers. Our data analyses emphasize the observations obtained with MSFC's ground-based vector magnetograph, and with the Ultraviolet Spectrometer and Polarimeter (UVSP) and Coronagraph/Polarimeter (C/P) instruments aboard the SMM.

Analyses continued using the data obtained by the Ultraviolet Spectrometer and Polarimeter (UVSP) instrument on the SMM spacecraft. One example is a study of oscillations in and other properties of the transition region (between the chromosphere and corona) in active regions, particularly above sunspots. The oscillations with periods of 120 to 180 sec occur only over the sunspot umbra, which is also the location of the strongest magnetic fields in the transition region as well as in the photosphere. An example of the time variation of the velocity, intensity, and longitudinal magnetic field for a pixel in the umbra is shown in Figure 17; the velocity oscillations are superimposed on a larger variation due to the orbital motion of the SMM spacecraft. The oscillations are also evident in the intensity signal, though not as strongly as in the velocity. No periodic fluctuations are visible in the magnetic field although the noise is high so that the upper limit is comparable to the mean value which is statistically signficant. The width of the C IV line at 1548 A, formed in the transition region, is narrowest over the umbra. However, the line intensity is not at a minimum over the umbra as might have been expected; rather, it is at an intermediate level. Both strong upward and downward flow velocities are seen over the umbra. On a larger scale, the flow velocities (primarily horizontal because they were observed near the solar limb) in the transition region are correlated with the magnetic field structure in that the flow seems to change direction at the same locations that the magnetic field polarity changes sign. In other words, the flow on both sides of a magnetically neutral line seems to be toward or away from that line. This work was done in conjunction with colleagues at Teledyne Brown Engineering, Huntsville, Alabama, and the High Altitude Observatory, Boulder, Colorado.

UVSP observations for the transition region (O V, 1354 A) and corona (Fe XXI, 1371 A) were compared with other SMM data and with radio observations from Itapetinga, Brazil. The transition region line, hard X-rays, and radio emission all show very spiky burst-like structure while the coronal line and soft X-rays show a rapid increase followed by an extended peak and a slow decrease. Apparently, the flare suddenly releases energetic particles which produce the hard X-rays and radio bursts and impact on the transition region to produce the O V emission. The Fe XXI emission and soft X-rays come from the extended heating of the corona. This work was in collaboration with colleagues at the Goddard Space Flight Center, Greenbelt, Maryland, and the Instituteo National de Pesquisas Espaciais, Brazil. (E. Tandberg-Hanssen/ES01/205-453-0027)

Henze, W., et al.: SMM/UVSP Observations of the Distribution of Transition Region Oscillations and Other Properties in a Sunspot. Solar Phys. (to be submitted)

Gurman, J. B., Leibacher, J. W., Shine, R. A., Woodgate, B. E., and Henze, W.: Transition Region Oscillations in Sunspots. Astrophys. J., 253 939, 1982.

Henze, W., et al: Observations of the Longitudinal Magnetic Field in the Transition Region and Photosphere of a Sunspot. Solar Phys. (accepted)

Athay, R. G., Gurman, J. B., Henze, W., and Shine, R. A.: Fluid Motions in the Solar Chromosphere-Corona Transition Region. II. Active Region Flows in C IV from Narrow Slit Dopplergrams. Astrophys. J. (submitted)

Poland, A. I., et al: The Impulsive and Gradual Phases of a Solar Limb Flare as Observed from the Solar Maximum Mission Satellite. Solar Phys., 78, 201, 1982.

Tandberg-Hanssen, E., Kaufmann, P., Reichmann, E. J., Teuber, D. L., Moore, R., Zirin, H., and Orwig, L.: Time Series of Radio, UV, Soft, and Hard X-Ray Data from Flare of November 1, 1980. (in preparation)

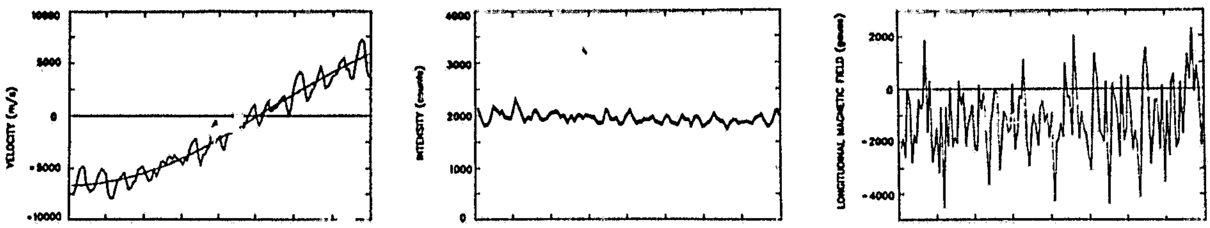

Figure 17. USVP Observations Using the C IV Line at 1548 A Formed in the Transition Region in Active Region 2744 on Oct. 23, 1980. (Each plot contains 135 data points covering an interval of 35 min.)

Solar Magnetic Fields

The FY82 activities of the MSFC Solar Magnetograph program were divided between continued data analyses related to SMM investigations, and extensive modifications to the MSFC magnetograph system to upgrade its performance capabilities.

A primary effort in data analysis has been the determination of vertical gradients in a sunspot's magnetic field using observations of the photospheric vector field obtained with the MSFC magnetograph together with the line-of-sight field component in the transition region as measured with the UVSP instrument onboard the SMM satellite. A theoretical potential field model was developed from MSFC observations in order to derive the variation with height of the sunspot field; representative results are shown in Figure 18. Vertical field gradients were calculated from the divergence-free condition for magnetic fields using the observed photospheric vector field. From these analyses, it was concluded that umbral fields decrease more slowly with height then previously thought and the transition-region fields occur at heights of 4000 to 6000 km above the photosphere.

One phase of an extensive research program to study magneto-optical effects as they influence vector magnetograph measurements was completed. This study demonstrated the presence of Faraday rotation in measurements of transverse magnetic field orientations in sunspot umbrae and indicated observational techniques which can be used to minimize these effects.

In collaboration with colleagues at the University of Alabama in Huntsville, calculations of magnetic-energy buildup were performed using a self-consistent MHD model of a sheared magnetic loop. The vector magnetic field and shearing motions of the loop were derived from observations taken at the MSFC Solar Observatory. The model produced magnetic-energy rates of growth comparable to energy-release rates seen in solar flares at the MSFC

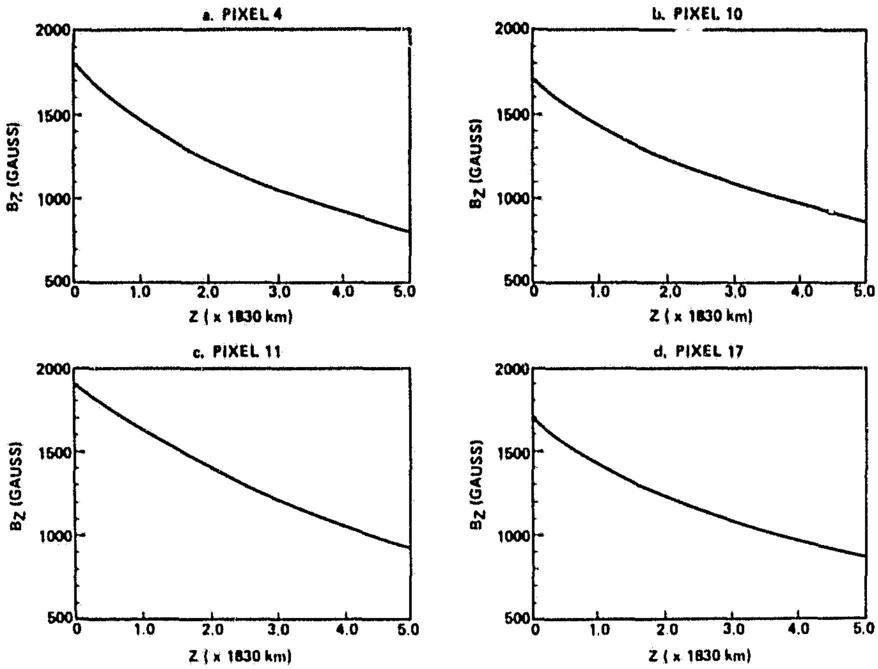

Figure 18. Variation of the Line-of-Sight Component of the Potential Magnetic Field with Distance Along the Line-of-Sight for Four Different Areas (Pixels) in a Sunspot.

Solar Observatory. The model produced magnetic-energy rates of growth comparable to energy-release rates observed in solar flares. This work was performed under RTOP 188-38-52, Office of Space Science and Applications, Dr. J. D. Bohlin.

At the invitation of IAU Commission 10, a review paper on studies of solar magnetic fields during the SMY was prepared and presented at a special SMY session during the IAU General Assembly in Patras, Greece.

In the upgrading program to increase the speed and sensitivity of the MSFC magnetograph system, a new CCD camera and electronic control system consisting of a high-speed adder and memory have been interfaced with a PDP 11/23 computer and 154-megabyte fixed disk. A new polarimeter package has also been designed and fabricated. Interfacing of the polarimeter, CCD camera, and remaining components of the magnetograph with the computer-controlled system is now in progress. (M. Hagyard/ES52/205-453-0118)

Patty, S. R.: Analyses of the Vector Magnetic Fields of Complex Sunspots. In The Physics of Sunspots, Lawrence E. Cram and John H. Thomas (eds.), Sacramento Peak Observatory, 1981, pp. 64-74.

Hagyard, M. J., West, E. A., Tandberg-Hanssen, E., Smith, J. E., Henze, Jr., W., Beckers, J. M., Bruner, E. C., Hyder, C. L., Gurman, J. B., Shine, R. A., and Woodgate, B. E.: The Photospheric Vector Magnetic Field of a Sunspot and Its Vertical Gradient. In The Physics of Sunspots, Lawrence E. Cram and John H. Thomas (eds.), Sacramento Peak Observatory, 1981, pp. 213-234.

Krall, K. R., Smith, Jr., J. B., Hagyard, M. J., West, E. A., and Cumings, N. P.: Vector Magnetic Field Evolution and Associated Photospheric Velocity Shear Within a Flare-Productive Region. Solar Phys., 79, 59, 1982.

Hagyard, M. J., Cumings, N. P., West, E. A., and Smith, J. E.: Solar Phys. (in press).

Henze, Jr., W., Tandberg-Hanssen, E., Hagyard, M. J., Woodgate, B. E., Shine, R. A., Beckers, J. M., Bruner, M., Gurman, J. B., Hyder, and West, E. A.: Solar Phys. (in press).

Schmahl, E. J., Kundu, M. R., Strong, K. T., Bentley, R. D., Smith, Jr., J. B., and Krall, K. R.: Solar Phys. (in press).

Hagyard, M. J., Teuber, D., West, E. A., Tandberg-Hanssen, E., Henze, Jr., Beckers, J. M., Bruner, M., Hyder, C. L., Gurman, J. B., Shine, R. A., and Woodgate, B. E.: Solar Phys. (submitted).

West, E. A., and Hagyard, M. J.: Interpretation of Vector Magnetic Data Including Magneto-Optic Effects: I. Transverse Field Azimuth Angle. Solar Phys. (submitted).

Strong, K. T., Benz, A. O., Dennis, B. R., Leibacher, J. W., Mewe, R., Poland, A., Schrijver, J., Simnett, G., Smith, Jr., J. B., and Sylvester, J.: A Multiwavelength Study of a Double Impulsive Flare. Solar Phys. (submitted).

Solar Activity Relationships

During the past fiscal year, investigations were conducted concerning statistical aspects of solar flares near the maximum of the present sunspot cycle, sunspot variation and associated phenomena (e.g., flare rate, gradual-rise-and-fall radio event rate, and coronal transient rate) during the present cycle, and association of interplanetary magnetic clouds with proxy coronal transient events based on ground-based and spaceborne observations extending more than a decade. Much of this work has been published or submitted for publication in NASA reports and various selected journals. The work has direct bearing on mission/payload planning exercises (e.g., Spacelab 2, Space Platform, etc.). (R. Wilson/ES52/205-453-2824)

Wilson, R. M.: Statistical Aspects of the 1980 Solar Flares - I. Data Base, Frequency Distributions, and Overview Remarks. NASA TM-82465, January 1982.

Wilson, R. M.: Statistical Aspects of the 1980 Solar Flares - II. Solar Activity Relationships and Additional Remarks. NASA TM-82475, February 1982.

Wilson, R. M.: Sunspot Variation and Selected Associated Phenomena: A Look at Solar Cycle 21 and Beyond. NASA TM-82474, February 1982.

Magnetic Changes Observed in a Flare

A fundamental problem in solar physics is that of the energy release process in flares. It is well accepted that solar flares are the explosive release of energy stored in the magnetic field above the photosphere in active regions. If the magnetic field in which a flare occurs is the immediate source of the flare energy, then a change in the field must accompany the flare, and the way in which this change occurs is a vital aspect of the energy release.

At present, solar magnetic fields can be directly observed only in the photosphere. Although it is expected that the magnetic changes wrought by flares above the photosphere (in the chromosphere and corona) should extend into the photosphere, few observations have shown this effect. Recently observers at Caltech's Big Bear Solar Observatory have reported magnetograph observations of transient reversals in polarity of small areas of photospheric magnetic flus in strongly impulsive flares; the magnetograms also show permanent changes in the magnetic flux in some of these flares (Patterson and Zirin, 1981 and 1982; Zirin and Tanaka, 1981).

Moore et al. (1982) found new observational evidence for flare-wrought magnetic changes in and above the photosphere and evidence that the transient reversed-polarity features seen in magnetograms in the impulsive phase of flares are artifacts of flare emission in the photospheric spectral line observed by the magnetograph. The evidence came from several complementary observations of a fairly large impulsive flare. The time development of the impulsive energy release was observed in microwaves by the Caltech Owens Valley Solar Interferometer and in hard X-rays by the University of California, Berkeley spectral analyzer on ISEE-3. Chromospheric and photospheric filtergrams from Big Bear and photospheric magnetograms, intensitygrams, and velocitygrams from Kitt Peak National Observatory showed magnetic structure, flare emission, mass motion, and magentic changes.

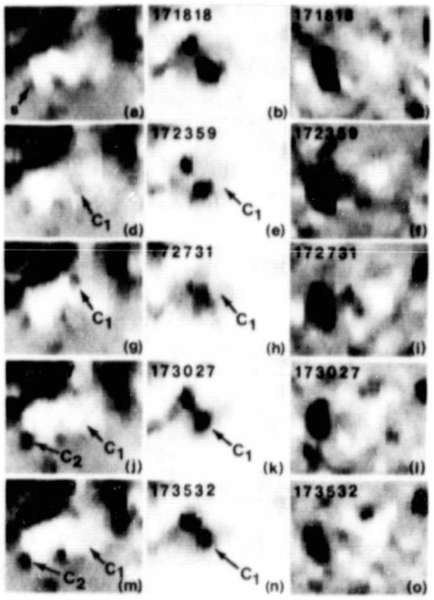

Figure 19. True and False Photospheric Magnetic Changes Produced by a Flare. These are Kitt Peak magnetograms (left), Intensitygrams (center), and Velocitygrams (right) in FeI 8688.

In Figure 19, the intensitygrams show the umbra and penumbra of the sunspot in which the changes occurred. In the magnetograms, positive polarity flux is light; negative polarity is dark. In the velocitygrams, flow toward the observer is dark; flow away is light. This area of the solar surface is 45^{o} west of central meridian (solar north is up, and west is to the right). The chromospheric filament explosion (not seen here) and impulsive peak of the flare was at 17:24:20 UT April 10, 1980; the time is given in each panel. Around this time, line emission in the positive polarity area of the sunspot produced a false transient polarity reversal in the magnetograms (C_1 in d, e, g, h). This was followed by permanent truncation of the umbra and weakening of the magnetic field at C_1 (in j, k, m, n). The negative flux (labeled s in panel a) also suddenly increased after the filament exploded (C_2 in j and m). The velocitygrams show that the flux decrease at C_1 was accompanied by down flow and the flux increase at C_2 was accompanied by upflow. The field-of-view is 38 x 32 inches.

From these observations, Moore et al. found: (1) A strong true magnetic transient, in the form of an explosive eruption of the field in the chromosphere and corona in and around a chromospheric filament; (2) The impulsive peak of the flare produced emission in the photospheric spectral lines observed by the Big Bear and Kitt Peak magnetographs; the emission produced a false polarity reversal in the magnetograms within a few minutes after the filament explosion, permanent changes in photospheric sunspot structure accompanied permanent changes photospheric magnetic flux. Apparently, these photospheric magnetic changes were caused by strong flare-wrought magnetic changes in the chromosphere and corona.

The photospheric changes in magnetic field and sunspot structure so far observed in flares are near the limit of resolution (1.0 arc second) of ground-based telescopes. Furthermore, the manner in which the field changes cannot be unambiguously determined from observations of the line-of-sight component alone, as has so far been the case. Hence, it is necessary to have very high resolution filtergrams of the photosphere and chromosphere and high resolution vector magnetograms if we are to advance our observational knowledge of the behavior of the magnetic field in flares. Photospheric field changes such as those reported here will be well resolved by the 0.1 arc second resolution of the 1.25 m aperture Solar Optical Telescope now being developed by NASA for flight on the Shuttle/Spacelab near the end of this decade. (R. Moore, ES52, 205-453-0118)

Moore, R. L., Hurford, G. J., Jones, H. P., and Kane, S. R.: Astrophys. J. (in preparation).

Patterson, A., and Zirin, H.: Astrophys. J., 243, L99, 1981.

Patterson, A., and Zirin, H.: Bull. AAS, 13, 821, 1982.

Zirin, H., and Tanaka, K.: Astrophys. J., 250, 791, 1981.

Computer Graphics for Analysis of MSFC Vector Magnetograms and SMM/UVSP Spectroheliograms

D. Rabin has developed a flexible computer program for the false-color display of spatial solar data. This program allows the investigator to tailor the characteristics of the display to his particular needs without the need for arithmetic manipulation of the input data. For example, by distributing color boundaries (or contour levels) nonlinearly within the range of the data, the program can make the correspondence between data value and color effectively logarithmic with negligible computation or delay, even for the largest images. A useful concomitant of this approach is that the investigator always sees and works with original data values, however nonlinear the display. The investigator may choose among several scale types; e.g., unipolar for radiant intensity, bipolar for radial velocity, or circular for the display of angles. He may rotate, flip, and squeeze the image in order to compare it with other images or to correct for known distortions. Finally, he may overlay contour maps, vector maps, or a coordinate grid on the false-color image.

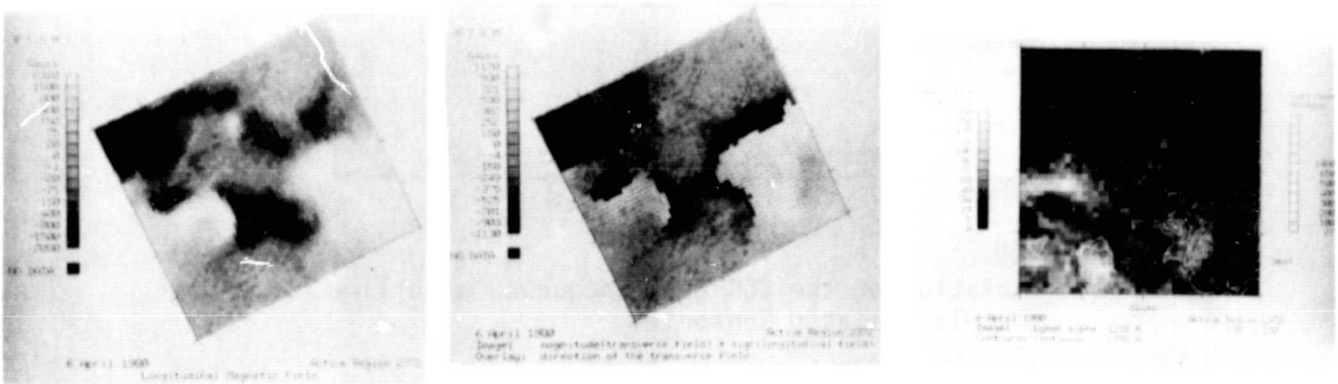

Figure 20. Comparison of the Photospheric Vector Magnetic Field of an Active Region with the Lyman Alpha Emission from the Chromosphere and Chromosphere-Corona Transition Region.

Figure 20 shows magnetic and UV images for a selected solar active region and compares the Photospheric Vector Magnetic Field of an Active Region with the Ly Emission from the Chromosphere and Chromosphere-Corona Transition Region: (a) Longitudinal (line-of-sight) magnetic field observed by the MSFC vector magnetograph; (b) Transverse magnetic field observed by the MSFC vector magnetograph; and (c) Ly spectroheliogram from the UVSP on the SMM. [The orientation of the transverse component is shown by the small dashes in (b). The magnetograms have been rotated so that the active region orientation matches that in the spectroheliogram (solar north up; west to the right). The contours superimposed on the Ly image (c) are from the photospheric brightness observed by the UVSP in the UV continuum at 2792 and show the location of sunspots. The field-of-view in (c) is not the same as in (a) and (b), but overlaps the same active region. The vertical segment of the boundary between the strong opposite-polarity flux regions in the lower central part of the magnetograms is located in the small sunspot near the lower edge of the spectroheliograms]. (R. Moore/ES52/205-453-0118)

Precise Measurement of Total Solar Irradiance

MSFC research in solar radiometry continued in FY82 with further laboratory testing of a Crystal Cavity Radiometer (CCR) as an advanced radiometric sensor concept. This unique concept uses the high temperature-sensitivity of quartz crystal oscillator frequencies together with the extreme oscillation stability of these crystals to produce a sensitive indicator for changes in temperature. High precision is achieved through the use of two matched crystal oscillators in a null mode with the frequency difference (beat frequency) proportional to temperature changes.

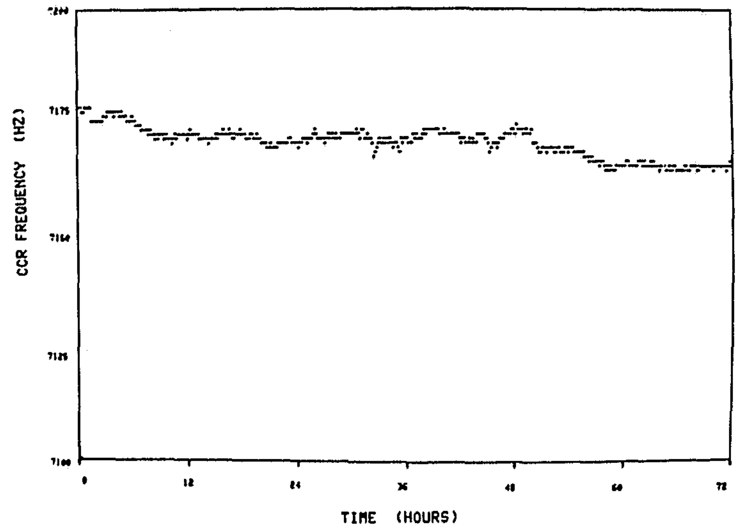

Figure 21. Variation of the CCR Beat Frequency with Time for a Completely Isolated Sensor.

To ascertain the basic sensitivity and stability of a CCR sensor, the beat frequency was monitored over a 3-day period with the CCR completely isolated from radiant sources. In Figure 21, the results of this test are shown, indicating a measured rms variation in beat frequency of 3.37 Hz at 7200 Hz. If this stability holds for the beat frequency at one solar constant, $\sim 10^{-5}$ Hz, then a CCR sensitivity of 2.7 x 10^{-5} is indicated, which is quite close to the design goal of 2 x 10^{-5}. This work was performed under RTOP 188-38-51, Office of Space Science and Applications, Dr. J. D. Bohlin. (M. Hagyard/ES52/205-453-0118)

GRAVITATIONAL PHYSICS

Superconductivity Research

Advanced research and development were accomplished toward meeting the requirements for the Gravity Probe-B (GP-B) experiment proposed by Stanford University. Some of the main areas include: coating a fused silica gyro rotor uniformly with a niobium film that will be superconducting, measuring the uniformity of this film with great precision, fabricating superconducting readout loops on a gyro housing half, and examining the characteristics of optically contacted surfaces at liquid helium temperatures (needed as a stable construction technique for the gyro). A coating uniformity to within 7.5 nm (0.3 microinch) has been specified as a goal, and a film of 2500 nm (approximately 100 microinch) thickness is desirable for ground testing purposes.

Superconducting niobium films have been coated on fused silica rotors to a uniformity of approximately 3 percent variation peak-to-valley on a macroscopic level (measurements integrate over an area approximately 3 mm in diameter and thus average microstructural variations). Specularly reflecting films are obtained below 750 nm (30 inches); increasing darker films are obtained for greater thicknesses as a result of scattering from larger microstructural features (very thick films acquired a velvet-like appearance due to growth of larger crystallites). Consistent uniformities are obtained utilizing a newly developed manipulator controlled by a microprocessor. Considerably better than 3 percent uniformities have been obtained about single great circles; investigations are underway to determine if uniformities can be improved further by reducing impurity variations as opposed to thickness variations.

New readout circuits on prototype gyro housing parts have been fabricated. These circuits involve multiturn superconducting loops with crossovers accomplished at the connector pads according to a recent design provided by Stanford University. External leads have been successfully connected to 1-mm square connector pads providing both superconducting joints and good bonding. (P. Peters/ES63/205-453-5134)

Liquid Helium Management Studies for Gravity Probe-B (GP-B)

The GP-B spacecraft requires a large quantity of liquid helium (LHe) for cooling of components to superconducting temperatures and for providing thrust for the propulsion system which will provide drag compensation (to 10^{-10} g). Asymmetries in the LHe configuration within the dewar (which holds the gyro package) can give rise to gravitational and gravity-gradient effects which can degrade the drag compensation system effectiveness. Mechanics of the LHe involve a balance of surface tension and centrifugal forces coupled with complex boundary conditions. Analyses have suggested an approach to managing the LHe configuration making use of a baffle system and an initial high-spin period. This approach will be tested in a model system which has been designed for a series of low-gravity experiments aborad the NASA KC-135 aircraft. These studies should answer specific questions about LHe behavior on GP-B as well as general results concerning the configurations and stability of free surfaces of liquids in rotating orbital spacecraft. Results should have broader application in the management of liquids (fuels, coolants, etc.) in low gravity. (F. Leslie/ES82/205-453-2047, and C. Schafer/ES82/205-453-1886)

ASTRONOMY

Infrared Telescope

Development continued on flight hardware of the Infrared Telescope (IRT) experiment scheduled for the Spacelab 2 mission in 1984. The IRT is a joint endeavor of the Smithsonian Astrophysical Observatory (SAO), the University of Arizona (UA), and MSFC. SAO is providing the Principal Investigator (G. Fazio), project management, and postflight data analysis; UA is responsible for the infrared optics; and MSFC provides the cryogenic system, mechanical equipment, and all integration and test functions. The University of Alabama in Huntsville has collaborated with MSFC in the development of the cryogenic apparatus.

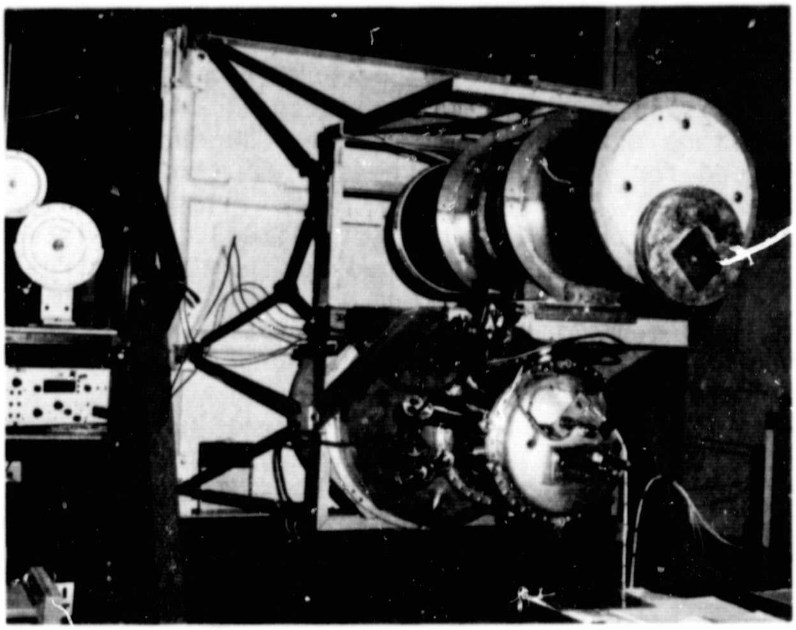

Figure 22. Infrared Telescope Flight Dewar and Dummy Cryostat in Launch Attitude during Dewar Thermal Performance Evaluation at MSFC.

The two major elements of the IRT have been qualified as subsystems. The infrared optics are carried in a helium gas-cooled, articulated cryostat which will scan about a single axis. Coupled with Orbiter motion, this will generate an extensive map of low-surface brightness and diffuse astronomical objects, and will produce data on the Orbiter/Spacelab induced environment and its effect on cryogenic infrared astronomy. Recently, the cryostat and optics subsystem satisfactorily completed its acceptance test. The 250-liter superfluid helium dewar has been thoroughly tested in several thermal performance evaluations which exercised a number of ground and on-orbit operations, including filling in the launch attitude, conversion to superfluid, stabilization, simulated gas flow to the cryostat, and liquid/vapor phase separation by a porous plug. Both dewar and cryostat subsystems are now ready for integration into the complete experiment assembly which will then be qualified for flight as a system. IRT delivery to the Kennedy Space Center is planned for the last quarter of 1983. (E. Urban/ES63/205-453-5132)

X-Ray Astronomy

The research program in X-ray astronomy has concentrated heavily on analysis and interpretation of data from the Time Interval Processor of the Monitor Proportional Counter aboard the HEAO-2 observatory. Several extremely interesting objects were observed, and many of the results have been published in the open literature. Of particular note has been the discovery of a 69 millisecond pulsation period from an X-ray source in a binary system in the Large Magellanic Cloud. This X-ray pulsar turns out to be the fastest known X-ray pulsar in a binary system and the third fastest pulsar ever observed.

Significant accomplishments were also achieved in support of the Advanced X-ray Astrophysics Facility. Specifically, detailed measurements of the X-ray scattering from a variety of reflecting surfaces have been accomplished. These tests, which made use of the X-ray calibration facility at MSFC, are the first where scattering data has been obtained with sub-arc-second angular resolution. As such, these data represent a unique data base for the understanding of X-ray scattering. (M. C. Weisskopf/ES62/205-453-5133)

Henry, J. P., Spiller, E., and Weisskopf, M.: Imaging Performance of a Normal Incidence Soft X-ray Telescope. App. Phys. Lett., 40, 25-27, 1982.

Skinner, G. K., Bedford, D. K., Elsner, R. F., Leahy, D., Weisskopf, M. C., and Grindlay, J.: Discovery of 69 ms Periodic X-Ray Pulsations in A0538-66. Nature, 297, 568-570, 1982.

Cline, T. L., Desal, U. D., Teegarden, B. J., Evans, W. D., Klebesadel, R. W. Laros, J. G., Barat, C., Hurley, K., Niel, M., Vedrenne, G., Estulin, I. V., Kurt, V. G., Mersov, G. A., Zenchenko, V. M., Weisskopf, M. C., and Grindlay, J. E.: Precise Source Location of the Anomalous 1979 March 5 Gamma-Ray Transient. Ap. J. Lett., 255, L45-L48, 1982.

Zombeck, M. V., Wyman, C. C., and Weisskopf, M. C.: High Resolution X-Ray Sacttering Measurement for the AXAF. Optical Engineering, 21, 63, 1982.

Leahy, D. A.: Matter-Antimatter Separation in the Early Universe by Rotating Black Holes. Ap. J., 249, 403-405, 1981.

Leahy, D. A. and Vilenkin, A.: Magnetic Field Generation by Rotating Black Holes. Ap. J., 248, 13, 1981.

Vilenkin, A. and Leahy, D. A.: Parity Nonconservation and the Origin of Cosmic Black Holes. Ap. J., 254, 77-81, 1982.

Leahy, D. A.: Scalar and Neutrino Fields in the Godel Universe. Inter. J. Th. Phys., 21, 703-753, 1982.

Gamma-Ray Astronomy

The latest in a series of balloon-borne observations in high-energy astrophysics was conducted on May 29-31, 1982. These investigations are directed at obtaining a better understanding of transient and perodic sources in the energy range above 30 keV by using an array of large-area scintillation detectors. The balloon flights also provide a test bed for the design and development of detectors and techniques for future, longer duration balloon flights and orbiting detector systems. The most recent flight provided an observation time of over 50 hrs at altitudes above 40 km.

Data analysis from a balloon flight in 1980 is now being completed. These data provided the best balloon-borne observations of a gamma-ray burst thus far obtained. It also provided the most sensitive observations of the pulsar in the Crab Nebula in this energy range. Several solar flares were also observed.

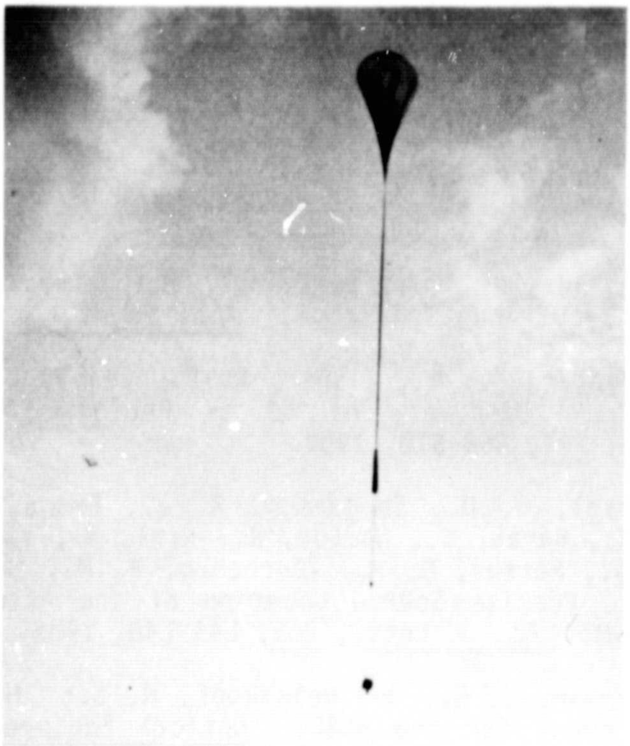

Figure 23. The Balloon-Borne Gamma-Ray Astronomy Detector Array Begins its Ascent to an Altitude of 40km after Launch from Greenville, South Carolina on May 29, 1982.

A new, on-board data system, designed and built at MSFC, was used in this latest experiment. This system is based on that being developed for the Burst and Transient Source Experiment (BATSE) on the Gamma Ray Observatory (GRO). It provides extensive real-time processing of large amounts of data in order to reduce the telemetry requirements. (G. J. Fishman/ES63/ 205-453-0110)

Cosmic Ray Research

The third in a series of balloon-borne cosmic-ray experiments designed to study cosmic rays above 10^{12} eV and the interactions produced by them was successfully flown from Greenville, South Carolina, on June 2, 1982. After gathering 39 hours of data at 38 km altitude, it was recovered near Roswell, New Mexico.

The series of investigations are being performed by a collaboration which includes members of several U. S. and Japanese universities. The experiments are called "Japanese-American Cooperative Experiments" (JACEE). The principal objectives are the study of the energy spectra and composition of the cosmic ray between 10^{12} and 10^{15} eV, and the study of hadron-nucleus and nucleus-nucleus interactions above 10^{12} eV. The hadron-nucleus interaction studies overlap and extend above center-of-mass energies available at colliding beam machines. The nucleus-nucleus studies are made at energies one to three orders of magnitude above that available from accelerators on Earth.

The principal instrument is a large stack of nuclear track emulsion etchable plastics, X-ray films, and lead plates called an "emulsion chamber." The cosmic-ray nuclei and their interaction products leave microscopic tracks that are analyzed after the flight. The first two JA balloon-borne experiments used 1 M^2 emulsion chambers, each weighing about 700 kg, composed of 300 layers of passive materials. These experiments produced new data on the cosmic-ray hydrogen and helium energy spectra. They also produced new results on the characteristics of proton-nucleus interactions in agreement with colliding beam results, and several nucleus-nucleus interactions that are anomalous compared to conventional models of such collisions. Figure 24 shows an emulsion picture of a collision between a cosmic-ray silicon nucleus of total energy 100 TeV with silver bromide in the emulsion. About 1000 charged mesons resulted, whereas a simple model of collisions between individual nucleus would predict a maximum of around 580.

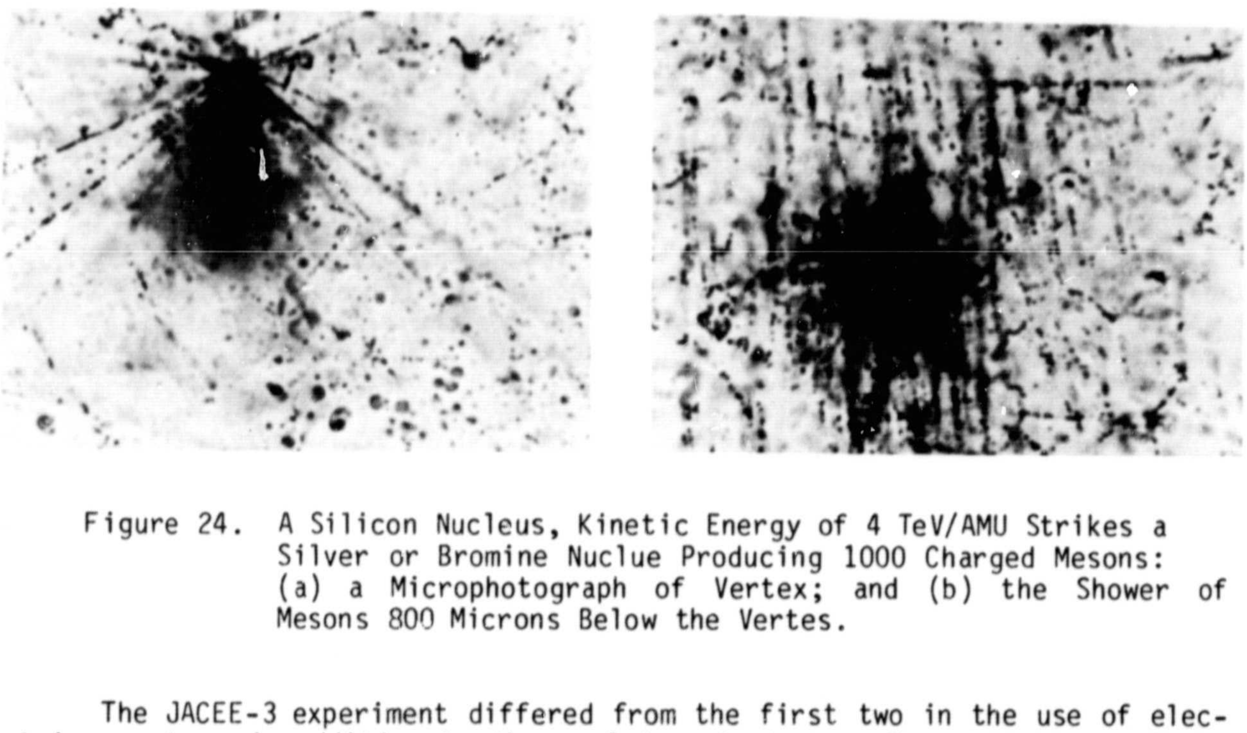

Figure 24. A Silicon Nucleus, Kinetic Energy of 4 TeV/AMU Strikes a Silver or Bromine Nuclue Producing 1000 Charged Mesons: (a) a Microphotograph of Vertex; and (b) the Shower of Mesons 800 Microns Below the Vertes.

The JACEE-3 experiment differed from the first two in the use of electric counters in addition to the emulsion chambers. The objectives of the JACEE-3 are to provide a sample of cosmic-ray nuclei characterized in atomic number and energy by electronic counters to be studied in the emulsion chambers. The electronic counters supply a "particle beam," and the materials in the emulsion chamber are used to study the nuclear and particle physics. The energy range is intermediate between that available with Earth-based accelerators and those studied in the JACEE-1 and -2 experiments. In the early stages of analysis, about 1000 interactions between incident atomic number 6 and 26 and between energies of 0.25 and TeV per nucleus have been identified for study. (T. A. Parnell/ES63/205- 453-5133)

MATERIALS PROCESSING IN SPACE

One of the major goals of the Materials Processing in Space (MPS) program is to utilize the unique low-gravity environment of space flight to vastly reduce or eliminate hydrostatic pressure, sedimentation, buoyancy-driven convection, and, in some cases, container walls in the processing of materials. Ultimately it is expected that new processes or products will emerge that will have sufficient value to justify the cost of processing them in space. The more immediate goal is to use this unique environment to increase our understanding of process control and in particular the effect of gravity on various terrestrial processes.

The MPS program is presently sponsoring some 60 investigations at a number of universities, private corporations, and government laboratories. The total program is summarized in NASA TM-82443, "Materials Processing in Space Program Tasks," published by MSFC. The results reported in this document are from investigations that have been supported by the MPS program at MSFC over the past several years and are representative of the work being accomplished in the program. (R. J. Naumann/ES71/205-453-0940)

Crystal Growth and Characterization

Theoretical and experimental work is continuing on the growth of alloy-type solid solution semiconductors, with emphasis on Hg Cd Te, by the Bridgman-Stockbarger method. The axial composition has been modeled assuming diffusion-controlled solidification. The variation of interface temperature with compositions and the variation of the distribution coefficient with compositions have been included, and the growth rate is determined by the applied thermal field and the local composition at the interface. By comparing the observed compositions in systems grown experimentally with the models, effective diffusion coefficients have been determined for the system. These diffusion coefficients are essential for determining the thermal gradient required to stablize the growth interface.

Other thermal properties required to model the growth of such systems are: thermal conductivities in both the liquid and solid near the melting temperature, solid and liquid-phase densities near the melting temperature, and selected points on the ternary phase diagram. These are difficult measurements because of the high vapor pressure of Hg at the temperatures of interest. Techniques have been developed for making these measurements at high pressures, and preliminary results are now available. One rather interesting result is that a liquid-phase density inversion exists in the Hg Cd Te system at values of x from 0.8 to 1.0. This is probably associated with the fact that HgTe expands when it freezes; therefore, one might expect a density inversion in the liquid phase, just as in H_2O. Since many other semiconductor materials also expand on freezing (e.g., Si, Ge, InSb, to name a few), they may also have density inversion in the liquid phase. This may have some important implications for the stability of such system in growth from the melt in a gravitational field. (S. Lehoczky/ES72/205-453-3090)

Undercooling Studies in Metastable Peritectic Compounds

A number of experiments have been carried out in the MSFC 34-meter drop tube in which a metallic sample is melted and allowed to solidify in free fall. In the absence of a container, most heterogeneous nucleation sites are eliminated and the melt can undercool far below the normal solidification temperature before it solidifies. Undercoolings in excess of 500 K have been observed in Nb alloys.

Solidification, when it occurs, usually originates from a single nucleation site and is extremely rapid, producing a single crystal with a highly dendritic structure. The rapid solidification can produce unique microstructures in bulk samples, similar to those produced in thin films by splat cooling.

Special emphasis has been given to the NbGe system in attempts to produce the metastable, high transition temperature, A-15 superconducting phase. By a combination of deep undercooling and rapid quenching, samples have been produced that exhibit a 4 K increase in T_c above normally solidified samples, indicating that at least some A-15 phase has been formed. This was confirmed by X-ray diffraction and microstructural analysis.

Improvements in sample preparation have reduced internal nucleation sites to the point that the degree of undercooling is limited by the fall time in the 34-meter drop tube. A new 100-meter tube has been constructed and has just been put in operation. This should dramatically increase the amount of undercooling possible. (M. Robinson/ES74/205-453-1887)

Model Immiscible Systems

One of the early goals of space processing was to form in situ composites from systems that have regions of liquid-phase immiscibility (monotectic alloys). As the melt is cooled through the two-liquid phase region in Earth's gravity, rapid phase separation occurs because of the differences in density of the phases. Early attempts to avoid this separation by cooling the system through the two-liquid phase region in a low-gravity environment also resulted in massive phase separation in which one component was more or less surrounded by the second component. This indicated that there were significant nongravitational effects operating during the cooling and solidification process. In order to study these effects in detail, several transparent organic monotectic systems were selected to serve as models or analogs to the metallic systems. Because of their transparency, such models can reveal details that are totally obscured in the metallic systems.

One such system, succionitrile/water, has a consolute temperature of 58°C and a monotectic temperature of 18°C which makes it a convenient model for laboratory study. Also, the densities of the two phases are similar and can be matched exactly at a particular temperature by substituting D_2O for some of the H_2O.

Two important nongravitational phase separation processes have been identified: critical-point wetting and spreading and droplet migration from thermal-Marangoni convection.

Critical wetting occurs in a region between a critical wetting temperature and the consolute temperature. In this critical region, the difference between the interfacial energies of each liquid phase and the container is greater than the interfacial energy between the two liquid phases; hence, Young's equation has no real solution for the contact angle. Physically this means that one of the liquid phases (the one that wets the container in preference to the other below the critical wetting point) will become perfectly wetting and will intrude between the container wall and the second liquid.

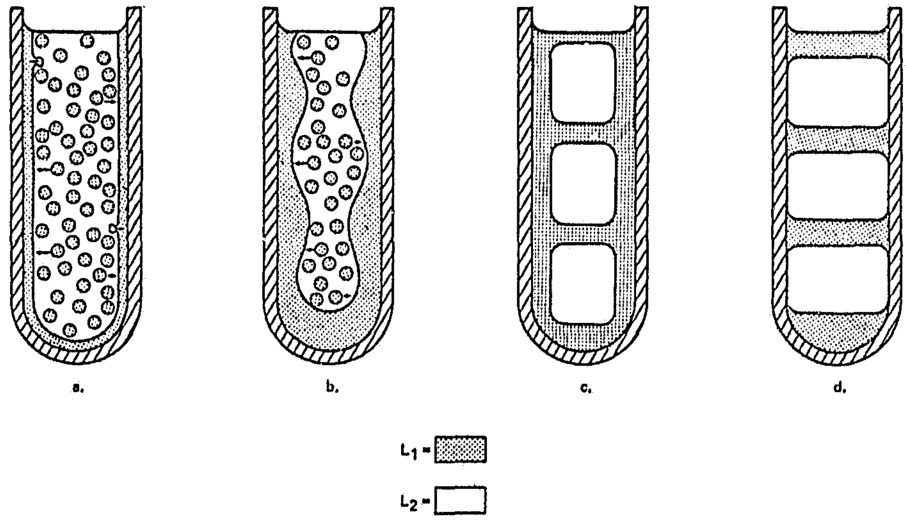

Figure 25. Phase Separation by Critical Wetting. As a binary solution is cooled into a region of liquid phase immiscibility, the minority phase nucleates to form droplets dispersed uniformly throughout the host. However, if the droplets perferentially wet the container, there is a temperature regime near the consolute point where they become perfectly wetting. Droplets near the wall spread to form a film of minority phase liquid between the host fluid and the container as shown in a. The resulting flow brings other droplets to the film where they also spread. As the film grows in a high aspect ratio container, Rayleigh instabilities occur (b.) which eventually isolate the host phase into large droplets (c.) as the system seeks to minimize its total surface energy. Finally, as the temperature drops below the critical wetting point, contact is reestablished between the host phase and the wall (d.). This effect is usually masked in a terrestrial laboratory because of gravity-driven flows arising from the density differences between the two phases.

When a monotectic system is cooled into the two-liquid phase region, the minority phase nucleates as small droplets that grow by diffusion until equilibrium is reached. If this minority phase critically wets the container wall, droplets near the wall will immediately spread over the wall. This will induce a flow which will bring other droplets to the wall where they undergo the same fate. This effect can be easily demonstrated in the laboratory by cooling a neutral-density, succinonitrile-rich/water solution below the consolute point. A film of water can be observed to form along the wall of the test tube. Soon Rayleigh waves can be seen on the surface, and eventually the system will decompose into large droplets of succinonitrile surrounded by water as the system seeks to lower its total surface energy (Figure 25). This seems to be the phase separation mechanism responsible for the results observed in the early attempts to form in situ monotectic alloys in space. This effect can be avoided by choosing the crucible material so that it is wet preferentially by the majority phase. Now as the critical wetting regime is traversed, the system is stable since the perfectly wetting phase is already in contact with the wall.

The second effect is more difficult to control. Because interfacial tension usually decreases with temperature, a minority phase droplet in a thermal gradient is subject to Marangoni flows that cause it to migrate in the direction of the gradient. The velocity of migration was calculated originally by Young, Block, and Goldstein (YBG). Experiments were carried out at MSFC in a two-liquid phase system that was heated from above and carefully insulated to avoid lateral gradients. Droplets of a more dense phase were caused to migrate upward against gravity. After correcting for gravitational effects, it was found that the migration was significantly lower than predicted by the YBG model. This is probably because in the two-liquid phase region there is a partial solubility of the two phases which depends on temperature. Therefore, minority phase droplets are in a solutal as well as a thermal gradient, which alters interfacial tension. The YBG theory will have to be modified to account for this effect.

Holographic microscopy techniques are being used to study the nucleation and growth of the second phase droplets and to study various agglomeration mechanisms. Models are being developed to describe the size and spatial distributions of the droplets which will determine the solidification conditions necessary to prevent phase separation by this mechanism. (D. Frazier/ES74/205-453-3090)

Crystallization Studies of Borderline Glass Formers

One possible application of containerless processing is the extension of the range of glass formation to systems that normally solidify in crystalline form. By eliminating container-induced nucleation, the melt can undercool well below the normal solidification point. Since viscosity increases rapidly with decreasing temperature, the system may be prevented from forming an ordered structure when it solidifies, thus forming a glass. In order to accomplish this, it is necessary to exceed a critical cooling rate in order to prevent nucleation of the crystallization phase.

Critical cooling curves are being determined for a number of these borderline glass-forming systems. One technique uses a strip heater made from a refractory metal foil (Pt, Mo, or Ta) to melt the sample. As the sample is allowed to cool, the nucleation and growth of the crystalline phase can be observed microscopically and correlated with the measured cooling curve. This determines the critical cooling rates required to form glasses in the presence of a heterogeneous substrate.

Another method will utilize a sting melting technique in which the sample is melted by a CO_2 laser. The cooling rates will be measured with a two-color pyrometer. Attempts are also being made to model the cooling of a sphere of semitransparent oxide melt. This technique may be able to provide the critical cooling rates for homogeneous nucleation.

Critical cooling rates of 250°C/sec have been determined for glass formation in 40 to 50 percent Ga_2O_3-CaO compositions on Pt. However, significant volatilization of Ga_2O_3 was observed which may have shifted the composition. Other systems being investigated are SiO_2-Al_2O_3 and CaO-Al_2O_3 prepared from both gels and the oxides. (E. Ethridge/ES74/205-453-3917)

Electrophoresis

An extensive modeling program has been carried out to determine the gravitational influences and limitations of continuous flow electrophoresis. This has been complemented by experiments in carefully designed, well-instrumented flow chambers that allow decoupling of the many complicating gravitational influences. It has been demonstrated that the electrophoresis chamber is sensitive to lateral and axial thermal gradients. Experiments have shown that lateral gradients as small as 0.1 K/cm are sufficient to produce sample stream meandering and loss of resolution in wide-gap machines. Lateral gradients are normally controlled in commercial machines by use of a very narrow flow channel, but at considerable expense in throughput and loss of resolution from wall effects. Adverse axial gradients, encountered when colder, denser fluid is above warmer, less dense fluid can cause flow reversal and essentially destroy the uniform, laminar flow through the chamber. During this past year, an instrumented chamber was used to observe flow under uniform lateral temperatures and various axial temperatures. Flow disturbances were observed for Rayleigh numbers greater than a critical value calculated for this chamber. The agreement between experiments and theory is remarkably close. In addition to establishing a clear rationale for performing electrophoresis in space, this research has led to two concepts in machines for terrestrial use.

One concept uses highly conductive, heat-sinked walls to reduce the lateral gradients and a channeled chamber coolant that assures a stable axial gradient. An aluminum electrophoresis chamber based on this concept has been built. Testing has been done on candidate insulating coatings for the metal walls. The insulation must be thin so the thermal conductivity of the system is not degraded, but the coating must be able to support the high electric fields and electrolytes necessary for electrophoresis.

Another method is a novel, moving-wall approach that allows the sample stream to be increased to the full width of the flow channel without introducing sample stream distortions. A laboratory instrument has demonstrated the basic concept. Polystyrene latex particles of known mobility were inserted as a ribbon through the entire thickness of the device, and deflection occurred without the disturbance of electroosmosis. The moving-wall device could be employed in low-g with even greater performance improvement and thus form the basis for the next generation of space electrophoresis devices. The design of a flight prototype unit is now underway, based on our experience with the laboratory unit.

Well-characterized biological samples are being prepared for testing the capabilities of the electrophoretic separator being developed by McDonnell-Douglas Astronautics (MDAC) as part of their commercial Joint Endeavor with NASA. Hemoglobin standards obtained from the Center for Disease Control (CDC) and pneumococcal polysaccharides obtained from Lederle Laboratories have been separated and analyzed inhouse and at MDAC with excellent agreement. They are stable samples that will be used to characterize the improvements in resolution and throughput achievable with the space instrument. (R. Snyder/ES73/205-453-3537)

Phase Partitioning

The possibility of maintaining a fine suspension of two immiscible liquid phases more or less indefinitely, and then effecting a controlled separation, gives a new dimension to the old technique of separation by phase partitioning. The material to be separated (e.g., cells or cell components) partitions itself in one phase or the other, depending on the interaction between molecules on its surface and the molecules in the two liquid phases. This can be controlled to an extent by addition of soluble salts to one or the other phase. Phase partitioning in microgravity allows a fine suspension to be maintained for sufficient time for the partitioning process to come to equilibrium. Researchers at the National Institute of Health (NIH) and the CDC have expressed considerable interest in this process, especially for the separation of large cells such as megakaryocytes. NIH has loaned MSFC three counter-current chromatography instruments for use in our laboratory to study separation efficiency. The latest is demonstrating the significant gains made by this new technology, and we are separating our standard red blood cell mixtures with reproducibility. The results of these separations will be compared with other reported separations and predictions of separations in weightlessness. An early low-gravity demonstration experiment is being planned to evaluate the process. (R. Snyder/ES73/205-453-3537)

TECHNOLOGY DEVELOPMENT

LARGE SPACE SYSTEMS

A number of projected space missions for the time period 1988 to 1995 (including space station, space platform, VLBI, and geostationary platform) involve the use of large space structures. To ensure that the LSS hardware and operations technology is available to meet these future mission needs, MSFC has implemented an LSS technology development program comprised of both ground and flight experiments. The ground-based program includes a broad range of future large systems technology requirements supported by basic R&T activities such as environmental effects on materials, thermal control, and space vehicle dynamics. Ground tests of selected structural elements (deployable masts/trusses) and assembly simulations in MSFC's neutral buoyancy facility have been underway for some time, and will establish the foundation needed to proceed with the flight test program. The flight test program, as outlined in Figure 26, consists of 5 basic missions of increasing complexity with time, with early emphasis on assembly and deployment techniques, and LSS dynamics. Mission needs for space fabrication technology are now perceived to be well down-stream (mid-90's or beyond); therefore, MSFC's activities and proposed flight experiments in this area have been deferred. Selected elements of the ground and flight programs are described below. (D. C. Cramblit/J. K. Harrison/PS04/205-453-0367)

Space Deployable Truss

A deployable truss, designed to the requirements of an early Space Platform/Space Station, was designed, fabricated, and delivered to MSFC. Automatic deployment under simulated zero-g conditions was performed using air bearings and a flat floor. The test article, shown in Figure 27, consists of the deployable truss deployment mechanism, two utility trays, and a representative complement utilities (power, data, and fiber optic cables). Hardpoints are incorporated into the structure to accommodate up to four payloads, each having a mass of 8,000 lbm. The deployed truss size is 55 inches high, 55 inches wide, and 550 inches long. Stowed dimensions are 55 inches high, 107 inches wide, and 60 inches long. Deployment is achieved by taking up two cables routed through the diagonal members on each side of the truss. Deployment tests were successful. Other versions of deployable trusses, designed to reduce the stowed volume, are under development. (E. E. Engler/EP13/205-453-3958)

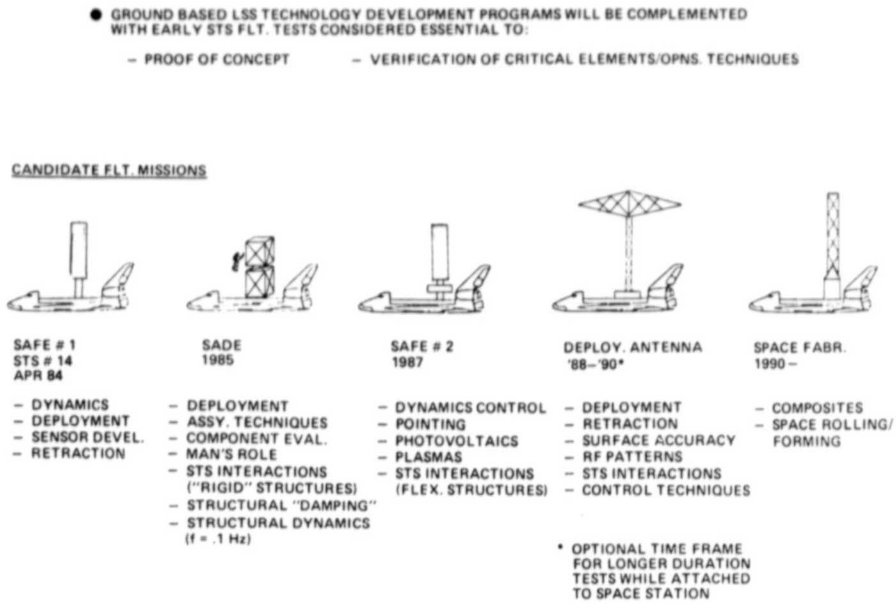

Figure 26. Baseline Large Space Systems Flight Program.

Beam Vibration Tests

The vibration testing of the one-meter size aluminum beams that were manufactured by MSFC's automated beam builder has entered the second phase. End fittings will be attached to beams of various lengths (6, 24, and 31.5 m) for future tests. The same series of vibration tests (random, sine, sweep and impulse) over a frequency range of 0 - 55 Hz will be done as in the first phase. The results from the first phase compared well with mathematical models developed to predict the behavior of the 16.5 m aluminum beam. The same comparisons will be made in the second phase. Figure 28 shows the three major phases of this effort. (J. K. Harrison/PS04/205-453-2817)

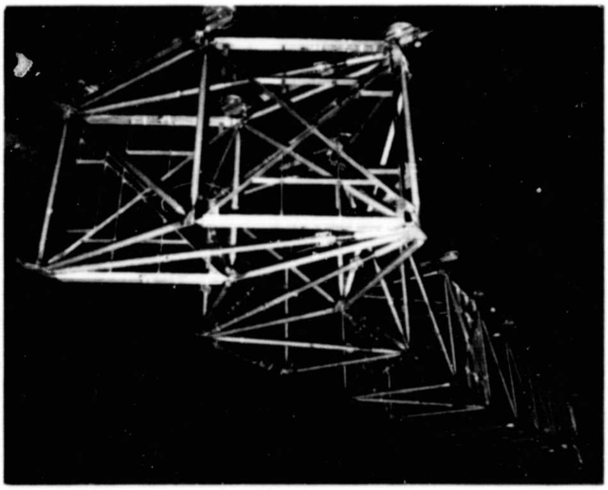

Figure 27. Deployment of the Space Deployable Truss.

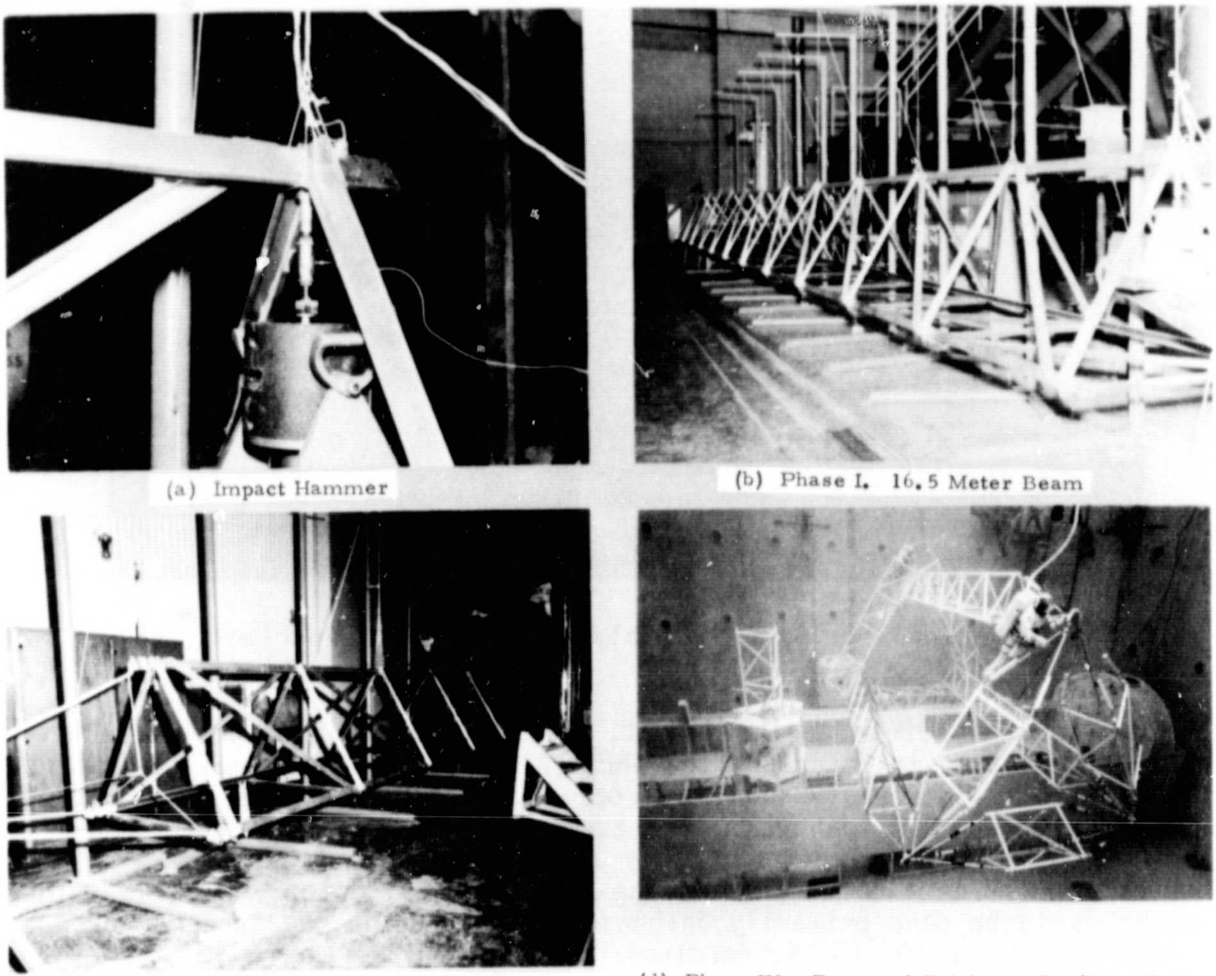

(a) Impact Hammer

(b) Phase I. 16.5 Meter Beam

(c) Phase II. 6-Meter Beam with End Caps

(d) Phase III. Proposed Tri-beam Configuration

Figure 28. Vibration Testing of Aluminum Beam Built by the MSFC Automated Beam Builder.

Structural Assembly Demonstration Experiment (SADE)

The primary purposes of this Structural Assembly Demonstration Experiment (SADE) are to demonstrate that the Shuttle has the capability to build a large structure in space, to measure the extent to which MSFC Neutral Buoyancy Simulator (NBS) can accurately simulate assembly activities in space, and to determine the mechanical performance of the truss in terms of deployment and assembly. The truss will be assembled in the Shuttle bay over a period of several hours using astronaut EVA assistance, tools, and other Shuttle resources (i.e. RMS) as well. The assembly procedure will be established in the NBS and then repeated in-orbit. The truss will remain

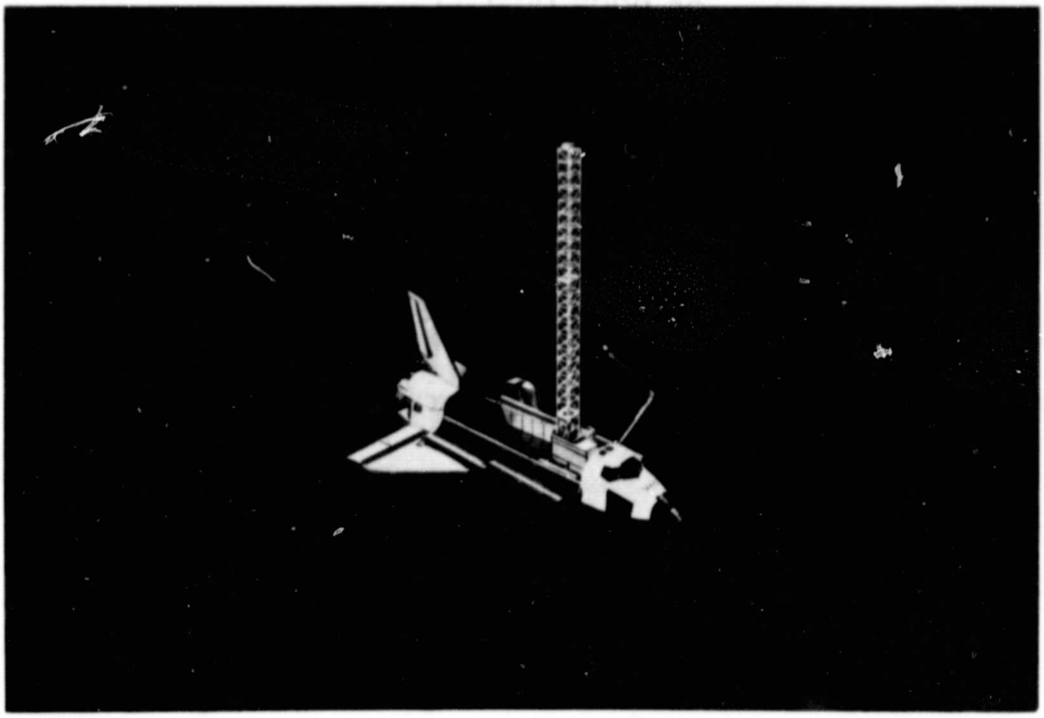

Figure 29. Structural Assembly Demonstration Experiment.

attached to the Shuttle during flight. After assembly is completed, some tests will be done to determine the Shuttle's ability to control structures of this size. Disassembly will then occur, and the materials and recorded data will be returned to Earth. The current SADE truss test article has a fully deployed length of approximately 115' and a cross section of 5' x 5'. The design will be a derivative of the current SASP deployable truss. The project is to be done primarily in-house. A sketch of the current concept is shown in Figure 29. (J. K. Harrison/PS04/205-453-2817)

Solar Array Flight Experiment (SAFE #2)

The SAFE #2 flight experiment is an evaluation in orbital environments of advanced photovoltaic, plasma physics, and large space structures system dynamics. The flight date is now planned for mid-1987.

The flight experiment permits full operating evaluation of advanced photovoltaic equipment in orbital environments in a manner that future vehicles can confidently utilize, with significant performance improvement. Included will be an evaluation of concentrator array designs (high and low concentration ratios), and advanced technology cells (GaAs, vertical function, multi-bandgap). The experiment also evaluates the operating limits on photovoltaic collectors imposed by plasma interactions. Plasma interactions as a function of cell voltage options from 200-1,000 volts will be evaluated relative to power loss and arcing potential. Design criteria applicable to future hi-voltage photovoltaic Space Station/Space Platform systems will be generated. Techniques for environment diagnostics and the monitoring/control of charge buildup/arcing phenomena will be demonstrated in a joint NASA/Air Force experiment utilizing spacecraft automatic active discharge system equipment to be provided by the USAF.

The experiment evaluates the dynamics of the 14" diameter by 105' long astromast structure that holds the photovoltaic array. This active control structural dynamic experiment is effected by the use of an "Advance Gimbal System (AGS)." The astromast structure (which deploys and holds the photocell blanket in the extended position in orbit) is mounted to the AGS and the AGS permits "shaking" this structure system to evaluate its modal frequency system characteristics. Control techniques for the active pointing and stabilization of large flexible structures will be generated. Gimbal mounted payload interactions design criteria will be generated; technology for both centralized and decentralized actuator/sensor systems for LSS control and vibration damping will be demonstrated. The flight experiment is integrated on a standard Spacelab pallet and utilizes planned instrumentation and computer facilities. (R. L. Middleton/PS04/205-453-0367)

Deployable Antenna Flight Experiment

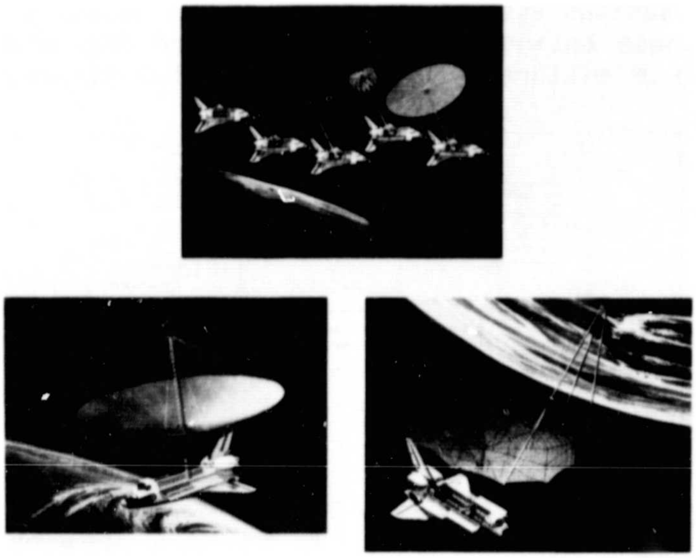

Figure 30. Deployable Antenna Flight Experiment.

Continuing design/definition and program planning in FY82 on the large antenna system flight test addressed prevailing needs for large space sensor capabilities on future applications of microwave radiometry, multi-beam communications, spaceborne radar, and radio astronomy. Numerous civil and military studies, technology efforts, and ground test programs are focused on large aperture requirements and development for improved mission performance. The proposed flight is a large structure system test to validsate the integrated performance of numerous component technologies being developed and tested by NASA and DOD. Candidate 50-meter diameter test articles (Shuttle-attached) are configured to evaluate the critical structural and RF performance parameters of large high precision, high gain antennas, including larger diameters and higher frequencies than the test antenna. A comprehensive flight measurement program including remote sensor instrumentation (for discrete measurement of structural nodes and surface deflections) and far-field antenna pattern measurements (for integrated structural performance and RF evaluations) is defined for precise measurement of static, dynamic, and thermal effects.

Control analyses and simulations of the Orbiter-attached antenna test contribute to development of broader capabilities for dynamic control of large space systems. The antenna studies are continuing the derivation of implementation schemes for a combined attitude-vibration control program for structural damping and precision pointing of the large antenna system. FY82 activities also include further definition and planning on structural ground tests to aid the design and manufacture of precision flight structures. (W. E. Thompson/PS04/205-453-2796)

Man/Machine Assembly Analysis

Man/Machine Assembly Analysis (MMAA) is a method for economically mixing large space system assembly techniques. Methods of assembly can be viewed as a continuum beginning with manual execution and progressing through remote operations to totally automated execution. A cost algorithm will provide the framework for performing the MMAA. Given any large space structure/system, the MMAA will assess the mission requirements, determine the costs for the various assembly options, define assembly requirements and constraints for those options, and finally define the most cost-efficient assembly technique or mixture of techniques for that structure/system.

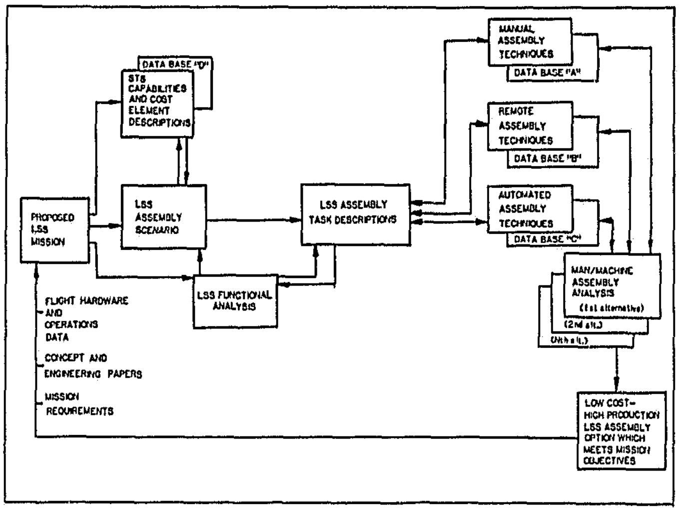

Figure 31. Man/Machine Assembly Analysis Methodology.

The analysis is functionally divided into two major sections, the data bases and the processes (Figure 31). The data bases include one each for manual, remote, and automated assembly techniques, and cost element descriptions for the Space Transportation System. Additionally, there are four process descriptions: one each for preparation of the Orbital system assembly scenario; preparation of the functional analysis; preparation of the task descriptions; and development of the MMAA itself.

Data have been collected for the data basses from various sources. Manual assembly techniques data have been the most easily obtainable, based upon flight (Skylab, SADE) and zero-gravity simulations (neutral buoyancy (Figure 32), zero-g aircraft, etc.). Remote data and automated data have been based upon paper analyses, with some support from ground simulations (Remote Manipulator System, Automated Beam Builder, Automated Orbital Servicer, etc.). Likewise, similar-function ground-based robots have provided useful data.

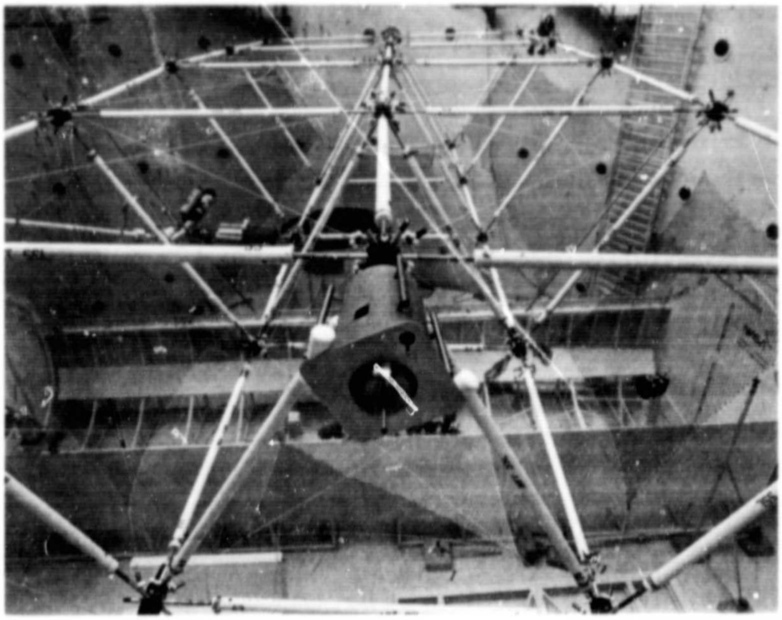

Figure 32. Zero-G Simulation with Large Space Structure in the MSFC Neutral Buoyancy Simulator.

The MMAA is planned for completion in May 1983. Prior to finalization, it will be exercised against one or more current large structure/systems in order to verify its definition. Once completed it will provide a tool for early decision-making in determining the most efficient assembly technique Further, the project will glean useful assembly requirements and constraints for the considered orbit system. (J. W. Stokes, EL15, 205-453-4430)

Watters, H. H. and Stokes, J. W.: Construction in Space - Toward a Fresh Definition of the Man/Machine Relation paper, entitled Astronautics and Aeronautics, Volume 17, No. 5, May 1979.

Space Applications of Automation, Robotics, and Machine Intelligence Systems (ARAMIS)

A major foundation to apply advanced automation to earth orbital activities was generated. A contract with the Massachusetts Institute of Technology, Space Systems and Artificial Intelligence Laboratories, supported by OAST resulted in a first time comprehensive survey and organization of present extended state-of-the-art of automation, robotics, and machine intelligence technology and its capabilities. These were matched with a comprehensive list of generic future earth orbital tasks providing numerous available technology options.

Presently, this available knowledge is being applied, through follow-on contract tasks, in the following areas:

Telepresence - A technology advancement program based on telepresence requirements leading to early and successive ground and space demonstrations.

Automation of Selected Prelaunch Operations - This ARAMIS application covers the automation of the Orbiter Hypergolic System, the application of expert systems to payload/Shuttle interface procedures, and to developing and modifying LPS system software. (Georg von Tiesenhausen/PS01/205-453-2789)

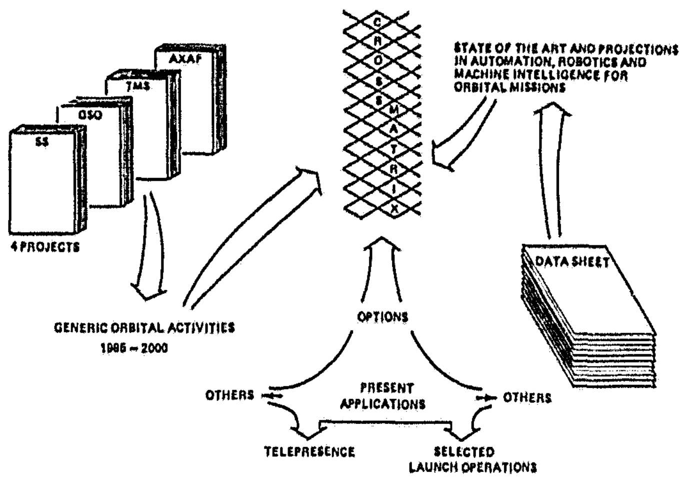

Figure 33. Space Applications of Automation, Robotics and Machine Intelligence.

Improvements of Modal Testing Methods

Modal structural dynamic testing is widely used in the transportation, aerospace, and propulsion industries to identify the frequencies and modes. Analysis may thus be verified before operation is risked. The dominant technique for modal testing of structures has been the use of single-point-excitation, with digital Fourier analysis techniques being employed for determination of frequency response functions (FRF's). Modal parameters (e.g., natural frequencies, damping, mode shapes) are derived from these FRF's by various curve-fitting techniques.

From both an analytical standpoint and an experimental standpoint, identification of modal parameters is more difficult if the system has repeated frequencies or closely-spaced frequencies. The more complex the structure, the more likely it is to have closely-spaced frequencies. It is therefore difficult to determine valid mode shapes using single-shaker test methods. Techniques for estimating experimental mode shapes by using a single column or a single row of the FRF matrix are well known and are incorporated in various modal analysis software packages. Because of the difficulties in obtaining accurate modal vectors for systems with closely-spaced-frequency modes by using only a single column or row of the FRF matrix, it is necessary to examine the possibility of using several rows/columns of the FRF matrix to obtain improved modal vector estimates. Analytical and experimental developments have led to promising methods for accomplishing this objective.

Based on research to date, the following conclusions may be stated:

a. Standard Asher tuning and minimum coincident response tuning both provide rational means for employing multiple rows or columns of the FRF matrix to improve modal vector estimates.

b. The use of synthesized frequency response functions rather than the original experimental FRF's has two advantages: (1) far less memory is required to store the synthesis parameters than is required to store a complete FRF, and (2) the analysis bandwidth can be reduced to obtain better estimates of the modal vectors. (L. Kiefling/ED22/205-453-2528)

Craig, Roy R.; Chung, Yung-Tseng; and Blair, Mark: Modal Vector Estimation for Closely-Spaced-Frequency Modes, University of Texas at Austin, Report CAR 82-1, February 1, 1982.

Turbomachinery Fluid Mechanics

The objective of this effort is to establish needed turbomachinery technology with fluid mechanics. This involves analysis, design, evaluation and improvement of rocket engine turbomachinery relative to fluid flow, the transfer of energy between fluid and rotor to produce pressure or extract work, internal flow control, and the influence of geometry on the flow.

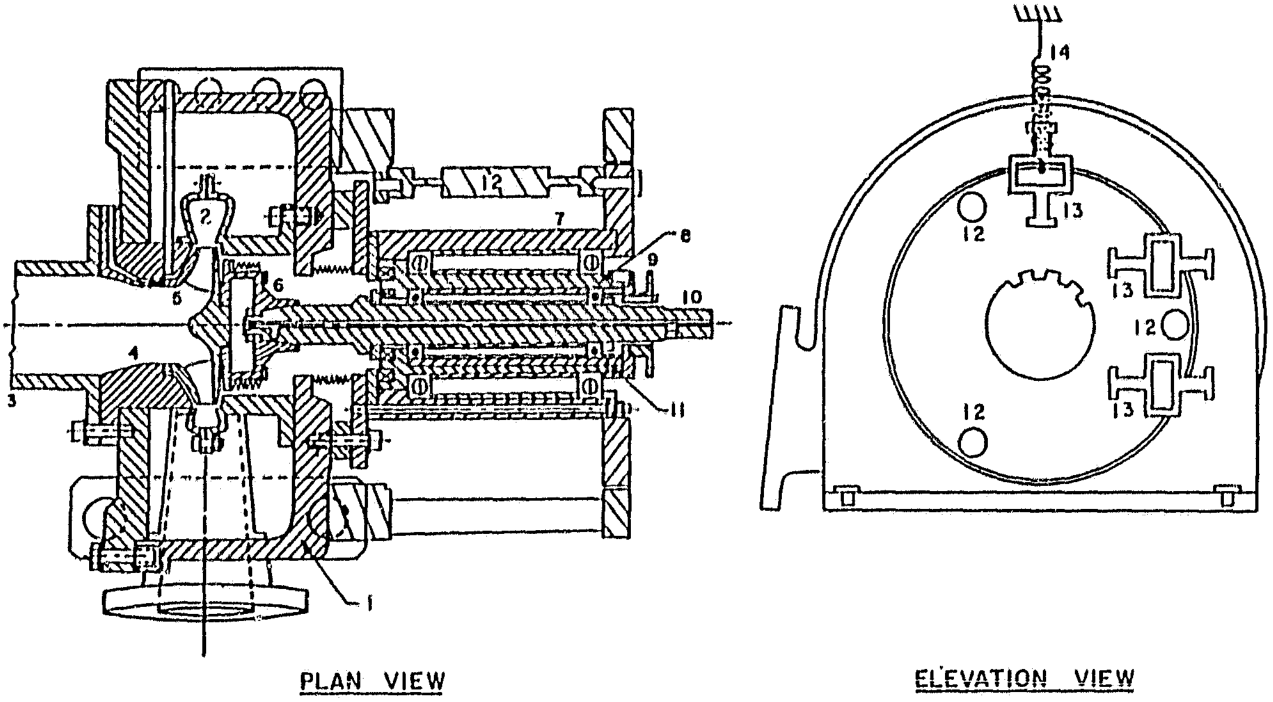

Figure 34. Schematic of Pump Housing and Force Balance Assembly of Rotor Force Test Facility. Pump Housing (1), Volute(2), Inlet Connection (3), Inlet Bell (4), Impeller (5), Internal Balance (6), Double Bearing Shaft (7), 8, 11), Orbiting Motion Sprocket (9), Main Shaft (10), Axial Retaining Flexure (12), External Balance Flexure Elements (13), and Retaining Spring (14).

This past year, a test rig for measuring impeller/diffuser dynamic forces was completed and operated (Figure 34). Figure 35 shows some of the results obtained for the impeller-volute combination with two different front and back seal clearances. The reduced data for the average force on the impeller and theoretical results along with other experimental results are given in Figures 36, 37, and 38 for comparison. Figure 39 shows the measured force coefficients used to determine the sources of large forces at zero flow. It was concluded that the force coefficient component is derived from fluid frictional effects and the induced pressure gradient acting on the entire exterior surface of the impeller. Typical non-dimensional hydrodynamic force matrices based on experimental data and theoretical results are in considerable disagreement, as shown in Figure 40. The measured data indicate that both diagonal and off-diagonal terms are of appreciable magnitude. The off-diagonal or cross-coupling terms (K_{XY} and K_{YX}) have opposite signs, indicating a tendency to excite a whirl motion of the impeller. Future tests will include measurements of the forces at non-zero whirl frequencies to obtain data on the rotordynamic effects of these hydrodynamic forces.

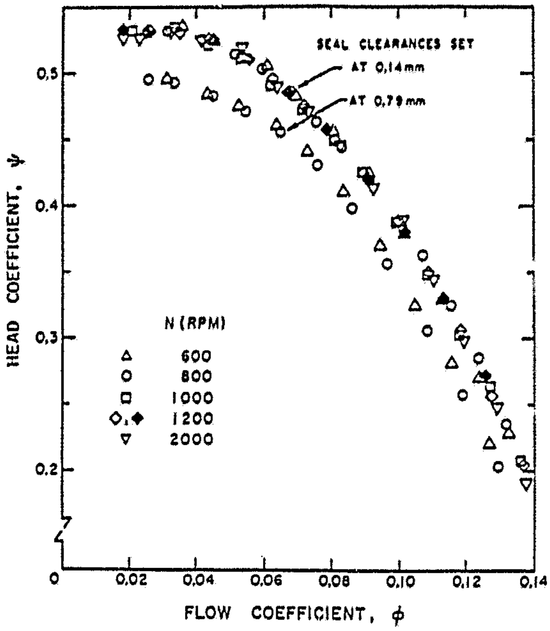

Figure 35. Performance Characteristic of Impeller X inside Volute A for Front and Back Seal Clearances of 0.14 and 0.79 mm. Open and Closed Symbols Represent Data for Omega > 0 and Omega < 0, Respectively.

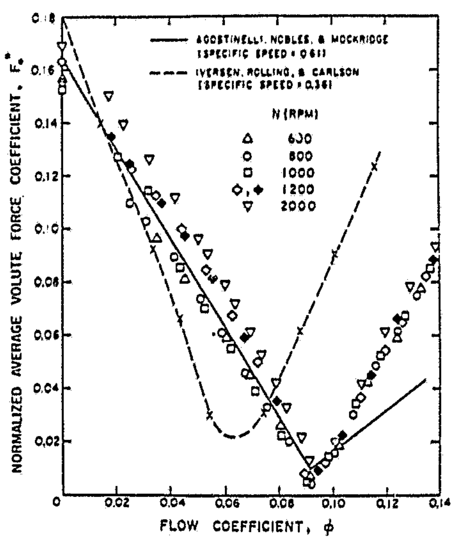

Figure 36. Normalized Average Volute Force for Impeller X, Volute A and Seal Clearances of 0.14 mm. Open and Closed Symbols Are the Same as in Figure 36. Comparison Is Made with Iversen Bearing Reactions and Agostinelli Experimental Data.

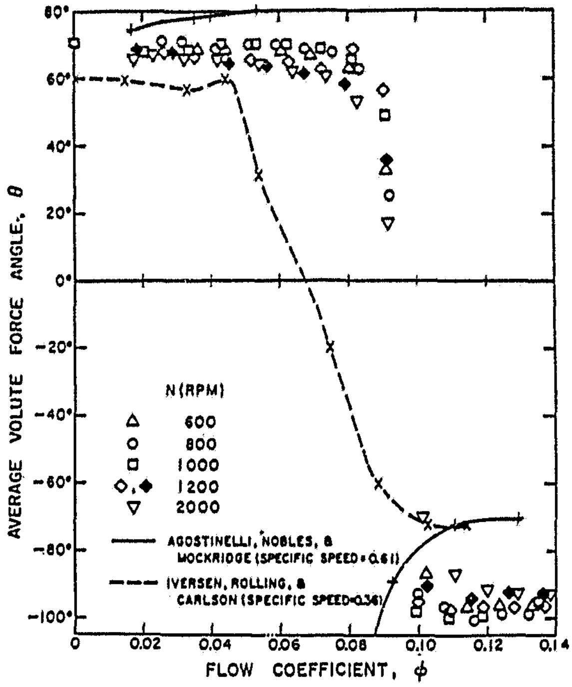

Figure 37. Direction of Average Volute Force Plotted in Figure 36 Expressed in the Volute Coordinate System. Theta is the Angle between the Direction of the Average Force and the Line Joining the Center to the Tongue of the Volute.

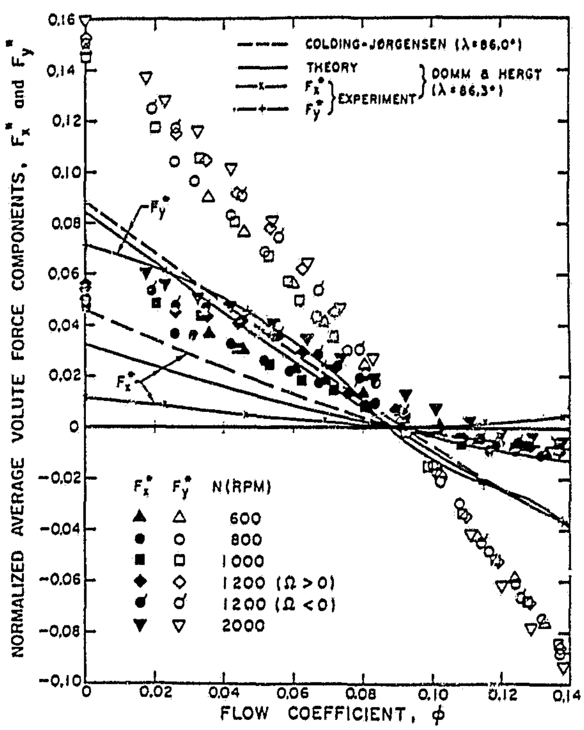

Figure 38. Normalized Average Volute Force Components from Figures 36 and 37 Shown Compared to Domm and Hergt, and Colding-Jorgensen. (Impeller X, Volute A and Seal Clearances Are 0.14 mm).

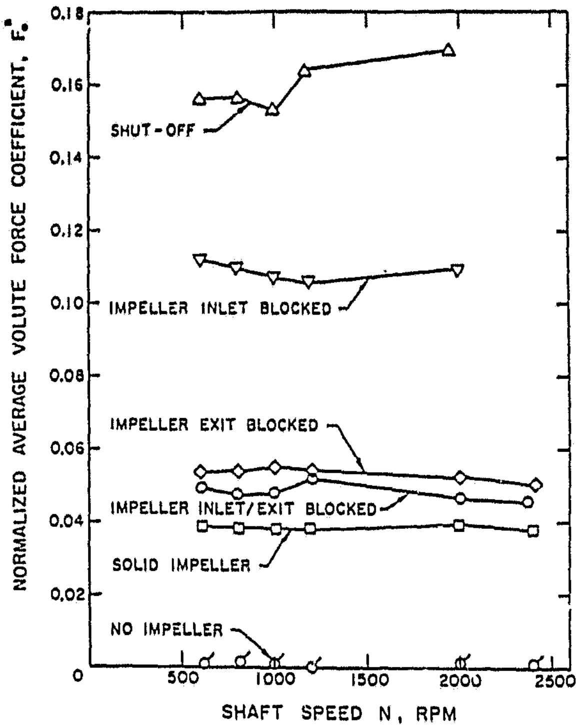

Figure 39. Normalized Average Volute Force as a Function of Shaft Speed for Various Auxiliary Experiments. (Impeller X, Volute A and Seal Clearances Are 0.14 mm).

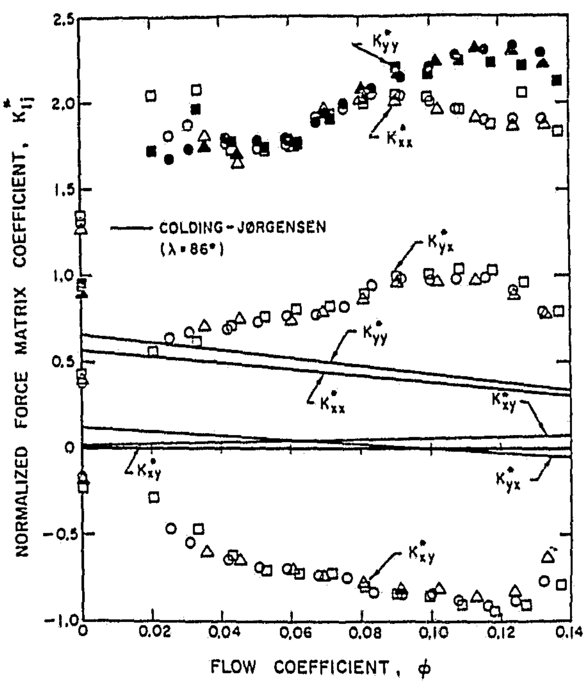

Figure 40. Force Matrix Coefficients, with Impeller X, Volute A and Seal Clearances at 0.14 mm. Triangles = Shaft Speed of 600 rpm; Circles = Shaft Speed of 800 rpm; and Squares = Shaft Speed of 1000 rpm. Values of K^*_{xx}, K^*_{xy} and K^*_{yx} Are the Open Symbols; K^*_{yy} Are the Open Symbols.

SSME HPFP Interstage Seal

Early in the Space Shuttle Main Engine (SSME) development, the high pressure fuel pump exhibited subsynchronous whirl which limited the SSME operation. The pump stability was improved by increasing the stiffness of the rotor, bearings, and bearing carriers, and also by incorporating annular interstage seals which provided stiffness and damping. The seal design was based on theoretical calculations which were experimentally verified only by water tests at a relatively low Reynolds Numbers. The HPFP interstage seals, however, operate at much higher Reynolds Numbers. Test data and dynamic analyses indicate that the HPFP is marginally stable at rated power level (RPL). The stability margin above RPL and at full power level (FPL) cannot be determined in view of lack of instrumentation internal to the pump.

A test program is being conducted to verify the theoretical analysis and to generate the necessary data for performance and seal design optimization which may be necessary for operation at FPL.

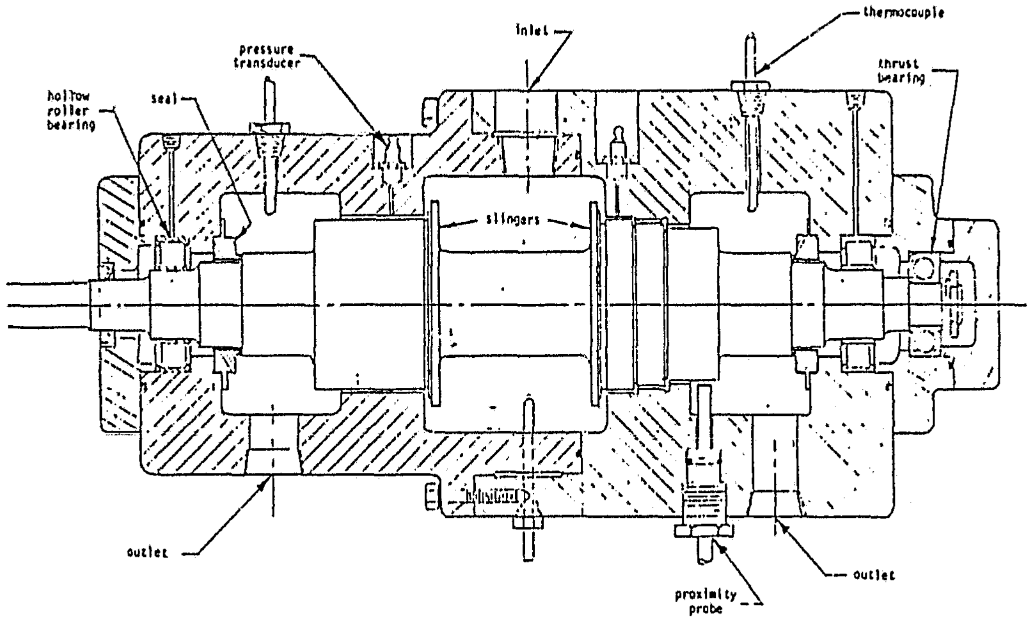

Figure 41 HPFP Interstage Seal Test Section.

A cross sectional view of the test article represented in Figure 41 shows the basic seals with stepped configuration currently used and an alternate convergent-tapered configuration being tested. Five rotors incorporating these two basic seal configurations in common but differing only in seal eccentricity and surface roughness were fabricated for testing. Specifically, eccentricity ratios of 0.0%, 25%, and 50% and surface roughness of 63 micro-inches (smooth), 0.001 inch, and 0.002 inch were chosen to examine the influence of dynamic eccentricity and surface roughness on both the sealing capability and seal dynamic coefficients. These rotors have each been subjected to a matrix of test conditions producing the combinations of axial and circumferential Reynolds Numbers encountered in the HPFP and indicated below:

a. R_a: 50,000, 75,000, 150,000, 325,000, and 400,000.

b. Rxzc: 40,000, 65,000, 90,000, 225,000, and 140,000.

The test fluid used to simulate the complete range of Reynolds Number is bromotrifluoromethane, CB_rF_3, which is manufactured by Dupont as a fire extinguisher fluid and refrigerant. This fluid has kinematic viscosity lower than that of liquid hydrogen and is nonflammable and nontoxic.

The test program is nearing completion. The static and dynamic test data generated from the tests are presently being reduced. A complete evaluation of the test data including comparison of the measured forces with theoretical prediction will be forthcoming. (F. F. Garcia/EP23/205-453-3812)

Erosive Burning in Shuttle Solid Rocket Motor

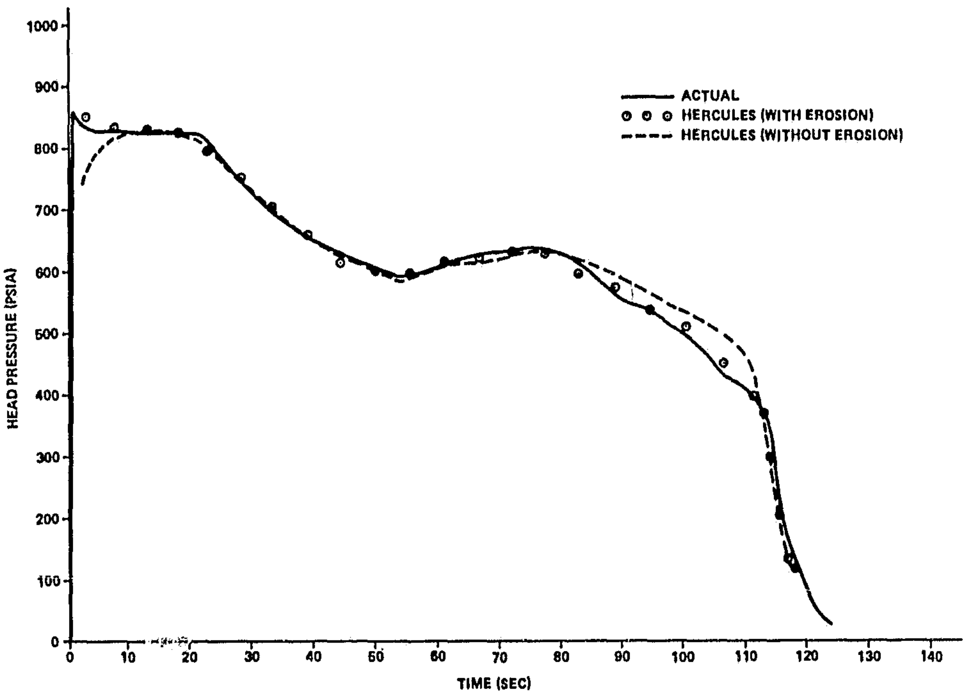

Figure 42. STS-3A Actual and Reconstructed (Hercules) Pressure-Time Traces.

Known models of Shuttle Solid Rocket Motor (SRM) performance have failed to produce pressure-time traces which accurately matched actual motor performance, especially during the first five seconds after ignition and during the last quarter of web burn time. Efforts to compensate for these differences in model reconstruction and actual performance have resulted in resorting to the use of a Burning Anomaly Rate Function (BARF). It was suspected that propellant erosive burning was primarily responsible for the variation of model from actual results. The three-dimensional "Hercules Grain Design and Internal Ballistics Evaluation Program" was made operational and slightly modified at MSFC, and an extensive trail and error effort was begun to test the hypothesis of erosive burning as an explanation of the burning anomaly. It was found that introduction of erosive burning using Green's erosive burning equation over portions of the aft segment grain and above a threshold gas MACH NUMBER did, in fact, give excellent agreement with the actual motor trace.

MATERIALS AND PROCESSES

Turbine Blade Coating Process

Recent occurrences of air foil cracks in flight engine turbine blades have re-emphasized the need for improved coatings, and work is being expedited to test the best coatings in a turbine engine rainbow wheel at Rocketdyne for final assessment and recommendations. Significant progress was realized in the turbine blade coating program with an attendant potential for improved SSME performance safety increased producibility and reduced engine maintenance costs. Turbine blades, vacuum plasma spray coated with NiCrAlY, CoCrAlY or NiCrAlY/Cr_2O_3 under contract with Howmet Corp., were evaluated and rated superior to standard SSME coated blades. Ratings were based primarily on 25 thermal cycles (Figure 43) in the MSFC Burner Rig Tester. This test showed there was no spalling on blades with improved coatings, while standard blades spalled. Currently, ZrO_2 thermal barrier coatings are being applied on top of the "M" CrAlY bond coatings. Fatigue and tensile specimens, machined from MAR-M-246 test bars (identical to the blades) are being vacuum plasma spray coated and diffusion bond treated in order to qualify the vacuum plasma spray process for flight hardware application. (R. R. Holmes/EH43/205-453-0643)

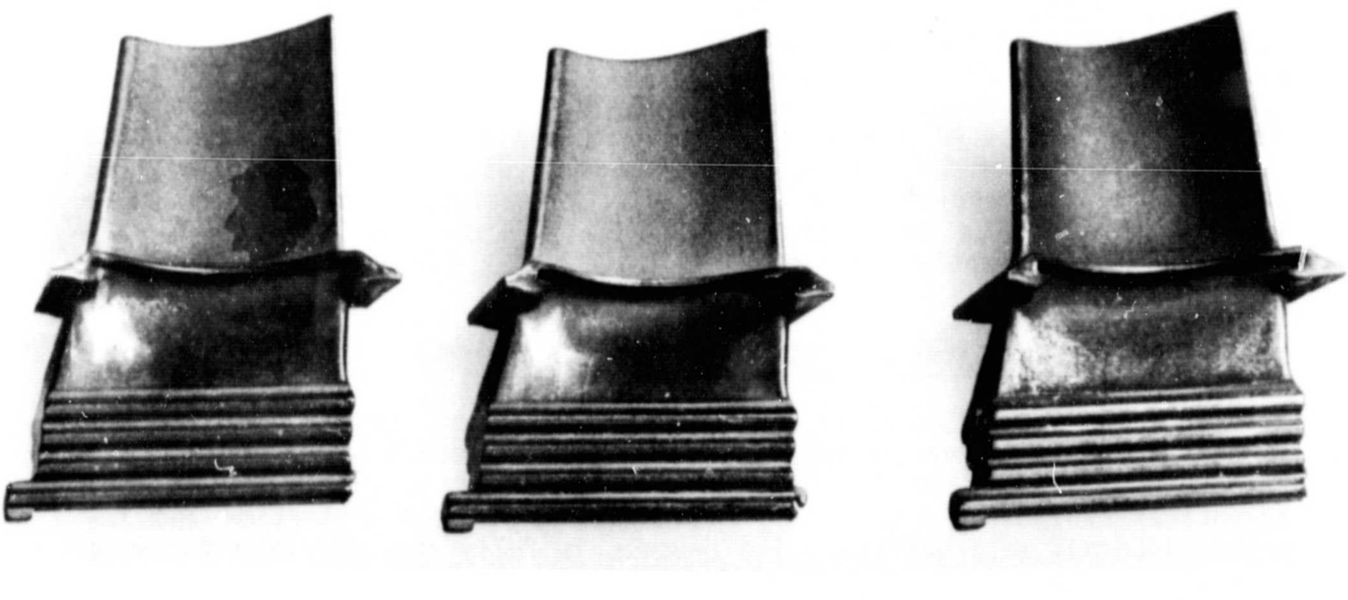

SSME BLADE NiCrAlY	TEST BLADE NiCrAlY	TEST BLADE NiCrAlY/ Cr_2O_3

Figure 43. Turbine Blades after 25 Burner Rig Cycles.

Hydrogen Resistant Alloys

In order to develop a weldable, corrosion resistant, high strength alloy (YS-160 ksi, UTS-180 ksi) immune to gaseous hydrogen embrittlement, chromium was added to the basic Incoloy 903 presently used for high pressure hydrogen applications. A factorial design of alloys with varying chromium and cobalt contents was used to optimize notched tensile strength in hydrogen. Alloys were melted in a vacuum induction furnace, cast, and hot rolled. Heat treatment consisted of solution treatment at 2200° F followed by aging at 1350° F for maximum strength. Test specimens were fabricated and tensile tests were run in 5000 psi hydrogen and in air to determine the amount of hydrogen degradation. So far, tests have indicated that low (10%) chromium alloys have the least (5% to 9%) degradation in high pressure hydrogen. Therefore, future work will be concentrated on the low chromium alloys. The heat treatment procedure will be optimized in order to maximize the tensile strength. Titanium, aluminum, carbon and columbium contents will also be optimized. After the alloy is fully developed, the alloy will be made in commercial quantities and tested for corrosion resistance, weldability, and fracture characteristics with the purpose of application in advanced high pressure O_2/H_2 propulsion systems.

High Speed Machining Technology

High Speed Machining (HSM) is a relatively new manufacturing technology with a high potential for improving machining efficiency in many applications. Lockheed Missiles and Space Company (LMSC), under contract to MSFC, has successfully demonstrated HSM on a subsection of an ET LH_2 Barrel Panel. A modified Sundstrand OM4 Ominimil was used with spindle speeds up to 18,000 RMP and table feeds up to 200 ipm. Cutting efficiencies (material removal) of 4.1 in^3/min/hp were achieved in the 2219-T87 aluminum. Conservative estimates of machining time reduction for ET Barrel Panels are significant --25% or $85,000 per tank. A better estimate of savings will be available at the conclusion of a productivity feasibility study in November 1982. It should be noted that metal removal rates of 300 in^3/min are possible with currently available HSM equipment. (James D. Hankins/EH44/205-453-1520)

Variable Polarity Plasma Arc (VPPA) Welding

Variable Polarity Plasma Arc welding development at MSFC and MCC/MAF is now available to replace the Tungsten Inert Gas method now used to fabricate the Space Shuttle External Tank. VPPA welding offers significant advantages of reduced precleaning requirements, reduced distortion and improved internal weld quality. The process is fully characterized for more ET applications with design allowable properties developed for joint thicknesses thru 5/8". The process advantages and production acceptance have been demonstrated on a major production fixture at Michoud by making a complete series of welds for test on a full scale barrel segment on the 5015 barrel assembly fixture. All welds exceeded preestablished acceptance criteria and the barrel assembly was made in a routine manner by production personnel. All welds were X-rayed and found to be free of defects. It is now anticipated that phased implementation of VPPA welding into ET production will begin in FY83. It is conservatively estimated that cost savings on the order of $200,000 per tank will be realized with full implementation of this new welding process. (Ernest O. Bayless, Jr./EH42/205-453-0011)

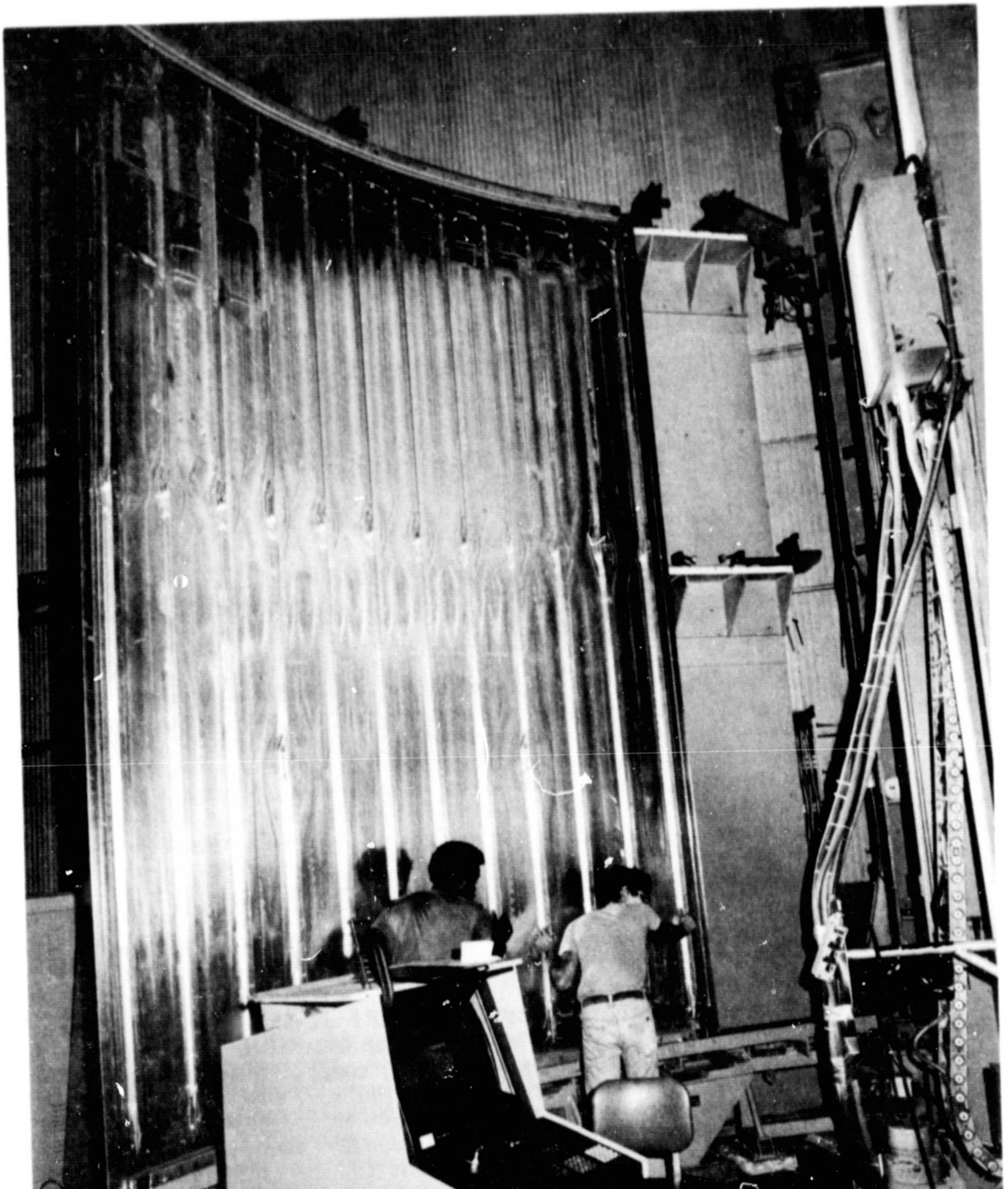

Figure 44. VPPA Welding of LH_2 Barrel from Scrap Parts.

ORIGINAL PAGE
BLACK AND WHITE PHOTOGRAPH

Alternate Thermal Protection System for ET Aft Dome

Figure 45. Large ET SOFI Spray Booth as Seen from the Control Room.

A cryogenic/thermal protective material, NCFI 22-65, was developed, utilizing the MSFC Spray-on-Foam Insulation (SOFI) facility, as a replacement/alternate to the SLA 561/CPP 488 (two layers) composite system now used on the Aft Dome of the Shuttle External Tank. NCFI 22-65 is an improved polyisocryanurate foam serving as both thermal ablator and cryogenic insulation. With an applied density of 2.6 to 3.1 lbs/ft^3 there is a significant weight reduction relative to SLA-561 (density 15 - 18 lbs/ft^3) and the CPR 488 (density of 2.2 - 2.6 lbs/ft^3) composite system. In addition, a significant materials and labor cost savings is projected for the life of the STS program. The new material and application process was developed as a joint effort by MSFC and MMC personnel in an MSFC facility which utilizes computers, robots, airbearing turntables and a sophisticated environmental control system. (Charles H. Jackson/EH43/205453-0643)

Biodegradable Organic Stripping Technique

A refurbishment process for the aluminum components of the Solid Rocket Booster (SRB) utilizing biodegradable, organic blasting material to remove protective coatings was developed and tested in the Materials and Processes Laboratory. This refurbishment technique offers various advantages over other conventional methods (chemical stripping, wire brushing, hand sanding) that are time consuming, expensive and require immediate waste disposal after use. There are several advantages with the use of this process: no major reconversion coating of aluminum is required; surface roughness is minimum; induced compressive stress is negligible; there is no pollution associated with the use of organic abrasive materials; and the time required for refurbishment is greatly reduced. This efficient, economical, non-polluting method of walnut hull blasting is now being used in the refurbishment cycle of the SRB aluminum components at KSC. (Gail H. Gordon & Wendell R. Colberg/EH43/205-453-0643)

Figure 46. Use of a Biodegradable Organic Stripping Material (Walnut Hulls).

ET SLA Vent Reduction Verification

A concept verification program for the reduction of SLA vents on Shuttle External Tanks (ET) was completed in the Materials and Processes Laboratory Spray-on-Foam-Insulation (SOFI) facility. The program was conducted as a joint effort by MSFC and MMC personnel utilizing state-of-the-art processing equipment consisting of computers, robots, airbearing turntables and spray formulators. On the ET, SOFI is applied over SLA 561 (a silicone base ablator) in various areas. In the past a large number of plastic vents were installed on the SLA surface prior to application of SOFI to allow escape of expanding (residual solvent) vapor, caused by SOFI exothermic reaction, that could result in lamination debonds. It was verified

ORIGINAL PAGE
BLACK AND WHITE PHOTOGRAPH

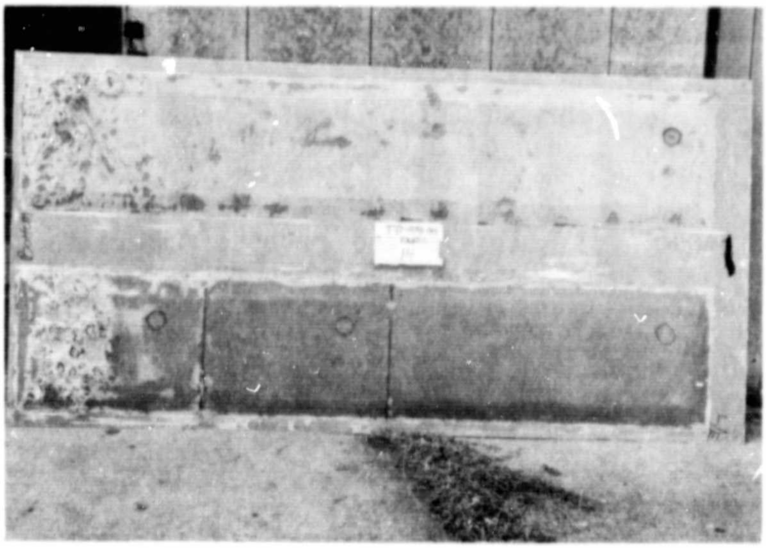

Figure 47. SLA Vent Reduction Verification Test Panel. (Panel on the top shows residual foam; panel on the bottom shows the SLA-561).

during the test program that the number of vents could be reduced by approximately 80% by selective placement on the surface to be covered by SOFI. The reduction was implemented on ET LWT-1 for a significant labor savings. Over the life of the STS program a cost savings of millions is projected. (C. H. Jackson/EH43/205-453-0643)

ELECTRICAL/ELECTRONIC SYSTEMS

Solar Cell Characterization

Various configurations of Back Surface Reflector silicon solar cells including small (2 x 2) cm and large (6 x 6) cm cells with conventional and wrap-around contacts have been subjected to 1 MeV electron irradiation and characterized under both earth orbital and deep space conditions of temperatures and illuminations. Current-voltage (I-V) data were generated from +80° C to -150° C and at incident illuminations from 135.3 mW/cm^2 (1 solar constant) to 11.6 mW/cm^2 (0.086 solar constant) for these cells.

The capabilities of the cells investigated in terms of photoconductivity (current density) and developed voltage generally were as expected from production run cells. However, some of the WAC cells had high open circuit voltage output (607 mV) at 135.3 mW/+25° C. The performance spread of the WAC cells was large with efficiencies ranging from 12.4% to 13.4% under earth orbital conditions; small series resistance contributed to some reduced output in these cells. The LILT flat spot performance problem identified earlier in BSR cells was found in the large cells in approximately the same severity and percentage of affected cells.

The large cells showed less resistance to 1 MeV electron irradiation than the 2 x 2 cm cells in terms of decreased current and maximum power output. The degradation shown by normalized current-voltage parameters as a function of irradiation is equal or slightly greater under LILT conditions than under high temperatures and intensities. The percentage change in current-voltage temperatures coefficients with the exception of voltage was less at LILT conditions. This work is documented in "Silicon Solar Cell Characterization at Low Temperatures and Low Illumination as a Function of Particulate Irradiation," a paper to be published in 1982 AGARD Conference Proceedings. (Ann F. Whitaker/EH12/205-453-4877)

Miniature Cassegrainian Converter

This past year a miniature cassegrainian concept for efficiently converting solar energy to electrical energy was evaluated from an analytical, as well as an experimental approach, to verify concept performance. A model of a nine-element miniature cassegrainian converter is shown in Figure 49. Emphasis this last year was placed upon experimental analysis. The nine-

Figure 48. Miniature Cassegrainian Energy Converter.

element model was evaluated in thermal vaccuum and natural sunlight to verify its thermal and electrical performance. This work is being conducted in conjunction with TRW Systems Group in an effort to improve efficiency and reduce cost of photovoltaic solar arrays. This effort was reported at the IECEC meeting in August 1982. (W. L. Crabtree/ EB12/205-453-2110)

Low Cost, High Concentration Ratio Solar Cell Array for Space Applications, August 1981.

Cassegrainian Concentrator Solar Array Exploratory Development Module, August 1982.

Automatic Rendezvous and Docking System

Many future space operations will pose challenging problems in the control of relative motion between spacecraft. Some of these will deal with the assembly of systems of modules into large structures. Others will arise from the need to retrieve nonfunctioning or uncontrolled spacecraft and payloads. In order to take full advantage of the Space Transportation

System and make the construction of Large Space Systems a reality, improvements in rendezvous and docking technology are needed. The objective of this work has been to develop techniques for automating the rendezvous and docking task. The fundamental technical problem involves devising a workable scheme to sense relative attitude and position errors between two vehicles and use this information to drive a control system on one of the vehicles to achieve automated docking. Two approaches have been developed at MSFC. One approach uses a scanning laser radar as the sensor and the other is a video-based technique. (Several additional video-based techniques were developed under contract NAS8-34679 with Martin-Marietta Company during FY82.) A preferred technique was selected from those studied to be further evaluated in a physical simulation to be conducted in FY83. (J. Micheal/ED15/205-453-4585)

Martin-Marietta Company Report MCR-82-569, entitled Development of an Autonomous Video Rendezvous and Docking System, Final Report, June 1982.

High Gain Antenna - Space Telescope

LMSC under contract with General Electric Space Division, Philadelphia, Pennsylvania, developed a modified version of the space-qualified Solar Maximum Mission (SMM) High Gain Antenna System. The High Gain Antenna Disk is a 50.3" diameter parabola weighing approximately six pounds. The reflector is constructed, for the first time, using graphite epoxy (GY70) face sheets bonded to and separated by aluminum honeycomb core sections. The core is subdivided into three circular segments; center, mid, and outer sections. The center core is 1/8", 8.1 lb/ft^3 hex honeycomb and the outer two core sections are 1/4" flexcore, 3.1 lb/ft^3 and 2.1 lb/ft^3 respectively. There are six layers of graphite fabric laid up to 0^o and $\pm 45^o$ wrap directions on both sides of the honeycomb core in the center area inside 4.0" radius and tapers out to a single layer on each side at the lip of the reflector. Titanium was chosen as the material for both the spool inserts and the cloverleaf center fitting over the lighter aluminum material because of its closer compatibility to graphite thermally (i.e., thermal coefficient of expansion). The graphite fiber-epoxy inner face sheet provides the reflecting surface which tests have shown to be suitable for operation over the required RF frequency range. The center fed turnstile feed used is the same design as provided for the SMM spacecraft. It is vertex mounted and the crossed dispoles are located at the reflector focus and are supported by a brazed coaxial section. All edges and corners have been designed in accordance with EVA safety requirements. (G. Emanuel/TA31/205-453-2387)

Gyro Noise Minization Technique - Space Telescope

Due to the extremely low jitter levels required for the Space Telescope Pointing Control System (.007 arc-sec), it became apparent that a significant improvement in gyro noise performance was required. The Space Telescope Pointing Control System uses a floated single degree of freedom gyro with a hydro-dynamic wheel rotating at 19,200 RPM. The gyro is basically the same unit as utilized on the High Energy Astronomical Observatories and the International Ultraviolet Explorer Satellite. To achieve the designed low noise characteristics, extensive testing and analysis were performed to identify the basic noise sources within the gyro with initial results indicating that the gyro electronics were a major noise source. The gyro gain (H/C) was then increased using a less vicous damping fluid, thereby allowing the gyro electronic gain to be decreased. Subsequent testing of development units confirmed a decrease in noise levels but not as extensive as modeling and analysis had predicted. It was concluded that the remaining prime noise contributor was mechanical in nature. Earlier experimental work done by both JPL and MIT's Draper Labs had indicated that a major source of mechanical noise in the gyro was due to gas turbulence inside the float. This turbulence is caused by nonlaminar gas flow generated by the gyro wheel and could be reduced by shielding the wheel to obtain laminar gas flow. An experimental float was constructed and tested on a special dynamometer to verify the noise reduction achieved by shrouding the wheel to reduce gas turbulence. Test data confirmed the noise reduction predications and the Space Telescope gyros are being modified to incorporate wheel shrouds within the float. Production units will be tested later this year to characterize the noise level of each flight sensor. (H. Krome/TA31/205-453-4122)

DATA BASES/DESIGN CRITERIA

Automated Vibroacoustics Data Bank

The Component Analysis Branch of the Systems Dynamics Laboratory has the responsibility for deriving vibration criteria and evaluating flight data for Space Shuttle components and payloads. This requires maintenance of an extensive vibroacoustics data bank containing vibration response spectra for many types of structures. In a new approach to automate this process, data are incorporated onto a computer disk file for compact storage and instant recall. A software package was developed which will retrieve, scale, and allow the user to formulate criteria approximately ten times faster and more accurately than the manual method used in early programs. Shuttle flight data evaluation and storage are accomplished in approximately one-fifth the time required previously without involving personnel or equipment outside the laboratory. This work was reported at the 1981 Shock and Vibration Symposium and also in NASA Technical Paper No. 1998. (R. Ferebee/ED23/205-453-3174)

Automation of Vibroacoustic Data Bank for Random Vibration Criteria Development, Proceedings of the 1981 Shock and Vibration Symposium, October 1981.

Application of a Computerized Vibroacoustic Data Bank for Random Vibration Criteria Development, NASA Technical Paper No. 1998, March 1982.

Effect of Plume-Induced Base Pressures on Launch Vehicle Aerodynamic Loads

The first Shuttle flights revealed an effect of the engine jets on the launch vehicle base pressure that was larger than predicted. They revealed also an unexpected additional lift on the rear of the Orbiter. In order to clarify the cause of this lift, force and pressure distribution tests were performed in MSFC's 14-inch wind tunnel on a Shuttle launch configuration model with solid jet plume simulators, adjusted to match the flight base pressure ratios. The resulting force and moment effects were consistent with the flight results, proving the base pressure increment to be the cause of the additional lift. The pressure distributions furnished a guide for preliminary Orbiter load corrections. The test series is a first step toward an inexpensive method to measure aerodynamic load effects of jet plumes for preliminary design of launch vehicles. (C. D. Andrews/ED32/205-453-3166)

Terrestrial Environment (Climatic) Criteria Guidelines for use in Aerospace Vehicle Development, 1982 Revision

Atmospheric phenomena play a significant role in the design and flight of aerospace vehicles and in the integrity of the associated aerospace systems and structures. Environmental design criteria guidelines in this report are based on statistics of atmospheric and climatic phenomena relative to various aerospace industrial, operational, and vehicle launch locations. This revision contains new and updated material in most sections. Specifically, aerospace vehicle design guidelines are established for the following environmental phenomena and presented by sections in NASA TM-82473: Winds, Inflight Thermodynamic Properties; Precipitation, Fog, and Icing; Sea State; Humidity; Atmospheric Density and Pressure (Surface); United States Surface Extremes; Worldwide Surface Extremes; Tornadoes and Hurricanes; Atmospheric Electricity; Cloud Phenomena; Four-D Atmospheric and Cloud Cover Models; Thermal Radiation; Atmospheric Chemistry; and Geologic Hazards. The last section in this document includes conversion constraints. Atmospheric data are presented and analyzed for application to aerospace vehicle design studies. The atmospheric parameters are scaled to show the probability of reaching or exceeding certain limits to assist in establishing design and operating criteria. Additional information on the different parameters may be found in the numerous references cited in the text following each section. (R. E. Turner/ES84/204-453-4175)

Induced Environment Contamination Monitor (IECM)

Early in the Space Transportation System development, concerns were expressed that the particles and gases emanating from the Shuttle would limit the performance of sophisticated sensors. Mathematical modeling indicated that with proper design, material selection, and operational considerations, the STS could provide a suitable environment for the anticipated experiments and payloads.

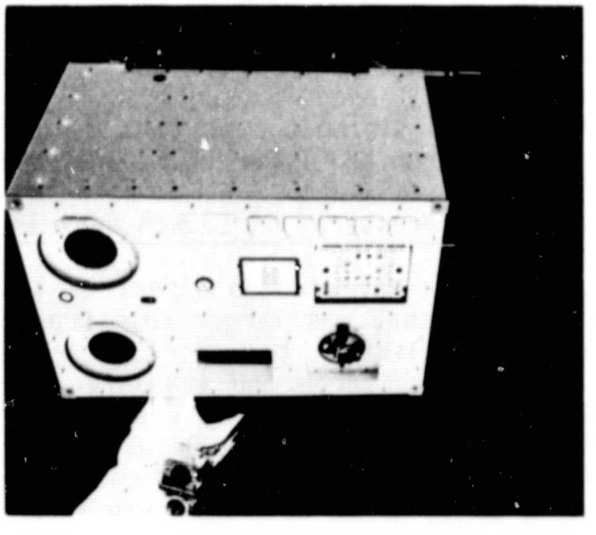

Figure 49. Induced Environment Contamination Monitor (IECM) Shown Attached to the Remote Manipulator System to Survey Orbiter Effluents during the STS-4 Mission.

The IECM (Figure 50) was developed to verify that the induced environment goals were met and to verify modeling techniques for prediction of the environments for future complex payloads. During the past year, the IECM has flown successfully on STS-2, -3, and -4 Orbiter Flight Test (OFT) missions. The results from the measurements acquired by the IECM during all phases of these missions indicate that with planned improvements to be implemented in the ground facilities, the Space Shuttle will provide an excellent science experiment platform, payload carrier, and retriever from the standpoint of induced contamination. The IECM also provides data which is being used to minimize the loss of operation time of sensitive instruments, yet avoiding deleterious contamination effects of necessary spacecraft operation such as engine firings and water dumps. (E. Miller/ES61/205-453-0130)

Miller, E. R. (editor): STS-2 Induced Environment Contamination Monitor (IECM)--Quick-Look Report. NASA TM-82457, January 1982.

Miller, E. R., and Fountain, J. A. (editors): STS-3 Induced Environment Contamination Monitor (IECM)--Quick-Look Report. NASA TM-82489, June 1982.

FACILITIES DEVELOPMENT

Bearing Test Facility

An MSFC, in-house, bearing tester and hazardous test facility have been designed and built for full scale cryogenic turbopump tests using liquid oxygen (lox). Future plans are to expand the facility to include provisions for liquid hydrogen full scale bearing tests. The present facility can accommodate lox bearing sizes from 45 mm to 85 mm bore and shaft speeds to 42,000 RPM. The tester and facility will be utilized to test various new bearing materials including new alloys and some powder metallurgy materials. Concepts being planned or being designed and manufactured out-of-house on contract are: powder metallurgy ball bearings (three different alloys and/or designs), various bearing alloys which have been surface altered with different ion implantation or ion plating processes, plus a magnetically levitated bearing is being studied. Various lubrication scheme studies and tests are also planned. Out-of-house feasibility contracts which culminate with the manufacture of bearings are intended to supply the bearing tester with test articles. All concepts, designs, and materials will be tested in direct comparison to the standard 440C angular contact bearings currently being utilized. A contract was also in effect in September 1981 for a study of currently available bearing computer programs and the analysis of data being generated by the bearing tester. The intent here is to have a bearing computer program altered and adjusted to predict cryogenic bearing life and other pertinent turbopump bearing design parameters.

The in-house bearing tester and facility were completed and the first lox bearing test was made June 18, 1982. The bearing data analysis and computer modeling contract has been in effect for nine months. The contractor, Spectra Research, Inc., has SKF's computer program "SHABERTH" and Battelle's model "BASDAP" both installed and operational on a Univac 1108 computer. The powder metallurgy contract was signed with TRW March 1, 1982. TRW has made a materials survey and has chosen six alloys for initial powder metallurgy tests. The roller bearing scope of work was completed, mid-May 1982, and the RFQ is currently out for bids. The magnetic bearing feasibility study was completed in March 1982. The second phase of this work, the design phase of the contract, is currently out for bid by SKF, a sole source bidder. Currently a scope of work is being prepared for the ion implantation and ion plating work efforts.

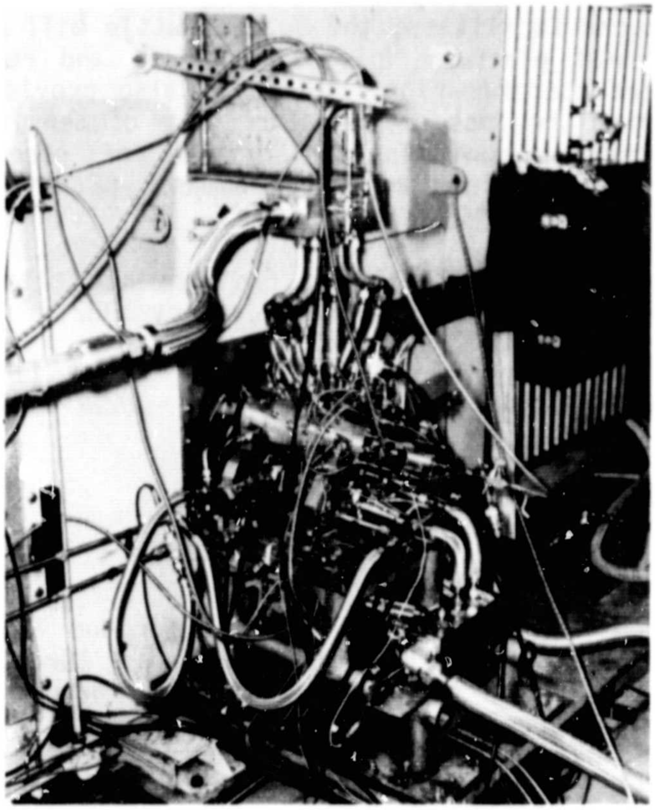

Figure 50. Lox Bearing Tester Installed in the Bearing Test Facility.

Drop Tube for MPS-Low-G Containerless Solidification

The "100 Meter" Drop Tube which is located in building 4550 began its operational phase in September 1982. This facility supports Materials Processing in Space Technology with research to better characterize and quantify the role of gravity inherent in terrestrial materials processing. Molten material samples are dropped from a furnace at the top of an evacuated tube and are solidified during free fall. Over 4 seconds of free fall time are available. The samples are recovered from a catch system at the bottom of the tube. Vacuum valves allow the catch system to be opened without losing vacuum in the rest of the tube. Three different type furnaces are available for the melt. These consist of an electron beam bombardment furnace, an electromagnetic levitator (induction heating) furnace, and a dripper furnace in which a sample is melted and forced out of a tube similar to an eye dropper. These furnaces are contained in a bell jar which can be isolated from the main tube with vacuum valves.

The Drop Tube is actually 341 feet long (104 meters) from the release point to the bottom of the catch system and is composed of 10.42 inch inside diameter stainless steel pipe. The tube is aligned so that the centerline of the tube, at any point along its length, does not vary more than 1 inch from a true vertical line from the center of the tube at the specimen

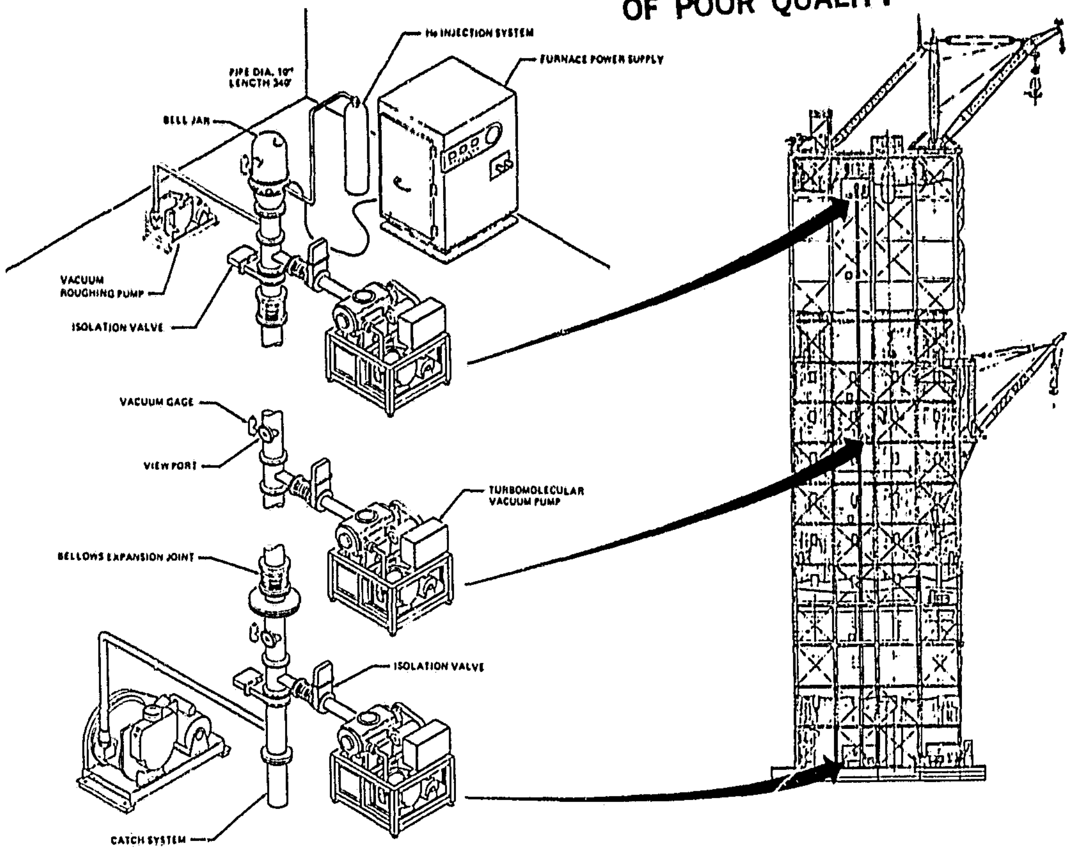

Figure 51. MSFC Drop Tube Facility.

release point. The Drop Tube is capable of attaining a vacuum in the 10^{-6} mm Hg range with the use of 6 turbomolecular and 2 mechanical roughing pumps. Vacuum valves are located in the pipe so that each pump can be isolated from the Drop Tube. Instrumentation and view ports are located at various points over the length of the tube. A data acquisition system, to record readings from thermocouples (furnace and specimen temperatures), optical pyrometers, infrared detectors and vacuum gauges, is located in the control room at the top of the tube. Missile grade air, gaseous nitrogen, argon and helium are available for repressurization of the tube to meet different test requirements.

Test Laboratory and Space Science Laboratory have worked concurrently to bring this facility to an operational state. The University of Alabama in Huntsville has supported Space Science Laboratory in its efforts. Two companies, which will be involved in early experiments with containerless solidification, are E. I. DuPont DeNemours and Company of Wilmington, Delaware and Deere and Company of Moline, Illinois. (Thomas L. Denton/ET45/ 205-453-4742)

High Voltage Power System

A versatile, multipurpose high voltage power system breadboard is functioning at MSFC as a test bed for high voltage, high power hardware and concepts. High voltage NiCd battery technology is being pursued as charge control techniques, pulse discharge, cell protection, and battery reconditioning are investigated. Programmable Power Processors (P^3) are being tested to determine capability, programmability, and applicability under various conditions and circumstances. The breadboard also provides the capability for testing a variety of high voltage switchgear for advanced electrical power systems. (J. R. Lanier, Jr./ EB12/ 205-453-4630)

NASA Technical paper 1939 entitled, Concept for a Power System Controller for Large Space Electrical Power Systems, November 1981.

Power Electronics Specialists Conference (PESC) paper entitled, A Programmable Power Processor for High Power Space Applications, June 1982.

☆U.S. GOVERNMENT PRINTING OFFICE: 1982—646-058/96